CR 172074

TRW

Study of Plasma Motor Generator (PMG) Tether System for Orbit Reboost

Final Report

June 1988

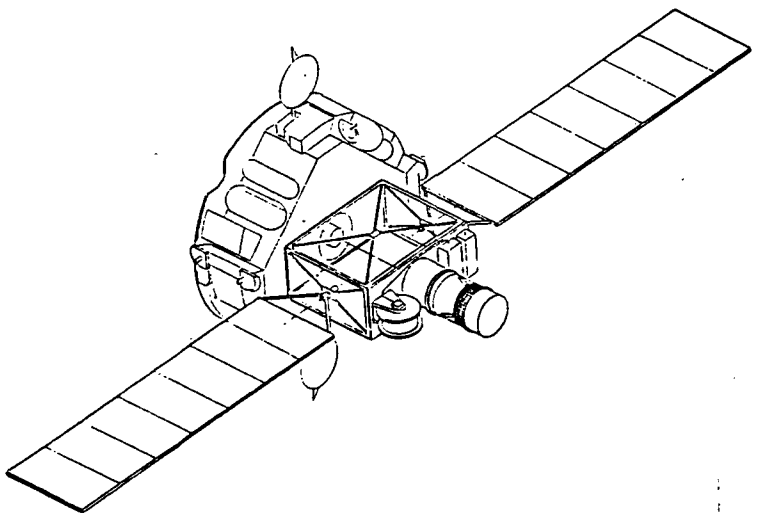

Prepared for:

National Aeronautics and Space Administration
Lyndon B. Johnson Space Center
Houston, Texas 77058
Contract No. NAS9-17751

CONTENTS:

1. Introduction and Task Description

This document contains a progress report on a system study by TRW begun in January 1987 of a 2 kW Plasma Motor Generator (PMG) Tether to be used for orbit reboost. Following the completion of the initial phase of this study in September 1987, additional tasks were agreed to and work on them began in March, 1988. These tasks fell into three categories: tests on the prototype tether fabricated during the first phase, simulations of the spacecraft and tether system after deployment using GTOSS and a brief investigation of the impact and feasibility of increasing the system to 20 kW and hosting it on the Orbital Manuvering Vehicle. Our subcontractor, Energy Sciences Laboratory (ESL) was assigned the responsibility of performing the simulations and some mechanical tests on the prototype tether to supplement those done at TRW.

A summary of the significant findings and issues from each task follows. Our recommendations for future work constitutes the third section. The Appendices contain a copy of the Final Briefing (Appendix A) the detailed reports submitted for each task and additional analyses.

2.0 Summary of Findings

This section contains a brief summary of the major findings of the three tasks. It is important to note that these tasks were performed to a fixed budget. As such, while some questions were answered, others were raised but could not be addressed.

2.1 20 kW PMG Tether Task

Appendix B contains the detailed report on this task.

The following is a synopsis of the findings: Because OMV can only provide approximately 1 kW to a payload, a substantial power kit would be required to provide the power to the tether. In the near term, photovoltaic arrays will be the only usable source for this magnitude of power. Assuming 12 w/FT^2 (129 w/m^2), two wings, 12 ft. by 73 ft. (3.6m by 22.2m) each, would be needed to generate the 20 kW. Scaling the 2 kW deployment design and the 10 km tether, the end mass at the start of deployment would weigh 2752 lb (1251 kg) and the experiment support equipment would weigh 1628 lb (740 kg). No batteries are included in the kit. While OMV is capable of handling this mass, the system cannot be launched cantilevered. Assembly on-orbit is required.

Several technical and programmatic issues arose including determination of a realistic stiffness for the arrays, their cost relative to the total package and the deployment and disposition of the large tether. The stiffness of the array panels will determine the acceleration limits and, hence, the thrusts modes of the OMV.

While OMV appears to be a feasible host for a 20 kW PMG Tether System, it would seem that further consideration of this upscaled concept should be deferred until a smaller system has flown.

2.2 Tether Characterization and Materials Testing

A number of tests were performed and measurements made at TRW on the prototype tether constructed during the first phase of this study. Complete results constitute Appendix C. The tether tested close to the calculated values for mass, sensitivity and tensile strength and met the physical performance goals. The tensile and torsional moduli would be improved by braiding the aluminum conductor. The DC breakdown voltage significantly exceeded expected service values. Based on various abrasion tests, it was determined that the FEP insulation without the glass braid would be adequate. Except for flexibility, the basic tether design meets or exceeds performance goals.

Materials testing was also conducted at ESL with particular attention paid to those characteristics that would affect deployment and behavior while deployed. Appendix D contains the description of the tests and the findings. The tether displayed the "pig-tail" effect after uncoiling. This effect radically lowered the effective modulus at low tension. Such a low modulus may be useful in reducing loads on the solar array. The wire "handedness" is part due to the pig-tail, as well as the fact that the wire was not counterwound, and allows transfer of some libration energy into torsional pendulum modes, a positive side effect. Damping could not be measured with confidence on the current test rig.

It would be beneficial from a systems standpoint if two more flexible tethers were fabricated with braided conductors, one with, and one without, counterwound conductors. Deployment testing should be performed on these tethers as part of the selection criteria. Test results comparison should yield additional design insights.

2.3 Simulations

Long term simulations of up to one week were performed using GTOSS with input parameters based on the nominal 2 kW PMG Tether System on OMV. In addition, an ESL program, DUMBBELL, was run to show the behavior of the system over several weeks but using a simple characterization of the tether and spacecraft. Appendix D details the various simulations and the results. In addition, two video tapes were produced that display some of the runs made with both programs.

The most striking result was the appearance of "jump-rope" resonances during a GTOSS simulation of the case of applying power to the tether during daytime only. Some control mechanism to eliminate this behavior must be developed. The continous power case did not result in this jump-rope effect. The usefulness of the DUMBBELL runs remains questionable and longer term GTOSS simulations are recommended to assess the simpler program's validity. Additional observations are included as Appendix E.

3.0 Recommendations for Future Work

The following activities merit special consideration as part of the preparation for developing the 2 kW PMG Tether System flight experiment: 1. perform more detailed host-platform system analyses; 2. build and test new prototype tethers reflecting the results and issues discussed in this report; 3. develop system controlability strategy and 4. continue and extend GTOSS simulations.

A series of experiments, beginning with the Hitchhiker PMG 1 tether package now scheduled for November 1989, should be designed and performed at the earliest opportunity to prove the concept of and to gain experience in deploying and operating an electromagnetic tether prior to proceeding with the full scale development of the flight experiment.

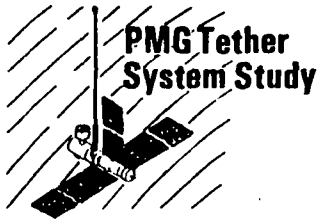

TRW Space &
Technology Group

PMG TETHER STUDY
TRW FINAL BRIEFING TO JSC/DR. JAMES MCCOY

DAVE YOUNKIN

22 JUNE 1988

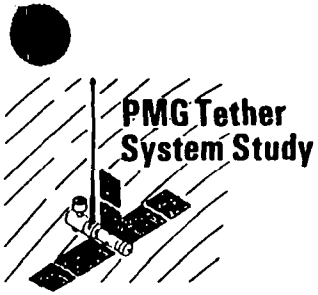

AGENDA

TRW Space &
Technology Group

- Introductions
- OMV Modifications for 20 KW PMG Tether System
  -- Dr. Neal Hulkower, TRW
- Mechanical and Electrical Properties
  -- Dr. Ron Rossi, TRW
- Deployment and Dynamics Evaluation
  -- Joe Carroll, ESL
- Conclusions, Recommendations

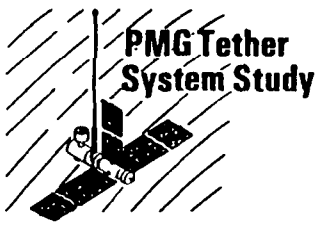

PARTICIPANTS

TRW Space &
Technology Group

- STUDY MANAGEMENT, TECHNICAL OVERSIGHT, BUDGET CONTROL, SUBCONTRACTING: YOUNKIN, SAKAGUCHI, LIEBE
- OMV STUDY TASK: HULKOWER, STROMMER, BIESS, ANDERSON
- TRW MATERIAL PROPERTIES EVALUATION: ROSSI, ET AL, APPLIED TECHNOLOGY DIVISION'S MATERIALS LAB
- DEPLOYMENT AND DYNAMICS: ESL: CARROLL, OLDSON, ET AL
  TRW: MEISSINGER, STUART

OMV WITH 20 kW PMG TETHER SYSTEM

TRW Space &
Technology Group

- TASK DESCRIPTION
- ASSUMPTIONS
- FINDINGS
- CONCLUSIONS: ASSESSMENT OF PRACTICALITY

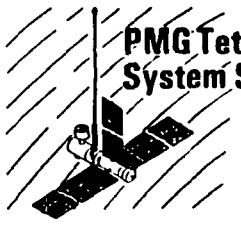

Task Description: 20 kW Tether on OMV

TRW Space & Technology Group

- Determine the top level impact on the OMV power kit to provide 20 kW of power to the PMG Tether System. Include the overall assessment of the practicality of such a design change.

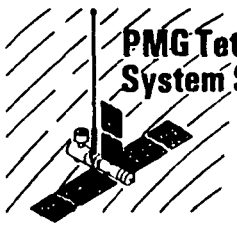

ASSUMPTIONS FOR 20 kW PMG TETHER ON OMV

TRW Space & Technology Group

- OMV POWER AVAILABLE TO PAYLOAD: < 1 kW
- POWER KIT REQUIRED TO PROVIDE 20 kW TO TETHER SYSTEM
- ONLY VIABLE POWER SOURCE AVAILABLE: PHOTOVOLTAIC ARRAYS
- SOLAR ARRAYS SIZED AT 12 W/FT^2
- THE 2 kW TRW DEPLOYMENT DESIGN WILL SCALE
- NO BATTERIES IN KIT: SUN-ONLY DUTY CYCLE

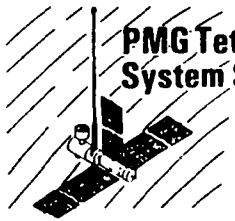

FINDINGS: OMV 20 kW PMG TETHER SYSTEM

TRW Space & Technology Group

o 20 kW SYSTEM WEIGHT (MASS) ESTIMATES:

END MASS	Weight (lb)	Mass (kg)
Plasma Contactor System (incl PWR Control Electronics)	240	109
Reaction Control System (RCS)	50	23
Structure	130	59
Tether (.81 cm diameter, 10 km)	2332	1060
Total:	2752	1251
EXPERIMENT SUPPORT EQUIPMENT		
Deployment Structure	40	18
Retrieval Reel	56	25
Plasma Contactor Assy	186	85
Power Control Equipment	200	91
Pallet	48	22
Truss	650	295
2 Solar Arrays (2 wings, 12′ x 73′ each) (incl drive assy)	448	204
Total:	1628	740

20 kW PMG Tether System on OMV

TRW

TRW Space &
Technology Group

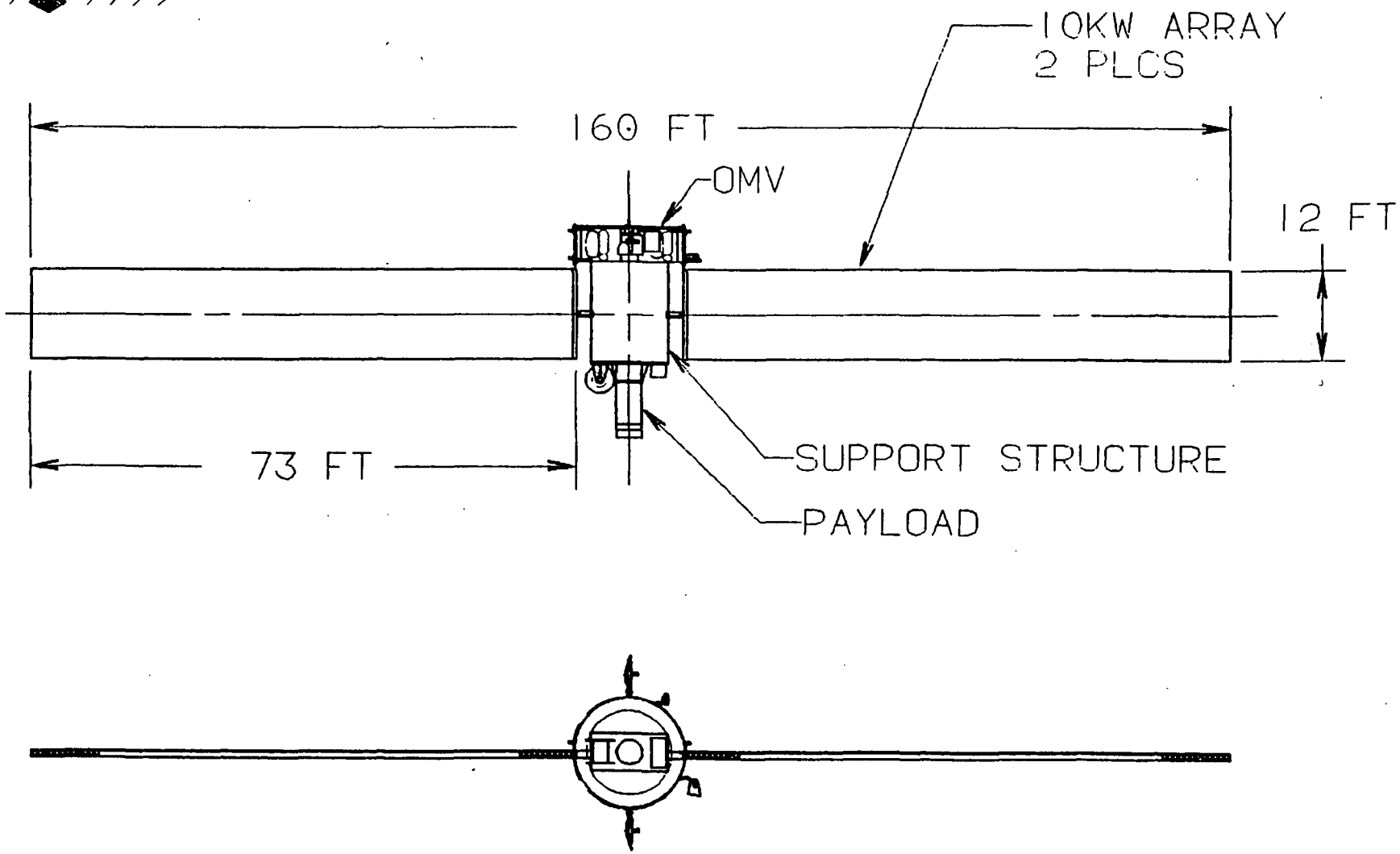

20 kW PMG Tether System on OMV
(CONTINUED)

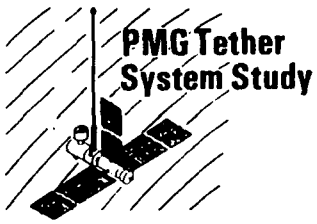

TRW Space & Technology Group

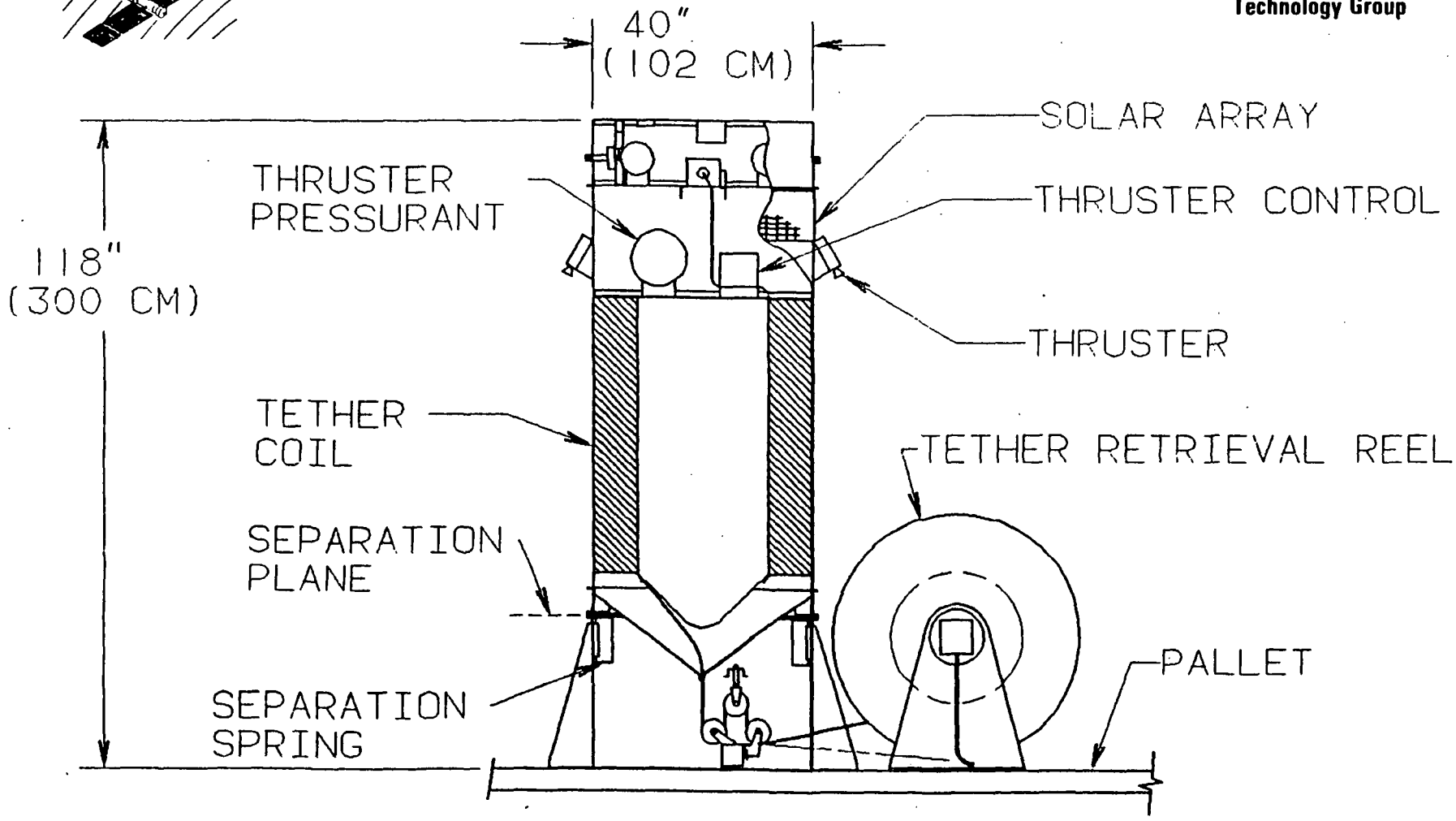

20 KW TETHER-END MASS DEPLOYMENT SYSTEM

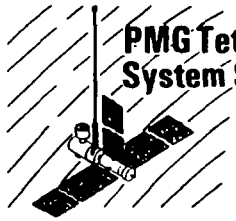

FINDINGS: OMV 20 kW PMG TETHER SYSTEM

TRW Space & Technology Group

- SYSTEM CANNOT BE LAUNCHED CANTILEVERED -- ASSEMBLY ON-ORBIT IS REQUIRED

- OMV IS WELL CAPABLE OF HANDLING PMG AND POWER KIT SYSTEM MASS

- OMV THRUST MODES WILL BE DRIVEN BY ACCELERATION LIMITS OF SOLAR ARRAYS

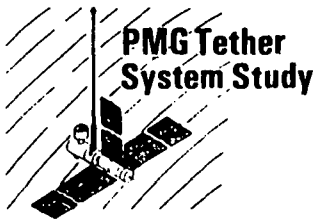

TRW

TRW Space &
Technology Group

Conclusions: Assessment of Practicality

- OMV a feasible host for 20 kW PMG Tether System
- Several technical and programmatic concerns must be resolved before further serious consideration is given:
  - -- Determine realistic stiffness for deployed solar array
  - -- Cost of Solar Array may overwhelm Tether System cost
  - -- Deployment of large tether must be studied in detail
  - -- Disposition of the large tether (retrieval or disposal) must be considered further
- Recommend deferring further consideration of this concept until smaller (e.g. 2 kW) PMG Tether System is flown or demonstrated.

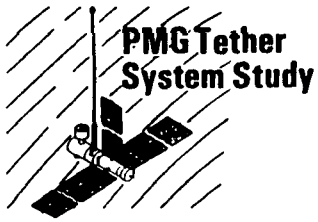

TRW Space &
Technology Group

Mechanical and Electrical Properties

- Task Description
- Findings, Conclusions

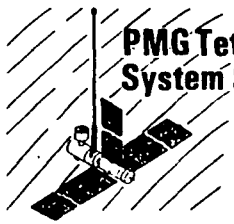

TRW

TRW Space &
Technology Group

Task Description:
Mechanical & Electrical Properties

- Determine mechanical strength and abrasion resistance of the PMG Tether.

- Determine electrical properties of the PMG Tether that may affect service performance. Determine breakdown voltage and the relationship between breakdown voltage and abrasion.

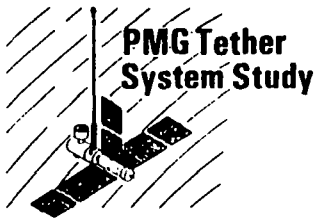

TRW Space &
Technology Group

MECHANICAL & ELECTRICAL PROPERTIES
FINDINGS AND RECOMMENDATIONS

- PROTOTYPE TETHER TESTED CLOSE TO THE CALCULATED VALUES FOR MASS, RESISTIVITY AND TENSILE STRENGTH, AND MEETS PHYSICAL PERFORMANCE GOALS

- BRAIDED CONDUCTOR RECOMMENDED TO IMPROVE TENSILE MODULUS AND TORSIONAL MODULUS

- DC BREAKDOWN VOLTAGE SIGNIFICANTLY EXCEEDED EXPECTED SERVICE VALUES

- FEP INSULATOR ADEQUATE FOR RESISTANCE TO ABRASIVE DAMAGE, SO GLASS BRAID NOT NEEDED IN ADDITION

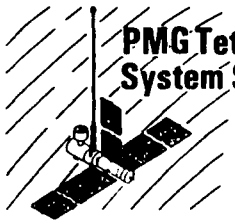

MECHANICAL AND ELECTRICAL PROPERTIES (FINDINGS, RECOMMENDATIONS--CONTINUED)

TRW Space & Technology Group

- OVERALL BASIC TETHER DESIGN MEETS OR EXCEEDS PERFORMANCE GOALS EXCEPT FOR FLEXIBILITY

- RECOMMEND CONSTRUCTION OF A SECOND MORE FLEXIBLE TETHER WITH BRAIDED CONDUCTOR FOR USE IN DEVELOPMENT TESTING

ENERGY SCIENCE LABORATORIES (ESL) TETHER MECHANICAL PROPERTY TESTS & LONG TERM PMG SIMULATIONS

TRW Space & Technology Group

- TASK DESCRIPTION
- FINDINGS, CONCLUSIONS

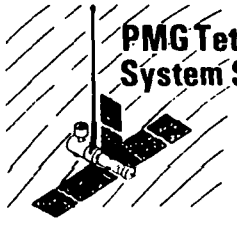

TRW Space &
Technology Group

ESL Task Description:
Mechanical Properties Tests

- Perform tests to determine tensile strength, modulus, and low frequency damping of the tether samples.

ESL Task Description:
Long-Term PMG Tether Simulations

- Study long-term stability issues using information from prior task and TRW system data. Critical issue: out-of-plane libration.

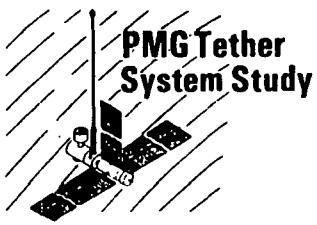

ESL Materials Testing Conclusions

TRW Space &
Technology Group

- Effective modulus at low tension is determined by 'pig-tail' stretching and is only about 2% as high as modulus at higher tension. Low modulus may be quite useful (loads on array, etc.)

- Wire 'handedness' (partly due to pig-tail) will transfer some libration energy into torsional pendulum modes.

- Damping cannot be measured with confidence on current test rig.

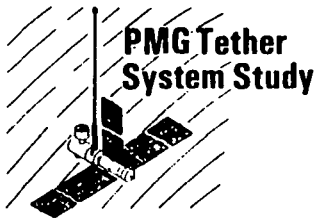

ESL Simulations Conclusions

TRW

TRW Space &
Technology Group

- Design to avoid jump-rope resonances.

- Long-term stability estimates different for GTOSS and DUMBBELL: most likely due to tether mass, extensibility, flexibility, and damping (low, but non-zero value used).

- Day-night continuous boosting has major advantages over day-only duty cycle:
  - -- 1/3 the libration amplitude
  - -- no eccentricity buildup
  - -- long-term stability less questionable

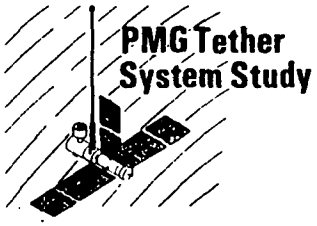

Overall Recommendations to Further PMG Tether Studies

TRW Space & Technology Group

- Continue to refine 2 kW PMG Tether System (versus upscaled systems)
- Further investigation and testing on present tether design is dictated
- Further dynamics analysis and development of system controllability strategy are needed
- Future studies should be sized to the task and funds of the investigation(s)
- Further Host-platform system analyses are needed

Interoffice Correspondence
TRW Space & Technology Group

TRW

Subject	Date	From
20 KW PMG Tether System with OMV Host Vehicle	3 May 1988	R. N. Strommer
To	**cc**	**Location/Phone**
Neal Hulkower	Dave Younkin	R11/2717 x22564

Reference: JN120488
NAS 9-17751, 1 Dec 1987
Plasma Motor Generator Contract Extension
Program, SOW Task 2.10.3

Introduction

This IOC contains the results of a brief study to define the general configuration of a 20 KW PMG tether experiment which utilizes the Orbiting Maneuverable Vehicle (OMV) as the host vehicle.

The referenced SOW task requests a determination of the top level impact on the OMV power kit to provide 20 KW of power to the PMG tether system. Since the OMV power capability is in the 1 KW range, 20 KW is impossible without a major change in design and mission for this vehicle which is now in development. Instead, this study assumes the OMV will be used as a host vehicle to provide on-orbit attitude control and communication for a self-contained 20 KW tether system.

The described configuration is a scale-up of the 2 KW system and concept 2 deployment recommended in the final report titled "Study of Plasma Motor Generator (PMG) Tether System for Orbit Reboost", dated September 1987.

This IOC includes a general description of the configuration, sizing of the solar array, a ROM weight/mass estimate and the OMV interface implications.

General Description

Figure 1 shows the overall configuration of the system on orbit before deployment of the PMG end mass. The major elements consist of a support truss structure which attaches to the payload mounting provisions on the OMV, two 10 KW deployable solar arrays and the PMG experiment (payload).

Figure 2 depicts the deployment concept (concept 2 of the final report) sized to accommodate the more massive tether. In this configuration the tether is housed in the end mass as it moves away from the host platform. The end mass is ejected from its base by releasing a clamp at the separation joint and preloaded spring actuators impart the initial velocity. Initial momentum will overcome tether friction until the increasing gravity gradient forces are enough to do the job. An RCS system offers attitude control for the end mass if needed and a backup force for tether payout.

Tether Description

The tether is 10 kilometers long and .32 inches (.81 cm) diameter. Its cross section geometry is similar to that defined in the final report consisting of a kevlar core with stranded aluminum wire (equivalent to a #2 conductor) surrounding it with an outer insulation and protective wrap. The weight is 2332 lbs. (1058 kg). This information is from R. C. Rossi, x64105, and he considers the diameter to be somewhat optimistic.

Power System Description

The power system was assessed by J. J. Biess, x63494, and is a scaled-up version of the one described in the final report except it has no batteries so it works only in the orbit boost mode. The reverse (orbit brake) mode has not been assessed but batteries required to absorb the power would cause a significant weight penalty. The power system is contained in four (4) 5 KW modules obtaining 120 VDC from the solar array. Each box is 16x20x5.5 inches high and, assuming 94% efficiency, dissipates 320 W per box for a total of 1250 W. Each box weighs 50 lbs.

Solar Array

The solar array area was determined using 12 W per ft^2. This value was chosen after a survey of other array systems and a phone consultation with R. M. Kurland, x50905. Mr. Kurland said this is an achievable output for a system to be used for one year or less in low earth orbit.

A flexible blanket wing using the astromast deploy method was chosen because there is some test and space experience for this scheme. It is also a weight efficient system. Weight and size were arrived at using configuration information from the "Advanced Photovoltaic Solar Array Design" final design review (TRW report 46810-6003-UT-00, dated June 1986, prepared for JPL).

The wing dimensions are 12x73 ft including several non-power producing leader panels in the folding blanket array. The weight of one wing is 224 lbs including deployment hardware and solar array drive.

Weight Summary

	Weight (lb)	Mass (kg)
END MASS		
Plasma Contactor System (incl PWR Control Elect)	240	109
RCS	50	23
Structure	130	59
Tether	2332	1060
TOTAL	2752	1251
EXPERIMENT SUPPORT EQUIP		
Deployment Structure	40	18
Retrieval Reel	56	25
Plasma Contactor Assy	186	85
Power Control Equip	200	91
Pallet	48	22
Truss	650	295
2 Solar Arrays (incl Drive Assy)	448	204
TOTAL	1628	740

OMV Interface

The OMV electrical interface is not yet fully defined. However, a connector is planned on the forward face which will provide power and communication circuits to be utilized by the OMV payload. The truss will be mechanically secured to the OMV forward face using bolt-on provisions for cantilevered payloads.

The overhanging mass of this experiment and its support hardware exceeds the OMV launch mode capacity by a factor of 6. This will require the system to be separately supported on the shuttle orbiter during launch then joined to the OMV on orbit. This situation is common to other projected OMV payloads and there will be developed methods for the joining operation.

The moment of inertia of the experiment and its support system is approximately 50,000 slug-ft^2 about the OMV center. This is well within the OMV capability which is designed to handle much larger mass systems on orbit.

Conclusions

It appears that a 20 KW tether experiment and its support hardware can use the OMV as a host vehicle. the OMV function would be to provide initial orbit location then attitude control after tether deployment. Primary power is furnished by the experiment support subsystem.

Several issues should be investigated before proceeding much further with this concept.

1. Determine a realistic stiffness for the deployed solar array analyze the effects of OMV thrust modes on orbit. This will require some understanding of the dynamics of the deployed tether on the system.

2. Define a development plan for deployment of this large tether. It would appear that considerable analysis and testing is required to determine feasibility.

3. A solar array of this size is feasible since there has been some analysis and testing done including deployment from the shuttle orbiter. However, this would not be an "off-the-shelf" subsystem and the cost of procurement of this space station technology system must be considered. It may overwhelm the cost of the experiment.

4. A decision should be made regarding disposition of the tether at the end of the experiment. Can something of this nature (.32 inch dia. x 10 km) be left as space debris? What are the operational problems associated with retrieval and what would be the cost of the retrieval system?

ORIGINAL PAGE IS
OF POOR QUALITY

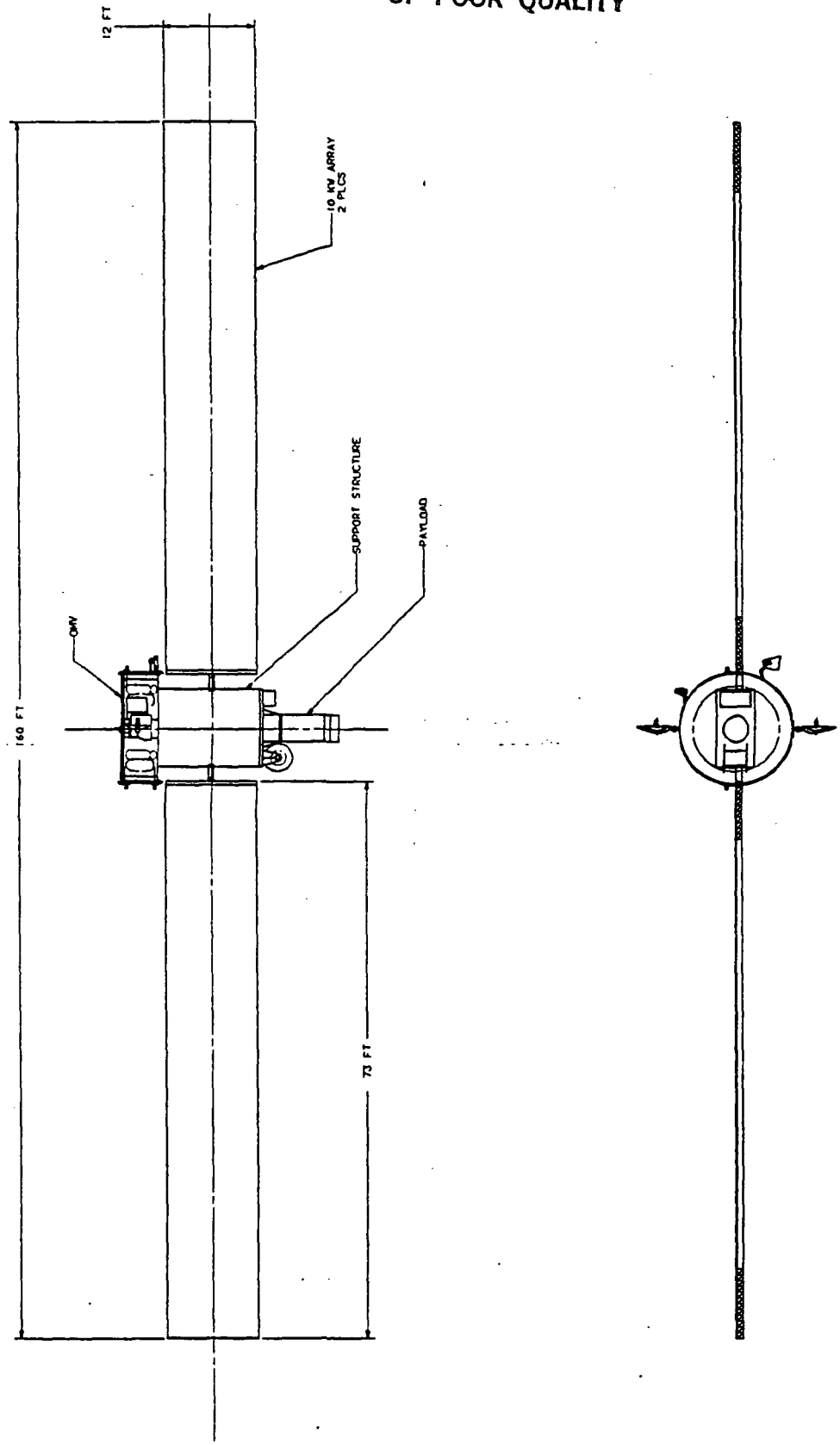

FIGURE 1

ORIGINAL PAGE IS
OF POOR QUALITY

STROMMER

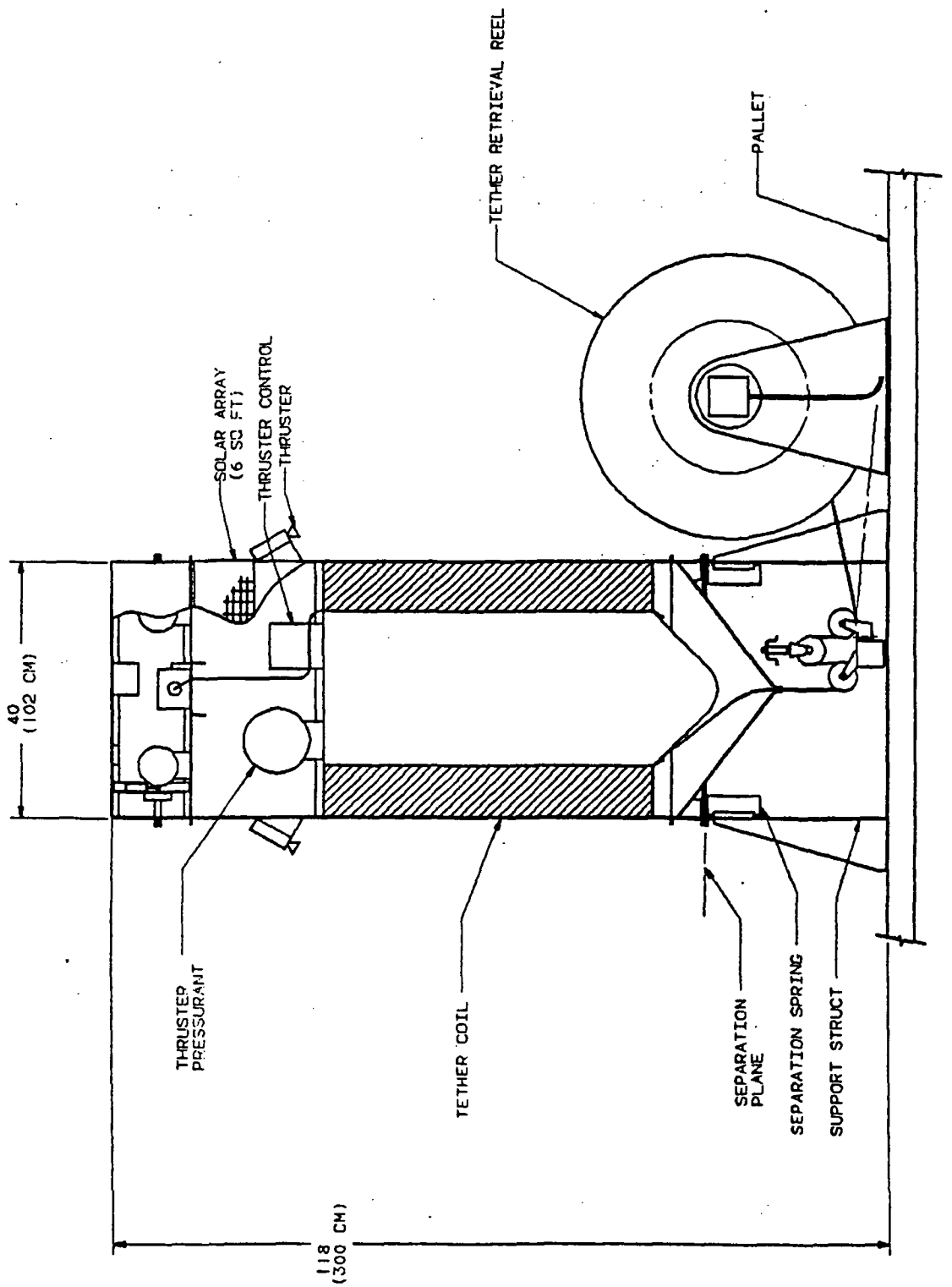

20 KW TETHER-END MASS DEPLOYMENT

FIGURE 2

Task 2.8.2-3 Tether Characterization

The manufacture of 1100 ft (335 m) of cable has been described in the Final Report[1] and its ground-based evaluation is described in this task. As explained in the Final Report, the constraints of time and manufacturing limitations on a small batch order required alterations to the design. Two major design changes were made: (1) the counterwinding of approximately equivalent proportions of the aluminum conductor to provide torsional balance was not done, and (2) the glass braid providing abrasion resistance and additional strength was not provided. Additionally, a 1.5 mil thick Kapton tape was wound about the conductor onto which a layer of FEP 8.0 mils thick was extruded.

In spite of the structural differences of the alternative design, several important cable characteristics could be determined relating to both materials and design. The absence of the glass braid gave the cable considerably more flexibility than that obtainable from the original design. From the point of view of the cable's dynamic mechanical response it would be desirable to eliminate the braid from the design. The alternative design provides the opportunity to evaluate the breakdown voltage, abrasion resistance and cable strength without the braid. Additionally, in contrast with other space tether designs, the conductor in the PMG design represents a major contributor to the dynamic response of the cable. The co-wound conductors provide a measure of the extent of mechanical anisotropy that can be built into the cable.

The tests presented in this section were selected and designed to provide data describing critical property performance of the cable. These properties are electrical, mechanical and abrasion resistance. The electrical tests include resistivity that define power losses, and breakdown voltage defining the dielectric effectiveness of the FEP insulator. Mechanical properties include both tensile and torsional modulus and tensile strength all of which determine the dynamic performance of the cable as well as its play-out characteristics. The abrasion tests describe the resistance of the outer layer to abrasion and were designed to relate to the effect an abrasive exposure may have on the breakdown voltage.

Mass

A measured length of cable (nominally 2 ft) was weighed on an analytical balance and from these measurements the expected weight of 10 km length was calculated to be 139.0 kg. The cable was then dissected and each component weighed individually. These weights are compared in Table 1 against the weight expected from the design of the cable.

Resistivity

The length of the cable was measured with a surveyor's tape (1107.71 ft), the resistance was measured with a Keithley 175 Autoranging Multimeter (3.061 ohms). The calculated resistivity was 2.763 ohms/1000 ft. which compares with a value 2.727 ohms/1000 ft calculated from the expected single conductor resistivity. The higher resistivity reflects the increased length of twisted wire over that of a single conductor of the same cable length. This value is reflected in an increase in conductor weight as well.

The measured cable resistance projects to a value of 90.7 ohms/for a length of 10 km whereas the expected resistance of the concept design[2] (#12 AWG, single conductor) is 86 ohms. The difference between these values is the consequence of a reduced wire cross section demanded by the constraints of the cable construction and by the increase length caused by the wire twist. The increased power loss (I^2R) over that of the concept design is less than 0.005 KW and affects the overall expected efficiency of the cable by less than 0.25%.

Compression Tests

A segment of cable was placed between platens in an arbor press and a load was applied until electrical contact was made. When the platens were 2" square blocks the load was 1500 pounds force. When one platen block was replaced with a 3/4" dia half cylinder block, the load measured on two segments was 1200 pounds force and 950 pounds force.

Tensile Strength

The strength of the cable was measured on an Instron mechanical testing machine at a cross-head rate of 0.05 in/min. Insulation at both ends of cable segments were stripped back, the conductor wires and Kevlar core were flayed and both ends were potted in epoxy to fabricate test sample having nominal 3" gage lengths. Failure of the cable was defined by failure of the Kevlar inner core. The distribution of strengths are presented in Table 2. By using an expected minimum strength for the Kevlar of 400 Ksi, a cable strength of 125.6 pounds was calculated. The average value of 139.5 pounds force for 5 measured lengths is in excellent agreement. The standard deviation of these measurements is 7.5 pounds force.

Tensile Modulus

The tensile modulus was calculated from the linear (elastic) portion of the stress-strain curve obtained from the cross-head displacement. The tensile modulus of a monolythic cylinder calculated for the cable from this method is 1.47×10^6 psi. By using the rule of mixtures for elastic moduli and assuming that the Kevlar core is fully loaded, the calculated effective modulus of the aluminum conductor is 1.07×10^6 psi, about 10% of its elastic modulus.

Torsional Modulus

The torsional modulus was measured on a Rheometrics Dynamic Analyzer by a method modified to account for the anisotropic properties of the cable. A short length of cable was prepared for the test by stripping back the insulator from both ends, flaying the conductor wires and Kevlar, and potting both ends in an epoxy resin. After curing, the epoxy ends were trimmed to fit the instrument grips. The tests were conducted by afixing one end to a stationary grip and measuring the torque necessary to rotate the other end to selected angular positions. The torsional modulus is calculated from the following equation for both right and left hand rotation and assumes the cable behaves as a monolythic cylinder.

$$G = \frac{Tl}{JO}$$

where T is the torque, 1 is the gage length, J is the polar moment of inertia and O is the angle of rotation. The term 1/J are constants of the test specimen so that the torsional modulus is a function of the torque to angle ratio.

Three specimens were tested with this method and the results are plotted in Figure 1. The data extrapolated to O degrees show that the modulus for left-hand torsion (with conductor twist) is 1.89×10^5 psi, 20% greater than for right-hand torsion (counter twist to conductor) which has a value of 1.57×10^5 psi.

Abrasion Tests

The abrasion tests were conducted by the cable vendor (Brand Rex, Div of Brintec) by two different methods. The first method was in accordance with MIL STD C 915 for cable insulation. In this method a segment of cable is fastened at one end to the machine's frame and to the other end is fastened a weight. The cable is draped over a rotating wheel onto which 2 knife edges are diagonally fastened. A low voltage DC bias is applied to the cable conductor so that the rotation will stop when the knife edge abrades through the insulation and makes electrical contact with the conductor. Abrasion resistance is measured by the number of revolutions as a function of load.

The second method is one developed by the General Electric Co. (called the GE method) and is similar in that the abrasion resistance is also measured by the number of revolutions as a function of load. However, in this test a section of cable is clamped to a supporting plate onto which a knife edge attached to an eccentric cam is made to oscillate. The knife edge is loaded with weights and is counted as complete back and forth cycles. The machine stops when electrical contact through the knife edge is made.

The relationships between revolutions or cycles and load is presented in Figure 2 and Table 3. The expected relationship is logarithmic as observed at loads greater than 2 lbs (1000 g) but fails at lower loads. The change in this relationship is the result of a change in failure mechanism. In this case, the low friction coefficient of the FEP insulator appears to contribute to knife edge sliding at low loads. Additionally, there appears to be evidence of cold flow that deforms the insulator and thins the insulator wall under the knife edge. Cold flow occurs from repeated load exposure; at low loads only cold flow appears to be operating and abrasion does not appear to occur until loads of 2 lbs or greater are applied.

Breakdown Voltage

The breakdown voltage was measured in both AC and DC potential fields. A 250 ft length of cable was passed through a 3500 VAC spark tester and the test was repeated at 10,000 VAC. The DC/AC breakdown relationship is 2.8 so that the comparable exposure to a DC potential would be 10 KVDC and 28 KVDC, respectively. The test was performed to verify manufacturing quality and to assure suitable performance criteria were met. No failures were experienced in these tests.

The DC voltage breakdown test was conducted on a loop of cable immersed in a 5% NaCl solution. The exposed ends of the cable were connected to the DC potential source, the solution was connected to ground. The DC voltage was raised at a rate of approximately 1 KV/sec and the maximum value was observed on a voltmeter. Two tests were conducted giving values of 44 and 50 KVDC. These values are significantly greater than the expected service values and provide confidence that a 10 mil layer of FEP/Kapton is adequate to meet the insulation requirements of the tether application.

After the test, the cable was cut at a distance of about 1 inch on both sides of the point of breakdown and the conductor was removed from the FEP shell. A careful cut was made through the remaining shell (including the Kapton overwrap) at a distance of about 1/16 inch away from

the point of breakdown which allowed the measurement of wall thickness at that point. The 50 KVDC sample had an insulator wall 9.5 mil thick, 8.0 mils of FEP and 1.5 mils of Kapton. The 44 KVDC sample had an insulator wall thickness at the point of breakdown of 10.5 mils, 7.5 mils of FEP and 3.0 mils of Kapton (overlapped layers).

Abrasion/Force Tests

The tests to measure the force required to cause abrasion was conducted on an Instron mechanical testing machine. A fixture was designed that contained a 0.120 inch hole through which the cable was pulled by the crosshead of the machine. The fixture contained a knife blade with a sharp edge (22° angle) that was positioned perpendicular to the cable and extending into the hole so as to remove a chord segment of insulation as the cable was pulled through the hole. The remaining thickness of cable was measured and plotted against the force required to remove the chord segment in Figure 4. The origin of the graph is the average diameter of the cable which was found to vary only a few tenths of a mil along the length measured. The linear relationship is a reasonable representation of the data.

Abrasion/Voltage Breakdown Tests

In order to evaluate the effect of abrasion on the breakdown voltage, segments of cable weighed with 1 pound load was subjected to 5, 7, 10 and 15 revolutions on the MIL STD C-915 test and the DC breakdown voltage subsequently measured. The results are presented in Table 4 and Figure 3. Also plotted are expected curves for 2, 3 and 5 pound loads with absicca values taken from Figure 2.

A second series of tests were conducted by exposing segments of cable to 400 oscillation cycles under a 500 g load on the G.E. test and subsequently exposing the cable to DC breakdown voltage. The results are presented in Table 4.

The reduced diameter at the abraded regions of test samples from both tests were measured at the point of breakdown and their values are plotted in Figure 5. A consistent relationship exists with the origin representing the interface between the Kapton and FEP. Also plotted on Figure 5 is the diameter of the cable measured perpendicular to the chord. The inverse relationship between perpendicular and parallel diameters suggests that standard abrasion tests on FEP insulation promoted a cold flow deformation rather than true abrasion. Nevertheless, the breakdown voltage is sensitive to the remaining thickness of insulation as shown on the left of the figure whether the action was from abrasion or from cold flow.

Discussion

The tests described in this section provide characterization data for critical properties of the cable that would be expected to affect its performance in the PMG tether application. Physical parameter goals such as weight, and diameter have been met; also the cable resistance meets our objective. It has sufficient strength to handle all forseeable loads placed upon it with adequate margin. The high tensile modulus and anisotropic torsional modulus are sure to affect its performance in space. Both of these properties can be improved by using braided conductors.

The abrasion tests are particularly valuable because they reveal whether the glass braid reinforcement originally designed for this cable is necessary. The data show that voltage breakdown values provide a high level of margin. Concern for abrasive damage that may degrade the insulator so as to compromise this performance was the basis for these tests. The maximum expected load on the cable is less than one pound force (5.1N ~3/4 lb). If the cable should become snagged against a sharp edge the data suggests that the low friction coefficient will allow the cable to pass undamaged. However, if we project a worse case scenario where the load is 2 pounds and the edge is a knife edge, Figure 4 shows about 0.002 inch of insulation can be removed and Figure 5 shows a breakdown voltage of 35 KVDC still provides comfortable margin. These data establish the adequacy of the FEP insulator without a glass braid thus reducing both rigidity and weight from the design.

Table 1. Mass Properties of 10 Km Cable

	Design	As Measured
Kevlar	3.3 kg	3.41 kg
Aluminum	87.2	87.80
Kapton	-	7.00
FEP	47.2	40.79
Total	137.7 kg	139.00 kg

Table 2. Cable Strength in Tension

Test	Load, lb
1	140.5
2	133.0
3	137.0
4	152.0
5	135.0
Ave.	139.5
S.D	7.5

Table 3. Abrasion Test Data

Test Method	Load	Revolutions/Cycles	Average
M.S. C-915	20 lb	1/2	
	10	1/2	
	5	1	
	3	3 1/2	
	2	9	
	2	4 1/2	
	1	35	
	1	49	
	1	22	31
	1	19	
	1	32	
G.E. (0.005 wire Tip)	500g	>7135	
(0.001 wire Tip)	500	126	
		64	72
		66	
		32	
(0.005 chisel Tip)	500	1188	
		476	1245
		1966	
		1350	
	1000	33	
		49	42.5
		66	
		22	
	1362	21	
		18	16
		16	
		9	
	1500	12	
		7	10.5
		11	
		11	

Table 4. Abrasion - Breakdown Voltage Relationship

Test	Load	No. of Cycles/ Revolutions	Breakdown Voltage (DC)
M.S.C-915	1 lb	5	22K
	1	5	19K
	1	7	16K
	1	7	14K
	1	10	12.5K
	1	10	12.5K
	1	15	0.5K
	1	15	7K
GE	500g	400	40K
		400	42K
		400	18K
		400	51K
		400	15K

Torsional Modulus

Figure 1 MODULUS OF RIGIDITY OF PMG Experimental TETHER

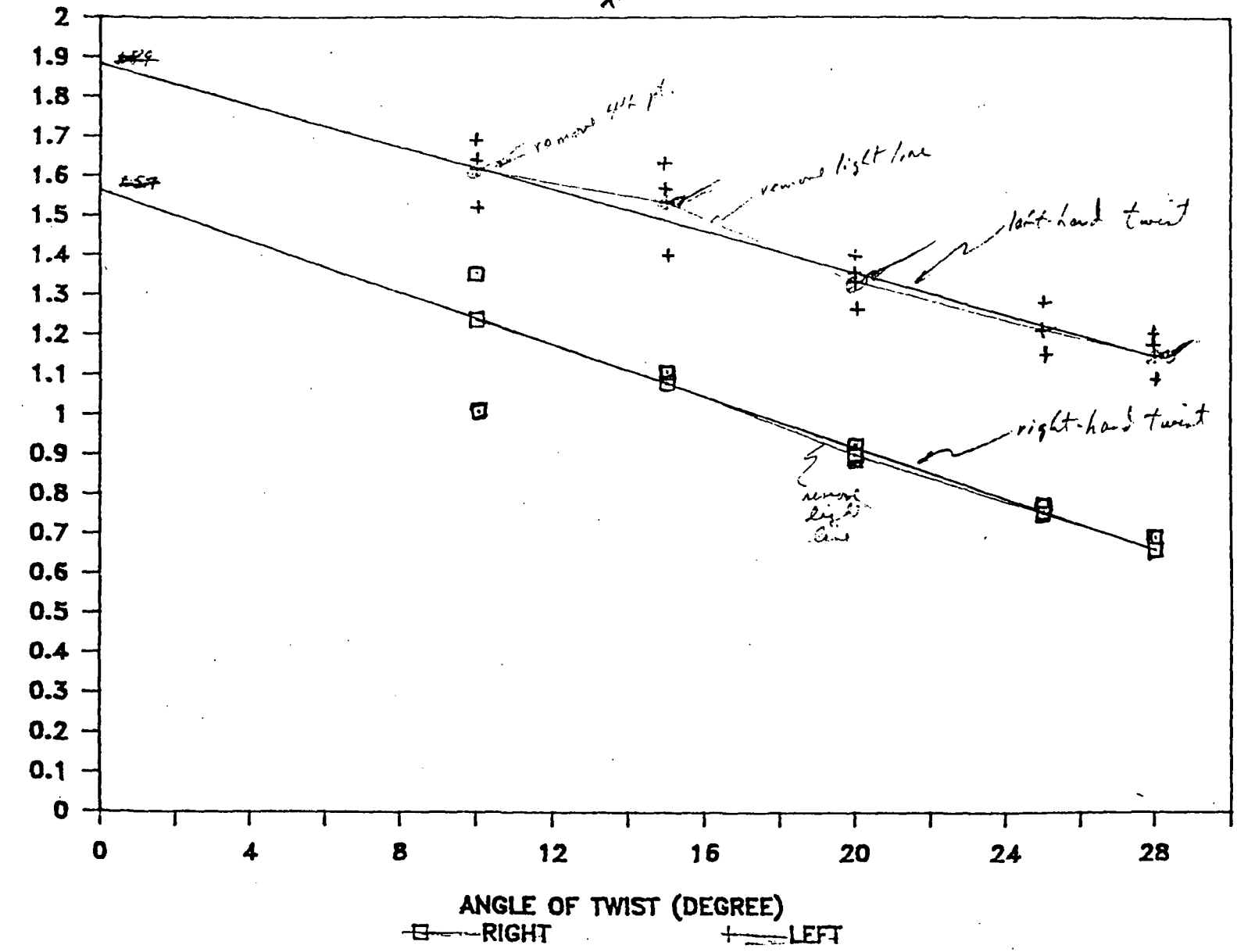

Fig. 2 Abrasion Resistance of ~~BMC Tether~~ Experimental Cable

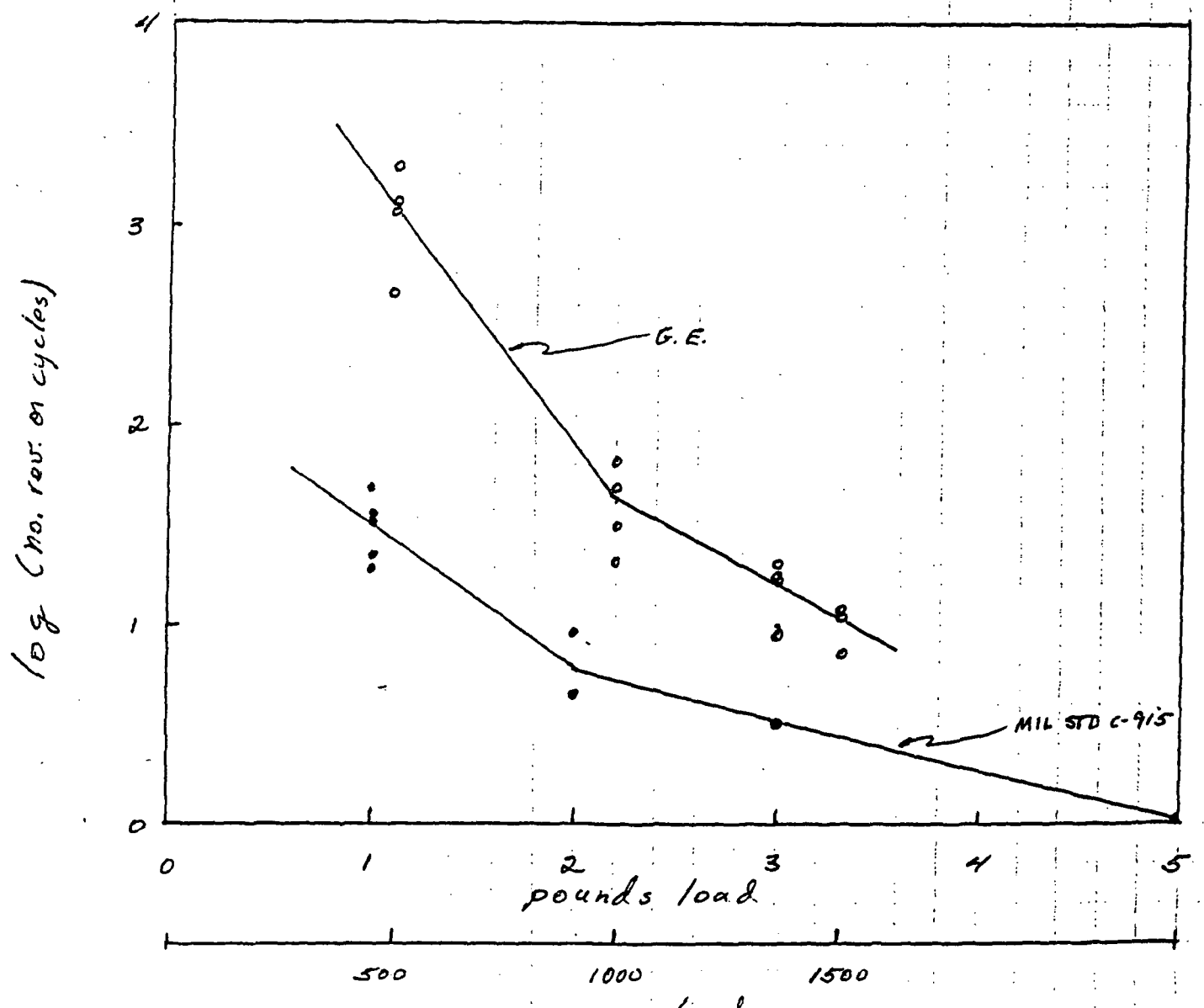

Fig. 3 Effect of Abrasive Exposure on Breakdown Voltage

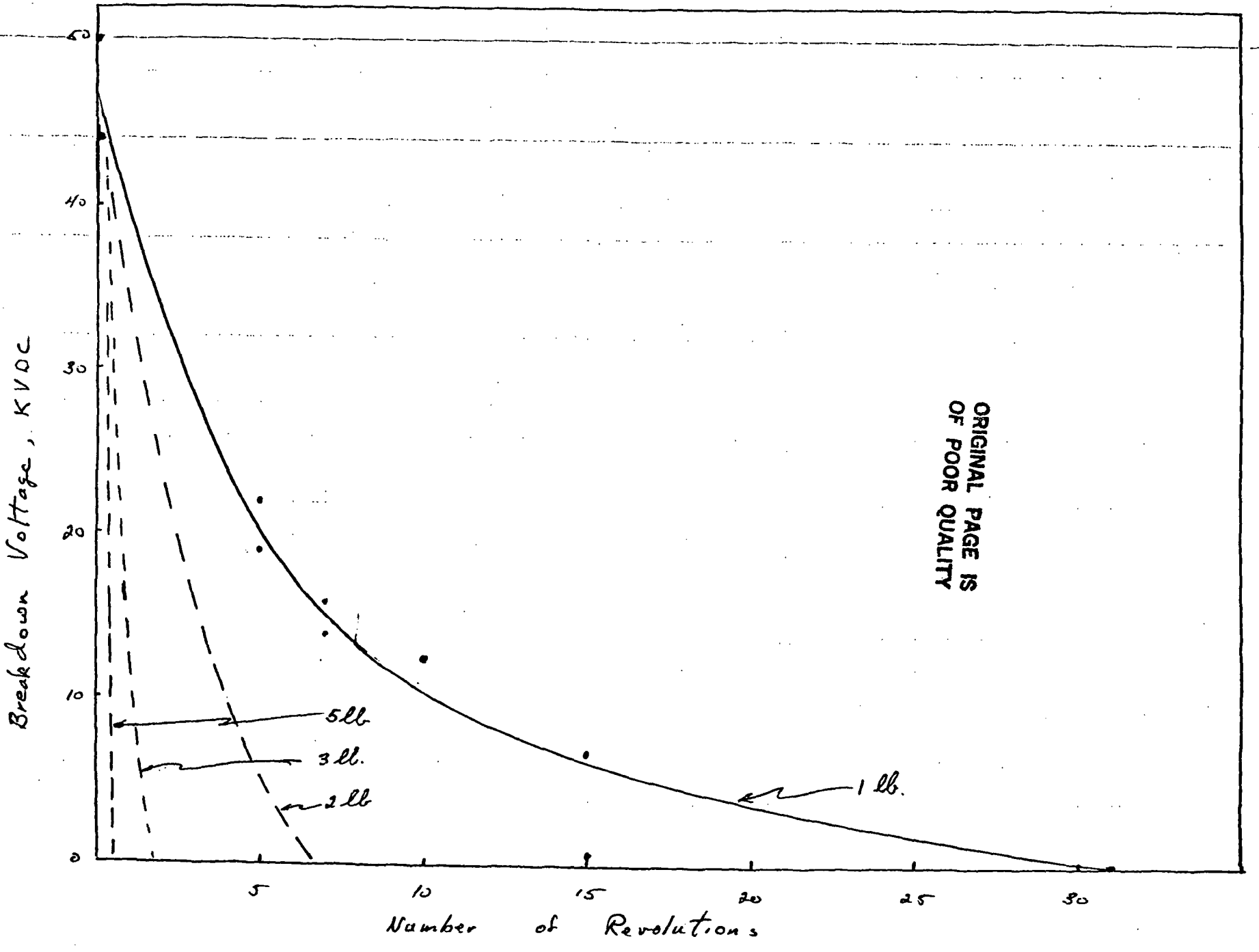

Fig. 4 Force Required to Remove Chord Segment from Cable

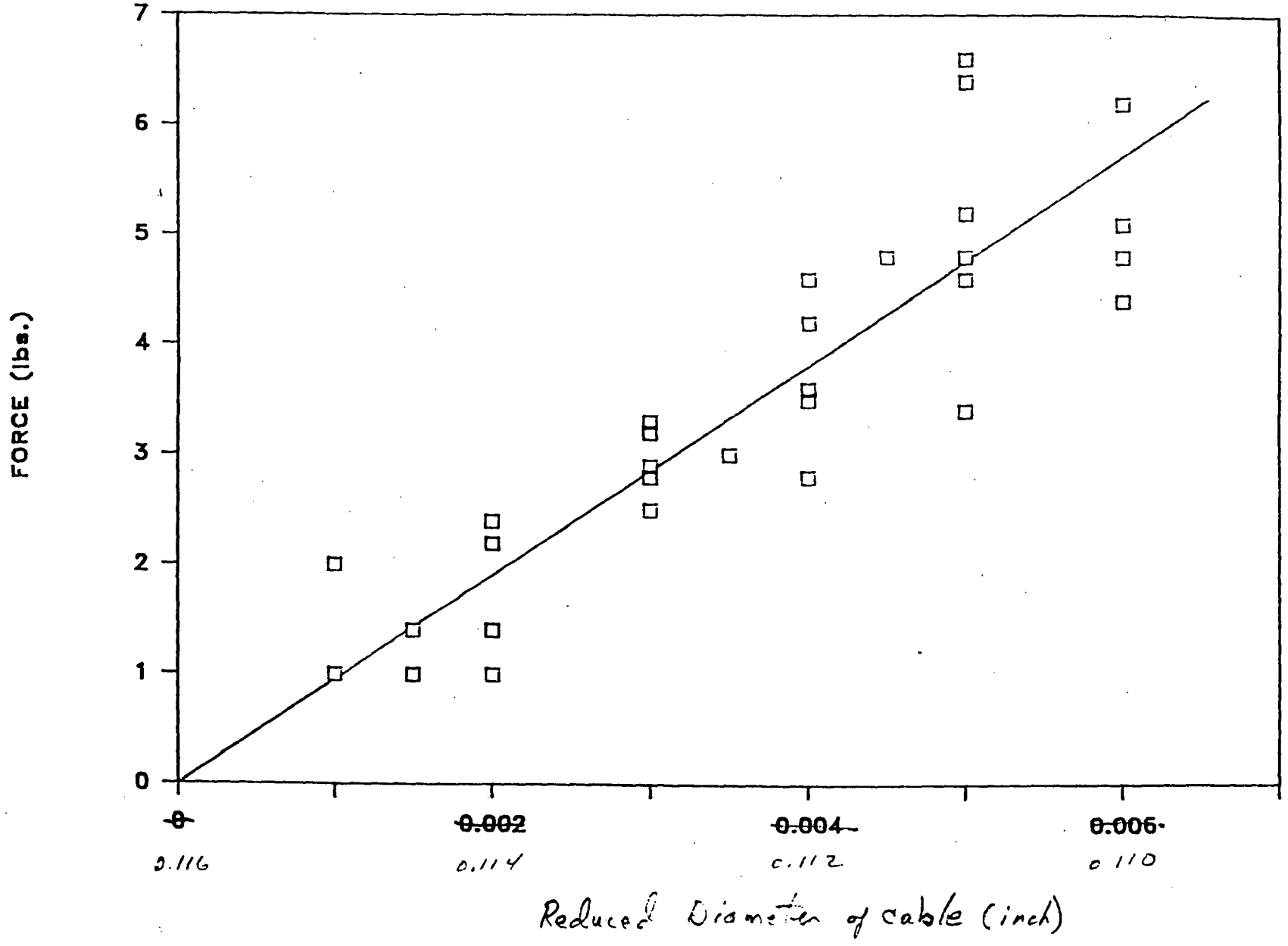

Figure 5. Relationship Between Breakdown Voltage and Cable Diameter

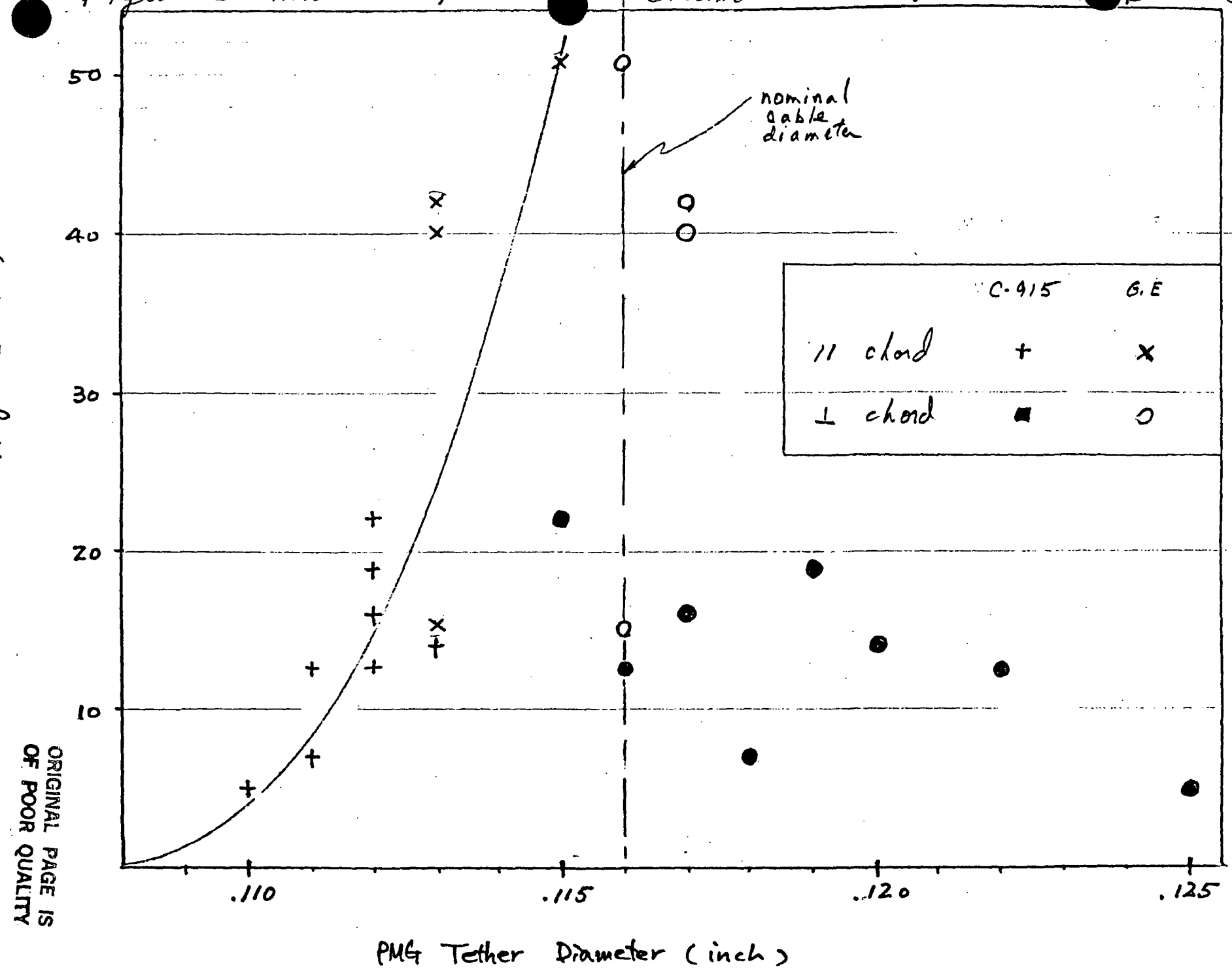

ESL REPORT TO TRW ON ELECTRODYNAMIC TETHER STABILITY

Joseph A. Carroll
and John C. Oldson
June 3, 1988

This report summarizes work done by ESL for TRW under purchase order DJ7201NB85, as a subcontract to contract NAS9-17751 between TRW and the NASA Johnson Space Center.

ESL's work covered the following areas:

Tether mechanical property tests (Task 4.2)
Long-term PMG Simulations (Task 4.3)

ESL personnel on the project were:

J.A. Carroll (tether tests and "dumbbell" simulations)
John C. Oldson (GTOSS simulations)
Matt Nilsen (test sample preparation).

In addition, our consultant David Lang of Lang Associates prepared a videotape of selected GTOSS runs of the PMG system.

Task 4.2: Mechanical Property Tests of Electrodynamic Tether

We prepared long and short tensile test samples with epoxy-potted terminations from the sample of electrodynamic tether provided to ESL by TRW and performed various tests at room temperature (24C). The sample preparation technique, test techniques, results, and our observations on the test results are described below.

Test sample preparation

The intended focus of these tests was damping. This requires a termination technique which minimize slippage and creep, plus a long enough sample length that intrinsic tether lossiness can be seen above the residual termination creep. We made two samples using tapered potted terminations as shown in Figure 1. One test sample was the longest that could be tested on our tester (2.7 m), and the other was about the shortest that could be tested (0.18 m). As shown in Figure 1, the insulation was removed over most of the termination length and the wires flared apart. Then the flared end was dipped in epoxy and pulled into the tapered bore of the termination, until the flared wires filled most of the bore, with only 1 cm of insulated wire remaining in the bore.

Tensile damping tests and results

The tests were done on an 2.7 meter long horizontal tensile tester fabricated in-house for other tether-related work. The tester uses a linear actuator with a 45 cm stroke, and a 4500 newton load cell based on 4 strain-gauges wired in bridge fashion. We mounted the sample on the tester, slowly stretched the sample until desired tension levels were reached, and then turned the actuator off to allow creep-relaxation of tension at constant length. Then the actuator was reversed to reduce the tension on the tether.

This procedure was done with both the long and the short sample, so we could separate termination effects from the intrinsic tether properties. We found that the shorter sample experienced significantly higher relaxation under tension. This indicated that residual termination-related effects were significant enough that we could not have much confidence in such tests.

Low-tension tests to characterize "pigtail" effects

The damping test data showed an interesting feature at low tensions (of order 4 newtons or 1 lb). The tether retains enough of a memory of its coiling pattern that the "pig-tail" effect radically lowers the effective modulus at such low tensions.

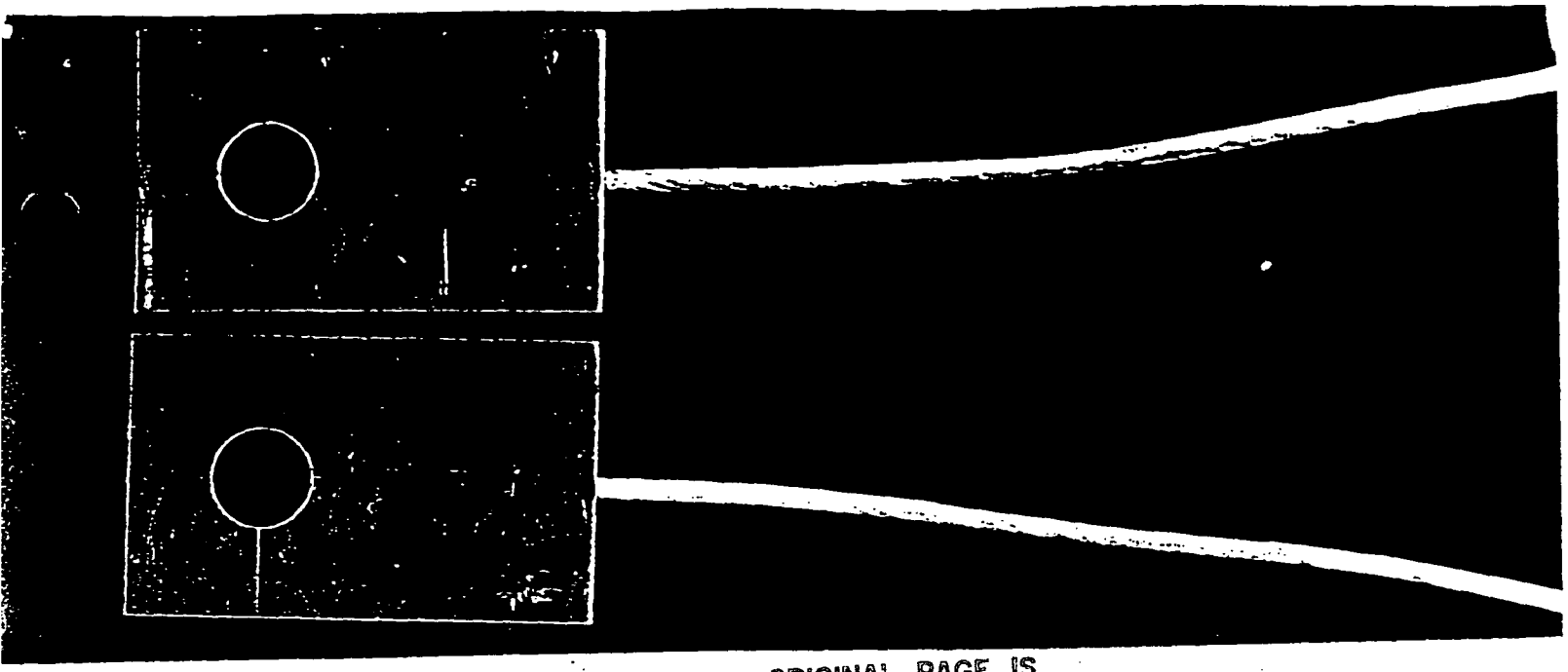

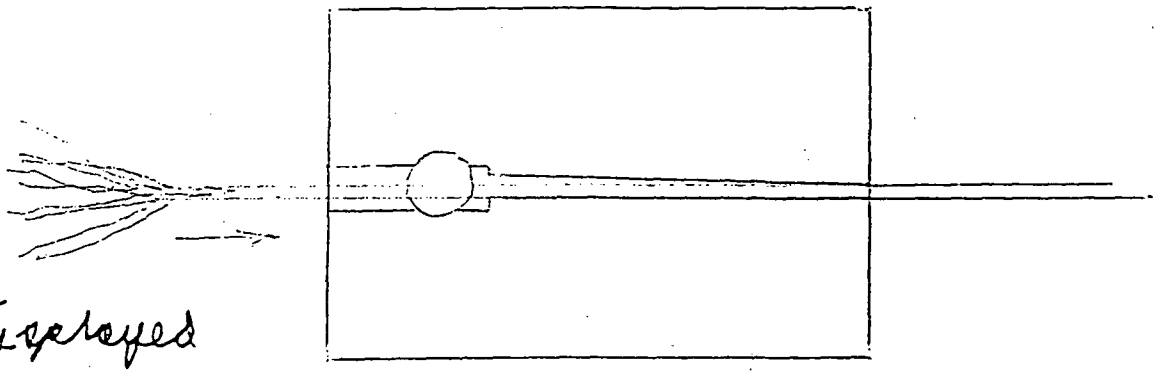

1) End is sleeved

2) End is dipped in epoxy

3) End is pulled into taper-reamed hole, until fairly tight.

4) Epoxy cured

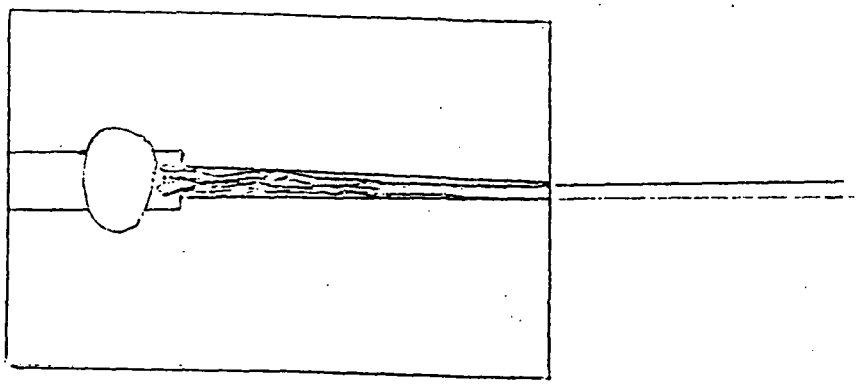

Figure 1. Epoxy-potted terminations

To make sure that the low modulus was not due to test artifacts, we made several minor changes in the test setup and repeated the tests. We did tests with the long and short samples, and the results assured us that the effect was not termination-related: the low-modulus region was much shorter with the short sample.

We also added supports just under the tether load path. This minimized catenary loads which would introduce a similar non-linear stress-strain relationship at low tension. (With somewhat more effort, we could re-orient the tester to the vertical to entirely eliminate this artifact.)

To further verify that the low-modulus region was mainly due to pig-tail effects, we manually straightened the tether so that the residual pig-tail effects were very small, and then re-tested it. Finally, we re-introduced a pig-tail by winding the tether on a small (0.127 m diameter) cylinder. We imposed one twist per turn in winding it, as would be done in winding tether for a SEDS-like deployment. We then unwound the tether and tested it again. The results are shown in Figure 2. The before and after "pigtail" tests (a and c) show a much larger low-modulus region than the "no-pigtail" test (b).

Discussion

If the PMG endmass weighs about 90 kg and a 10 km PMG tether 140 kg, the equilibrium gravity-gradient tether tension is about 4 newtons (1 lb). This means that the tension during the PMG mission will be well within the low-tension non-linear stress-strain region shown on these tests, unless a far more flexible tether is used. The effective modulus near 4-5 newtons tension (the tangent modulus) is only 2% as large as in the steep nearly-liner portion of the load curve. This is enough to increase the period of the fundamental longitudinal "bobbing" mode from about 80 seconds to 600 seconds.

Because of the rapidly changing modulus in the few-newton tension range, increasing the endmass (which increases tether tension and system stability) is likely to decrease the bobbing period rather than increase it.

Tests of Torsional Stiffness and Equilibrium Twist

We also tested our long tether sample to determine torsional stiffness and torques introduced by load changes. These tests were done with the long (2.7 m) sample. The tether was hung vertically by clamping one termination to an overhead HVAC duct flange. A 100 gram plastic bar 1.27 cm in diameter and 62 cm long (with 18 cm radius of gyration) was inserted through the transverse mounting hole at the lower end of the tether. The average tension along the tether length was about 2 newtons.

Figure 2a

TRW
PMG wire
With
pigtail
(as supplied)

2.7 l/m sample

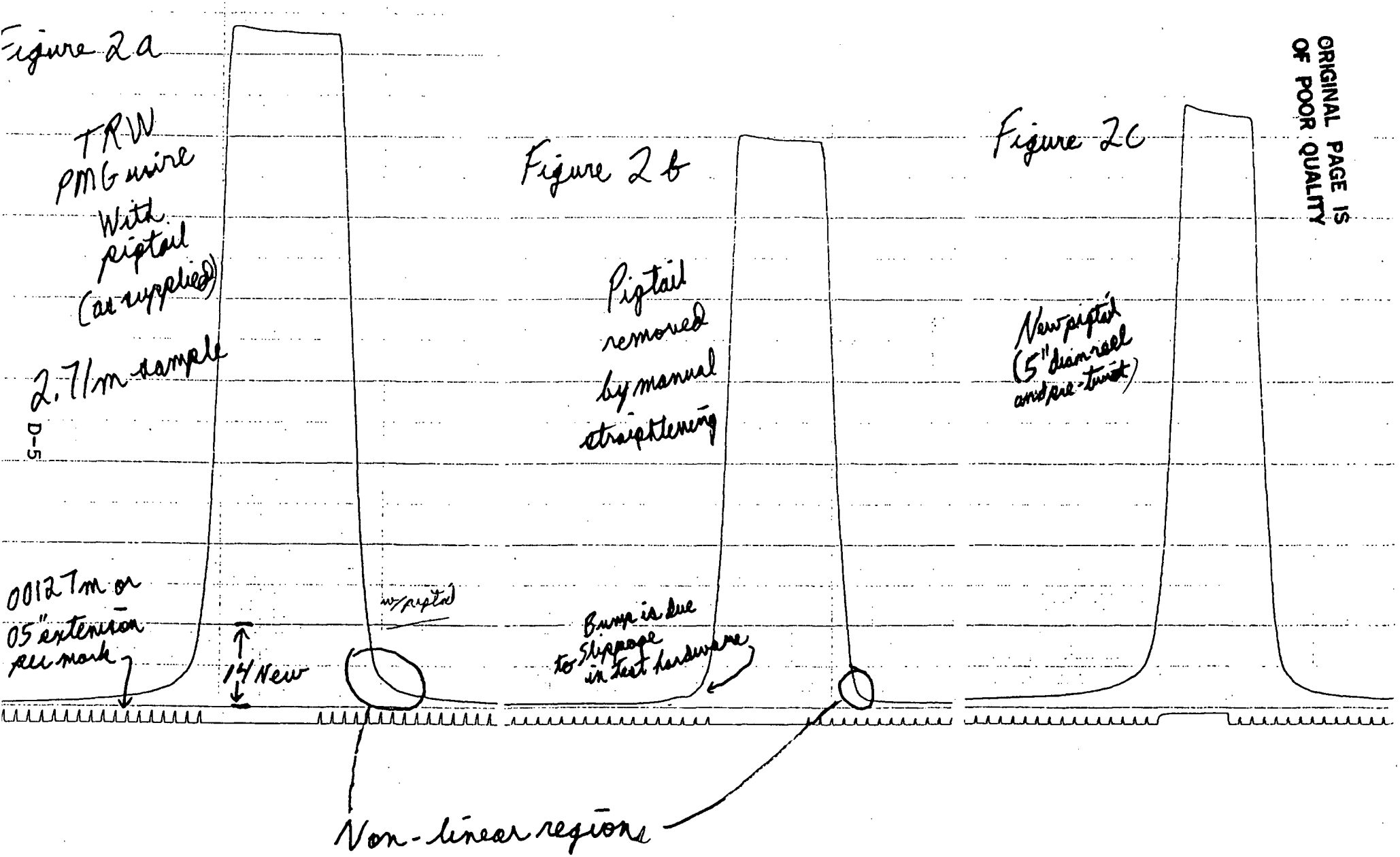

Figure 2b

Pigtail
removed
by manual
straightening

Figure 2c

New pigtail
(5" diam reel
and re-twist)

We then rotated, held, and released the bar. The torsional pendulum period was 4.3 seconds when the tether was straight, and 4.5 seconds when a moderate pigtail effect was re-introduced as described in the previous section. Thus as might be expected, the torsional stiffness is far less dependent on pigtail effects than the axial stiffness is.

If we assume a 90 kg endmass with a radius of gyration of 30 cm, the period for PMG endmass torsional oscillations will be Sqrt(90/0.1 * 10000/2.7) * 30/18 times as long as in our test, or about 13,000 seconds. Since this period is about 2.5 orbits, the resulting torsional oscillation behavior will be strongly affected by the once-per-orbit rotation of the tether system.

We also tested the tether to determine whether a small load change caused a change in the equilibrium twist. Such a change could drive torsional oscillations. We clipped a small weight (66 grams, or 0.65 newton) to the bottom of the tether. Careful marking of the bar orientation allowed us to determine that the load change caused the tether to twist about 1.3 degrees when the tether was straight, and 1.8 degrees when it had a pigtail. Such a load change is comparable to that caused by a few degrees of in-plane libration. Based on this, over a 10 km length, a 1 newton variation in load will cause a change of 20-28 turns in the tether's "zero torque" twist.

It is possible that thermal effects will have comparable effects on the tether's zero-torque twist, particularly since the core, wire, and insulation have greatly different thermal expansion coefficients.

Final Comments on Test Results

We decided to perform the variety of tests described above when we realized that our short test samples and current test setup would not allow us to get valid axial damping data. We believe that the phenomena characterized are relevant to PMG equipment and mission design, and that similar effects are likely even with a moderately more flexible tether. And even if a nominally twist-balanced tether is used, there will be some residual torques and torque changes with load. These effects do add some complexity to the tether dynamics analysis that will be required before the PMG experiment is flown, but the effects need not be undesirable.

For example, the greatly reduced effective modulus at tensions of a few newtons will minimize the transient forces on OMV-mounted solar arrays. In addition, the highly non-linear stress-strain curve at even lower tensions (<1 newton) will replace any sudden slack/taut transitions with the far more gradual transitions seen in the test data.

In addition, it seems likely (though not certain) that tension variations which cause alternate straightening and bending of a pigtail may provide higher damping than pure stretching behavior would.

The change in equilibrium twist with load may allow useful damping of low-frequency axial load changes, by converting some of the oscillation energy into a torsional pendulum mode and then damping that mode. Most of the torsional pendulum energy will go into the smaller end mass, and it may be fairly easy to design a torsional oscillation damper into that end mass. One possibility is an appropriate xenon tank geometry plus vanes: this may provide useful amounts of damping at low cost (at least until the xenon supply gets low). Any other weak yaw oscillation damper could perform the same function.

Suggested future work

As indicated by the above discussion, pig-tail and other effects associated with the existing wire design may actually make a stiff wire advantageous. Hence a wire as stiff as the existing one may be preferable to a more flexible wire--providing that the stiffness does not make deployment difficult or unreliable. We propose that deployment tests be done in follow-on work.

The high ballistic coefficient of this wire in cross-flow (about 10X that of the SEDS tether) means that air drag effects will be fairly small (comparable to gravity effects), so deployments in air should be fairly representative. In-air deployments will be far simpler to set up and perform than in-vacuum deployments. Deployment of short existing lengths of wire from various sizes of spool should allow determination of deployment performance from different spool geometries. We believe this should allow a determination of the "deployability" of the existing tether from a SEDS-like deployer.

If such deployment tests indicate that the wire is deployable on a simple deployer, then further electrical and mechanical tests on the tether would be in order. These tests should be done at a variety of temperatures spanning the expected use temperatures in orbit (probably about 200K to 300K).

TASK 4.3 LONG-TERM PMG SIMULATIONS

We prepared input databases for GTOSS based on system data provided by TRW and our own measurements. The detailed inputs are shown in Table 1. A sample GTOSS input deck is shown before the GTOSS graphs.

Table 1. Nominal parameters for GTOSS simulations.

Satellite mass:	2235 kg.
Tether mass:	139 kg.
Tether length:	10 km.
End mass:	90 kg.
Tether modulus:	0.55 GPa. (80 ksi)
Tether diameter: (effective)	0.2413 cm. (0.095 in)
Starting altitude:	401.4 km.
Starting inclination:	28.5 deg.
Starting lat., long.:	0, 0 deg.

Power: 2 kw continuous and 2 kw daytime only boost

Variations:

Tether mass:	69.5 kg (half of nominal)
End mass:	180 kg (twice nominal)
Tether modulus:	55 GPa (100X nominal)
Starting long.:	180 deg. (opposite nominal)

We have run 6 GTOSS simulations of one day or longer, for a total simulated time of over 22 days. Runs were done using a rented Levco Prodigy SE board in a Macintosh SE, which yielded about a six-fold increase in speed. For the original tether modulus of 55 GPa, a time step of 0.2 sec. was used, giving a simulation speed somewhat faster than real time. For the nominal case (low modulus tether), a time step of 1.0 sec. allowed one week of simulation to be done in one day. The continuous power simulations assumed a constant 2 kw of orbital energy increase (boost), while the daytime power only simulations assume 2 kw of boost power is used only while the satellite is sunlight. Table 2 shows the 6 cases.

Table 2. GTOSS simulations.

Run 1: 1 week total, Continuous power

Run 2: 1 week total, Daytime power only

Run 3: 2 days, High modulus (55 GPa), Daytime power only

Run 4: 270,000 sec., High modulus, Light tether (69.5 kg.), Continuous power

Run 5: 200,000 sec., High modulus, Light tether, 180 deg. longitude start, Daytime power only

Run 6: 100,000 sec., High modulus, light tether, heavy endmass (180 kg.), 180 deg. longitude start, Daytime power only

Graphic output was generated by the standard GTOSS programs set up for Macintosh use, along with the commercial software CricketGraph for generated plots. Because our Macintosh configuration does not allow for more than about 2 days of data to be saved, longer runs were generated by merging 2 data sets. For the 1 week runs, this leaves a gap of 200,000 seconds on graphs of the entire interval.

The standard data shown are the in and out-of-plane librations of the end mass relative to the satellite, and the altitude of the satellite. In most cases, the tension at both ends of the tether, orbital inclination and eccentricity, and tether voltage are also shown.

The constant-power simulations show very docile behavior, and we have difficulty imagining ways in which a constant-boost-power operation could get into difficulty, except by driving the system so hard that the in-plane angle gets large (i.e., long-term boosting or deboosting at over 10 kw for the system parameters specified). However, note that the simulation over a one week period does not show a steady state behavior. The out-of-plane libration amplitude is still building at the end of the week.

As expected, the daytime-power-only case has much larger libration amplitudes. The out-of-plane libration amplitude builds up to about 20 degrees in less than one day (this is for a power level that gives an equilibrium in-plane angle of 1.75 degrees in full-time operation). However, by the time the libration amplitude grows to 20 degrees the frequency of free out-of-plane libration drops nearly 3%, which limits the further growth of the out-of-plane libration. Thereafter the system "breathes" diurnally, as the geomagnetic field rotates with the earth and varies the orbit inclination with respect to the geomagnetic field between a minimum of 17 degrees and a maximum of 40 degrees.

In cases where operation starts when the geomagnetic inclination is near maximum (i.e., when the satellite orbit ascending node is near the international date line), the libration amplitude builds up quicker than when operation starts with the ascending node near 0 longitude, but in either case, the limiting amplitude is similar.

Simulations with factors of two change in the tether and the endmass show the qualitatively expected behavior. Out-of-plane libration builds up more slowly with both the heavy endmass and the heavier tether.

GTOSS simulation videotape

Dave Lang prepared an animated version of Runs 4 and 5, with simulated durations of about 2 days each. Each case is shown at a slow and a fast speed. The animations give information about the actual behavior of the tether itself which cannot be deciphered from raw data or static graphs. In particular, the behavior of the daytime only power case is very interesting. Near the end of the run, it is showing an obvious "jumprope' motion, with a frequency very near to six times the orbital frequency. It may be possible to detune the frequency of this mode to lessen its amplitude.

Suggestions for future work

Longer runs are needed to show the behavior of the system over a time-scale of several weeks. This would also allow a better check on the validity of the Dumbbell simulations. In addition, long-term simulations of various control strategies should be done to see if librations can be kept to an acceptable amplitude over long periods.

Guide to the DUMBBELL Videotape

To save time, the videotape was shot simply by pointing a camcorder at an IBM-PC monitor, running the program, and making comments as the program ran. The display is sketched below:

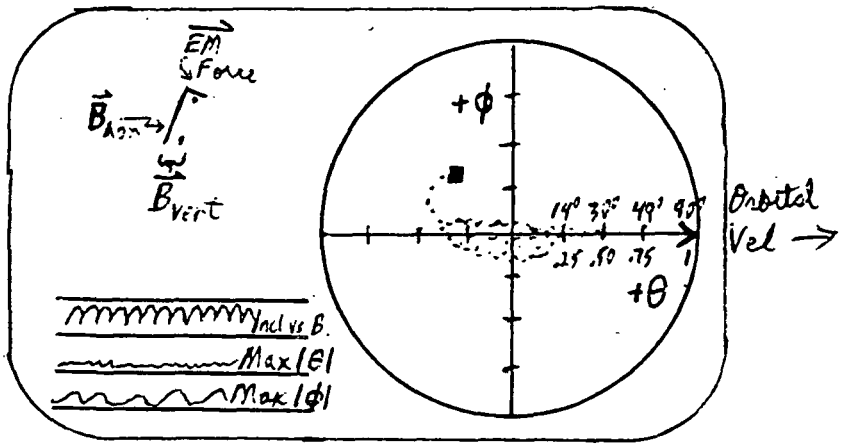

The large circle on the right indicates the possible range of motion of a small upper end mass tethered to a larger object, as viewed from above in a LVLH reference frame moving with the dumbbell. The orbital velocity vector is to the right, as shown by the arrow. Thus what is seen is a projection of the endmass's position onto a horizontal plane. The marks on the screen show equal increments in in-plane and out-of-plane displacement, with each mark indicating a displacement of 1/4 of the tether length. This corresponds to libration angles of 14, 30, 49, and 90 degrees.

The endmass position is represented by the small moving square. Its position is calculated at 10 second intervals, and plotted at 40 second intervals. At 80 second intervals, a "dot" is left behind the square as it moves away. This provides a graphic record of the envelope of attitude oscillation and of changes in that envelope over time.

At the upper left the B-field and electromagnetic thrust vectors are shown. The reference frame is the same LVLH rotating frame used in the large display, with the same overhead perspective. Hence the two lines on the screen represent the horizontal components of the field and the thrust vector. The field line orientation is mostly out-of-plane (vertical on the screen) for low-inclination orbits. The thrust vector line runs mostly east (to the right for a low-inclination orbit). The thrust vector line appears and disappears as current is turned on and off. Note that the component to the right is the in-plane force, which can be much larger than the net boosting force if Cos(Theta) is small.

state0		orbit		current		control law			
Theta0	Phi0	Incl	OrbPh0	Limit	EqTheta	DC	Sun	2Ph	NoI
0.0°	0.0°	28.5°	0.0°	2.00	1.75°			X	

OrbIncVsB: 0-40 deg

MaxPhi: 0-40 deg

MaxTheta: 0-40 deg

MaxCurrentMult: 1-2

state0		orbit		current		control law			
Theta0	Phi0	Incl	OrbPh0	Limit	EqTheta	DC	Sun	2Ph	NoI
0.0°	0.0°	28.5°	0.0°	2.00	1.75°		X		

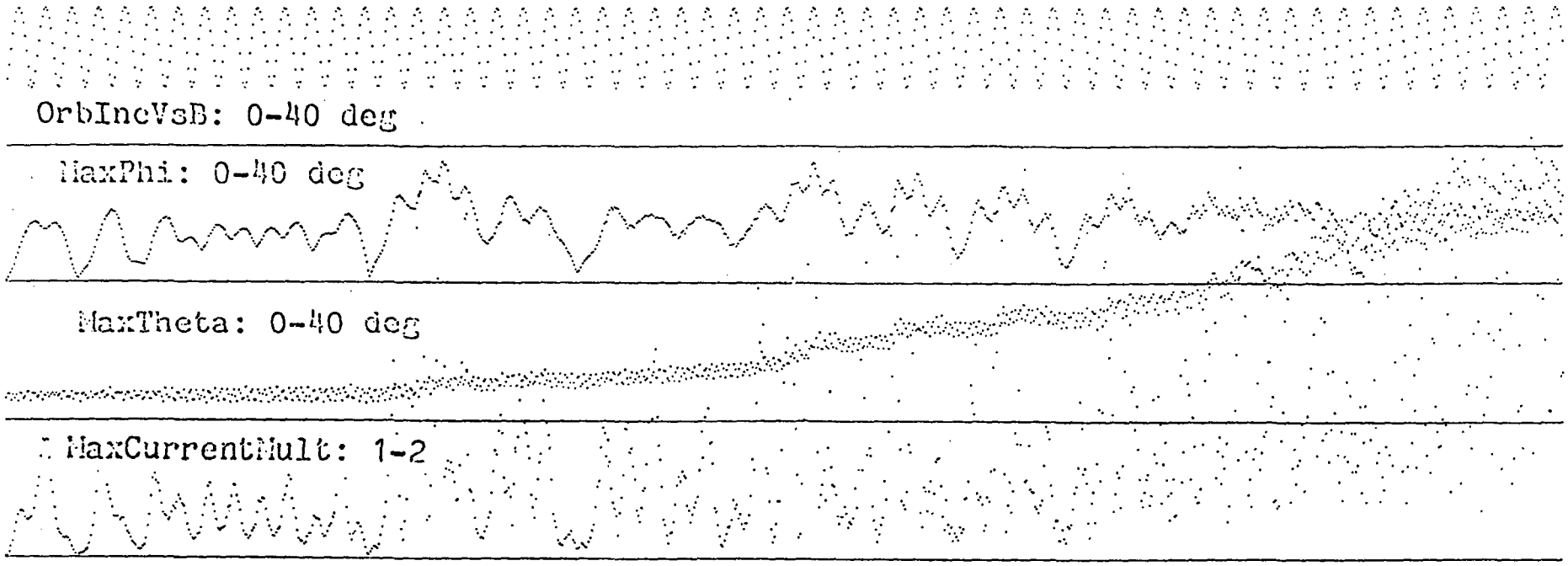

state0		orbit		current		control law
Theta0	Phi0	Incl	OrbPh0	Limit	EqTheta	DC Sun 2Ph MoI
0.0°	0.0°	28.5°	0.0°	2.00	1.75°	X

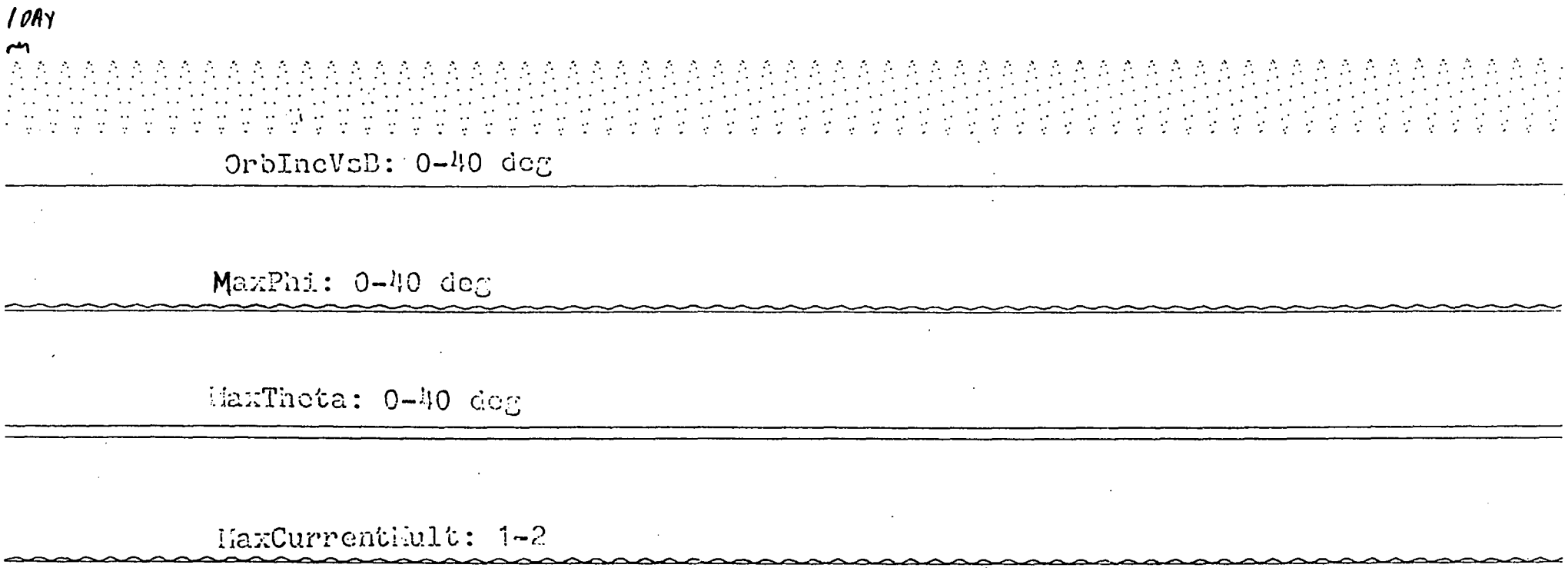

DUMBBELL is written in Borland Turbo-Pascal 4.0. It runs on IBM/PC-compatible micros and generates a graphics display as it runs. With an 8087 co-processor, double-precision numbers, and 10-second timesteps, the program takes about 8 seconds per orbit.

DUMBBELL Inputs

The program begins with a default set of inputs, and the user supplies replacement values interactively. The parameters are:

Theta0:	Initial in-plane libration angle in degrees.
Phi0:	Initial out-of-plane angle in degrees
Incl:	Orbit inclination in degrees
OrbPh0:	Initial orbit phase (from ascending node), in degrees
Limit:	Maximum current allowed, compared to vertical tether
EqTheta:	Equilibrium theta due to electrodynamic torque

Theta and Phi are "clock" and "cone" angles in a local-vertical, local-horizontal reference frame, with positive theta indicating displacement of the upper (smaller) end mass in the direction of the orbital velocity vector, and positive Phi representing a displacement to the left of the velocity vector. The initial Theta and Phi rates are both assumed to be zero. The current limit parameter comes into play when the libration angle is large. With Limit=2.0, when libration causes the EMF to go down to less than half the value for a vertical tether, then the current is limited to twice the vertical-tether current. Also, if the libration angle is large enough to make the EMF change sign, the current is turned off entirely.

The control law options are:

DC:	Fixed power (and hence fixed force along velocity vector)
Sun:	Fixed power in sun, no power in shade
2Ph:	Fixed power within 45 deg of nodes; no power otherwise
NoI:	No current; over-rides the EqTheta input.

Explanation of DUMBBELL Viewgraphs

Each viewgraph lists the inputs at the top, and four key output parameters plotted at a rate of one data point per orbit. The top value (OrbIncVsB) is the "geomagnetic inclination" of the orbit, halfway through that orbit. It varies from 17 to 40 degrees each day for all the runs shown. Below that are MaxPhi and MaxTheta, the maximum absolute Phi and Theta displacements during that orbit, with 0 degrees at the bottom of each plot and 40 degrees at the bottom of the next plot upwards. Finally, "MaxCurrentMult" (with a range of 1.0 to 2.0) is the relative current required to give a fixed boosting force. Note that when this value is above "Limit" (the input parameter), the net power is scaled back to stay within the limit, but the plot shows the current that would have been used without the Limit constraint.

Simulations of Dumbbell Behavior

The slow execution speed of GTOSS severely limited the number of long-term GTOSS runs possible under this contract. To supplement the GTOSS work, we wrote a simple rigid-dumbbell electrodynamic tether simulation program, DUMBBELL. It runs fast enough to allow us to simulate months of dynamic behavior in a few hours. The key program assumptions and results are described below.

"DUMBBELL" Program Description

DUMBBELL models the attitude motion of a rigid dumbbell in circular earth orbit, in response to gravity gradient and electrodynamic torques. It models gravity gradient attitude dynamics using the general equation of attitude motion listed in the Appendix to the paper "The Behavior of Long Tethers in Space" (David A. Arnold, in Journal of the Astronautical Sciences, Jan-Mar 1987). The length-change terms are set to zero. Note that this equation linearizes gravity and assumes a spherical earth.

DUMBBELL does not model perturbations due to air drag or earth oblateness on the attitude motion of the object. However it does take into account the effect of nodal recession on the phasing of the day/night cycle with respect to the orbit's ascending node. This typically goes through a complete cycle in roughly 50 days. The earth's magnetic field is modeled as a simple dipole tilted 11.5 degrees with respect to the earth's axis of rotation. The field rotates with the earth. This causes the "geomagnetic inclination" of the orbit to vary over a 23 degree range each day: from 17 to 40 degrees and back for a 28.5 degree orbit inclination. This variation in geomagnetic inclination causes the out-of-plane component of electrodynamic force on a vertical tether to vary from Tan(17) to Tan(40) times the in-plane component. Since the in-plane "boosting" force and torque are constant (for a constant-net-power control strategy), the out-of-plane forces vary by almost a factor of 3 during the day. The motion of the field with respect to the orbit also causes the orbit's ascending node with respect to the field to oscillate, over a total range of about 80 degrees for a 28.5 degree orbit.

DUMBBELL does not include the offset of the earth's magnetic field from the center of the earth, or the higher harmonics of the field. When an electrodynamic tether is operated on a constant-net-power basis, variations in field strength cause EMF and thus current variations that compensate for the field-strength variations. We did not model higher-order terms of the field because of time limitations, and because higher harmonics are smaller and mostly average out over time due to the earth's rotation under the orbit.

Near the end of the B-field and thrust vectors two small bright spots can be seen moving around on the display. The left-to-right distance between the end of each vector and the nearby spot represents the vertical component of that vector, on the same scale as the horizontal component. If the spot is to the right of the tip of the vector, then the vertical component is upward; if to the left, then the vertical component is downard. We have found it instructive to freeze the display and position two pencils in front of the screen to show the tether and field orientations. This allows visualization of the tether, field, and thrust vectors in 3-D.

At the lower left is a summary set of plots similar to the DUMBBELL viewgraphs, except that the order is different: OrbIncVsB is shown on top, followed by MaxTheta and then by MaxPhi. This plot uses 1 column per orbit and takes 720 orbits to "march" across the screen. If the run lasts over 720 orbits, then the plot starts over at the left side and superimposes new data on the old data.

To provide a proper context for understanding the effects of electrodynamic forces on the tether, the video starts off with several cases of free libration: in-plane, out-of-plane, and combined, with amplitudes of 15 and 30 degrees. Then tether electrodynamic forces are added, first as a small perturbation on a large free libration, and then for the two cases of greatest practical interest: "DC" and "Sun-only" boosting at the 2-KW level, using the baseline TRW PMG hardware design. Because of the duration of the last two simulations (several hours run time), only selected portions of each run are shown. In tabular form, the cases shown on the video are:

CASES SHOWN ON "DUMBBELL" VIDEOTAPE:

	Theta0	Phi0	Power
Short runs:	15	0	0
	30	0	0
	0	15	0
	0	30	0
	15	15	0
	30	30	0
	30	30	2KW
Long PMG runs:	0	0	2KW "DC"
	0	0	2KW when in sun

```
$TR4301    GENERIC RDB NAME FOR SERIES
     TRUN43: 3 BEAD SOLN FOR TRW PMG OMV, grav grad. start
     downward DEPLOY AT 400 km, 28.5 DEG ORB, 2 kw cont.

  1  1.0           DELTAT: REF PT
  2  610000.           TMAX
  3  500.0          N, THE RDB SOLN OUTPUT INTERVAL = N * DELTAT
  4  400000.           START RDB OUTPUT AT THIS TIME
 16  43.00         RUN NUMBER

C QUICK LOOK PAGE FORMAT CONTROL
117  1.            SELECT QUICK LOOK PAGE FORMAT
381  2.0           CHOOSE TOSS OBJ FOR QUICK LOOK (IF APPROP)
382  2.              "       "
385  2.              "       "
421  1.0           CHOOSE TOSS TETHER FOR QUICK LOOK (IF APPROP)
422  2.              "       "
433  2.              "       "
435  1.0           CHOOSE FINITE SOLN FOR QUICK LOOK (IF APPROP)
442  1.            BEAD NUMBER TO DISPLAY FOR QUICK LOOK (IF APPROP)
443  2.              "     "
444  3.              "     "

C GTOSS EXECUTION CONTROL DATA
111  1.0           INVOKE RP PARTICLE DYNAMICS
112  0.0           INVOKE RP EULER ANGLE DEFINITION
113  2.            NUMBER OF LAST TOSS OBJECT BEING SIMULATED
114  1.            NUMBER OF ATTACH PTS ON THE REF POINT

C BASIC REF PT GEOMETRY
455  0.            INVOKE AERO DRAG ON REF PT
456  0.0           REF PT AERO REF AREA (SQ-FT)
457  0.0           REF PT DRAG COEFF
 20  153.196       REFERENCE PT MASS (SLUGS)
 21  50000.        IXX: REF PT (SLUG-FT**2)
 22  50000.        IYY
 23  50000.        IZZ

C REF PT TRANSLATION STATE INITIALIZATION
100  0.0           TRNS IC OPT: =0. FOR TOPO;   =1. FOR INERTIAL
 81  0.0           XIO REF PT POSITION (FT) (INER FRAME)
 82  0.            YIO  "        "
 83  0.            ZIO  "        "
 84  0.0           XIDO REF PT RATE (FT/SEC) (INER FRAME)
 85  0.            YIDO  "       "
 86  0.            ZIDO  "       "
101  1316800.0     REF PT  ALT (FT)
102  0.0           REF PT  TOPO LONGITUDE (DEG)
103  0.0           REF PT  TOPO LATITUDE (DEG)
107  12005.12      VXTO (FT/SEC) RP INER VEL COMP (RP TOPO FRAME)
108  22110.67      VYTO    "           "
109  0.            VZTO    "           "

C REF PT ROTATION STATE INITIALIZATION
 90  2.0           EULER IC OPT: =0. FOR ORB;  =1. FOR TOPO;  =2. INER
104  0.0           PITCHO (DEG) EULER ANG ICS
105  0.            ROLLO          "
```

```
106  0.            YAWO            "
 87  0.0           OMXBO: REF PT BODY ANG VEL (ORB RATE = .069
 88  0.            OMBYO           " (ORB RATE=-0.0692)
 89  0.            OMZBO           "
  0                END OF REF POINT AND TEST BED DATA

======> GENERAL <======= READ-IN LTOSQ ARRAY HERE - INTEGER CONSTANTS
 125     0 TOSS-WIDE EULER ANGLE DEFINITION
  23     1 INVOKE TOSS-WIDE PARTICLE DYNAMICS
  24     1 TOTAL NUMBER OF TETHERS
 129     1 NUMBER OF FINITE TETHERS
 234     5 ASSIGN PWR GEN SCENARIO 2 TO TOSS TETHER #1
 198     1 TYPE OF FINITE SOLN #1 (0=MODAL, 1=STD BEAD MODEL,4=frozen)
 284     1 grav grad start for tether #1
 207     3 NUMBER OF BEADS FOR FINITE SOLN# 1
 194     0 EVAL OPTION -GRAV GEN FORCES, FOR "ALL" FINIT TETH SOLNS
 195    -1 EVAL OPTION -AERO GEN FORCES, FOR "ALL" FINIT TETH SOLNS
 196     0 EVAL OPTION -ELEC GEN FORCES, FOR "ALL" FINIT TETH SOLNS
 130     1 ASSIGN FINITE TETHER SOLN 1 TO TOSS TETHER #1
  25     1 OBJ # TO WHICH "X" END ATTACHES-TETHER #1
  50     1 ATT PT #, FOR "X" END OF TETHER #1
  75     2 OBJ # TO WHICH "Y" END ATTACHES-TETHER #1
 100     1 ATT PT #, FOR "Y" END OF TETHER #1
   0     0           END OF DATA
   ---------------------- READ-IN JTOSQ ARRAY HERE - INTEGER VARIABLES
   0     0           END OF DATA
   ---------------------- READ-IN FTOSQ ARRAY HERE - REAL CONSTANTS
 145          0.0    FINIT TETH INTEG INTVL: SOLN #1  <---<<<<<<<<<
  25       12.820    SPRING RATE - MASSLESS TETHER #1
  50      32808.5    UN-STRETCHED LENGTH - TETHER #1
  75          0.0    DAMPING CONST - MASSLESS TETHER #1
 100       9.3268    LINEAL DENS (LMB/1000FT) FOR FINITE TETH SOLN 1
 109     80000.      YOUNGS MODULUS (PSI)     FOR FINITE TETH SOLN 1
 118     .09500      ELASTIC DIA (IN)         FOR FINITE TETH SOLN 1
 127       0.01      BETA DAMPNG FAC (/SEC)   FOR FINITE TETH SOLN 1
 154     .11420      AERODYNAMIC DIA (IN)     FOR FINITE TETH SOLN 1
 181        9.0      INITIAL CURRENT (AMPS)   FOR FINITE TETH SOLN 1

C DEFINE ELECTRO POWER GENERATION SCENARIO NUMBER 5
 389      2.0        TYPE:day/night 2kw constant
 394      0.0        ABSOLUTE TIME(SEC) TO START POWER GEN SCENARIO 5

 404     -2.0          day PWR LEVEL (KW) - PERIOD 1,  SCENARIO 5
 414      100.         MAX LIMIT CURRENT (AMPS) - PERIOD 1,  SCENARIO 5

 424     -2.0         night PWR LEVEL (KW) - PERIOD 2,  SCENARIO 2
 434      100.        MAX LIMIT CURRENT (AMPS) - PERIOD 2,  SCENARIO 5

 504     0.0         BEGINNING PWR LEVEL (KW) - PERIOD 6,  SCENARIO 5
 509     0.0         ENDING    PWR LEVEL (KW) - PERIOD 6,  SCENARIO 5

 335      1.0        PWR MULTIPLIER (DEFAULTS TO 1.) - TOSS TETHER #1
   0            0.0       END DATA

   ---------------------- READ-IN DTOSQ ARRAY HERE - REAL VARIABLES
   0            0.0       END DATA
```

```
======> OBJECT 2 <====== READ-IN LTOS2 ARRAY HERE - INTEGER CONSTANTS
  18     1 # OF ATTACH POINTS ON THIS OBJECT
  19     0 .GT. 0 INVOKES AERO CALC ON OBJECT
  21     2 LICTRN SELECTS TRANS STATE IC OPTION, =0 FOR TOSS INER COORDS
  22     5 LICROT SELECTS ROTAT STATE IC OPTION, =0 FOR DIRECT COS ENTRY
   0     0          END OF DATA
   ---------------------- READ-IN JTOS2 ARRAY HERE - INTEGER VARIABLES
   0     0          END OF  DATA
   ---------------------- READ-IN FTOS2 ARRAY HERE - REAL CONSTANTS
   3        6.167      INITIAL MASS FOR THIS OBJECT
   4         10000.0 INITIAL IXX FOR THIS OBJECT
   5         10000.0    "    IYY       "    "
   6         10000.0    "    IZZ       "    "
 102             0.0 AERO REF AREA (SQ-FT)
 103             0.0 DRAG COEF

  40             0.0 INITIAL POSITION X COORD (OF OBJECT WR/T RP)
  41             0.     "        "     Y   "          "      "
  42        32808.5   "        "     Z   "          "      "
  43             0.0 INITIAL RATE X COORD (OF OBJECT WR/T RP)
  44             0.     "        "   Y   "          "      "
  45             0.     "        "   Z   "          "      "

  46             0.0 INITIAL OMXB ANG RATE (INER) OF OBJECT
  47             0.     "    OMYB   "    "
  48             0.     "    OMZB   "    "
  49             0.0 INITIAL EULER PITCH OF OBJECT
  50             0.     "           ROLL
  51             0.     "           YAW
   0             0.0       END DATA
   ---------------------- READ-IN DTOS2 ARRAY HERE - REAL VARIABLES
   0             0.0       END DATA
>>>>>>>>>>>>>>>>>>>> END OF TRUN40 <<<<<<<<<<<<<<<<<<<<<<<
>*************************************************************
 -1
```

RUN 1

1 week
Continuous power

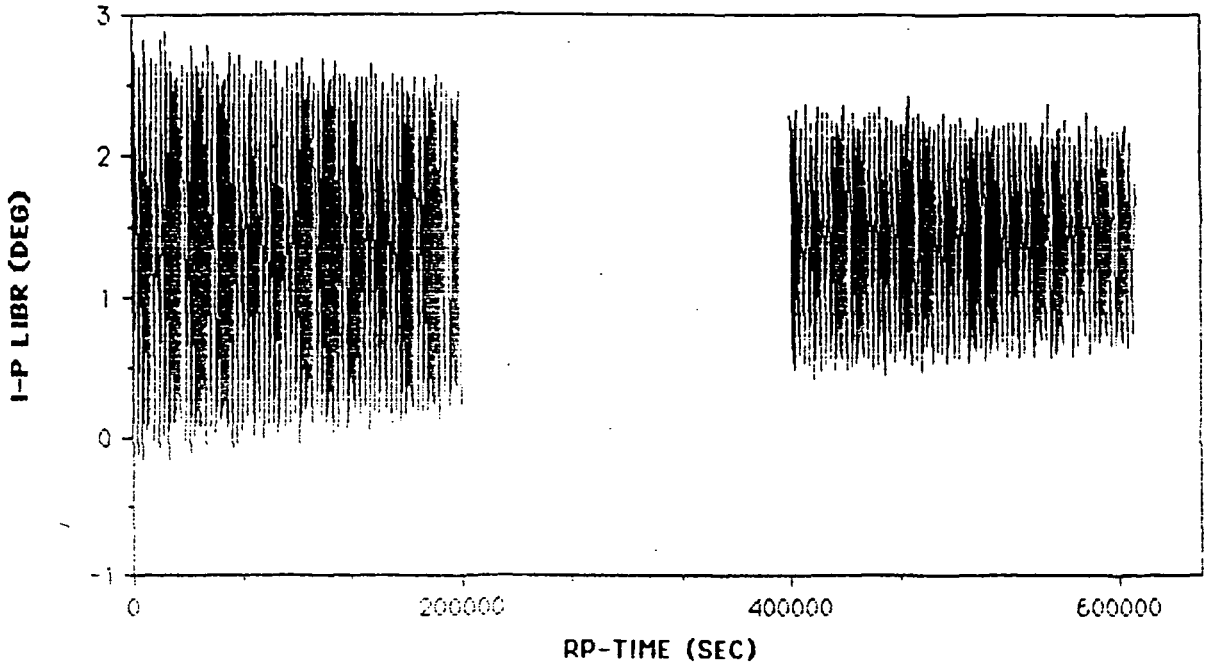

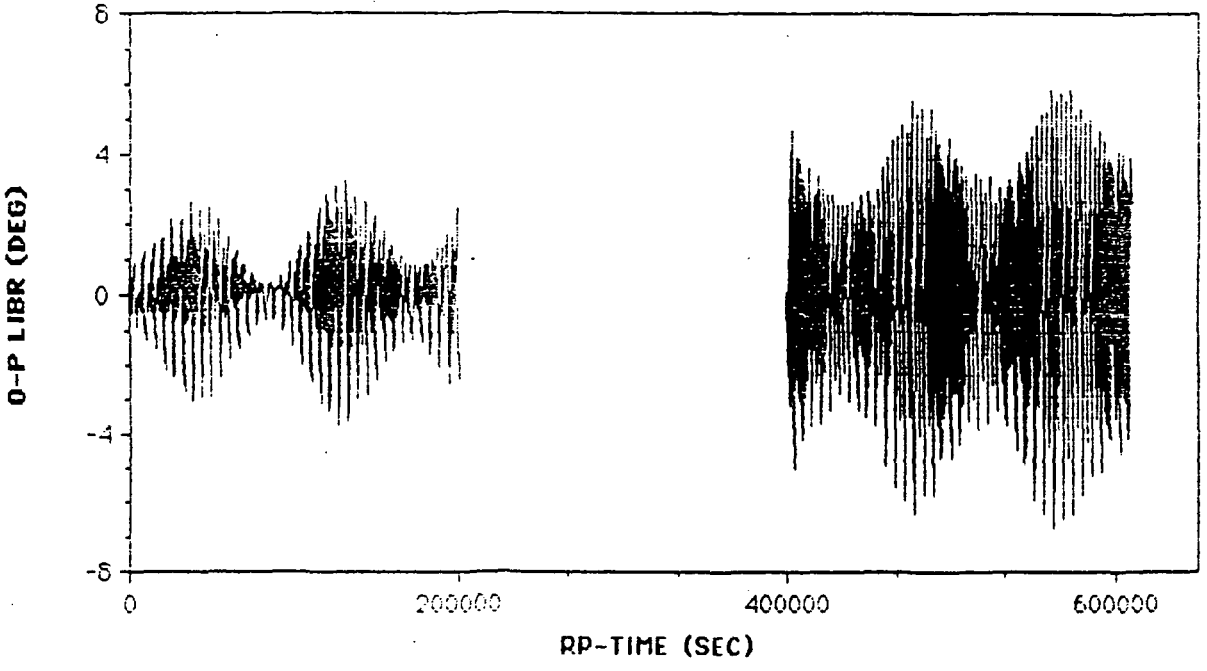

RUN 1

1 week
Continuous power

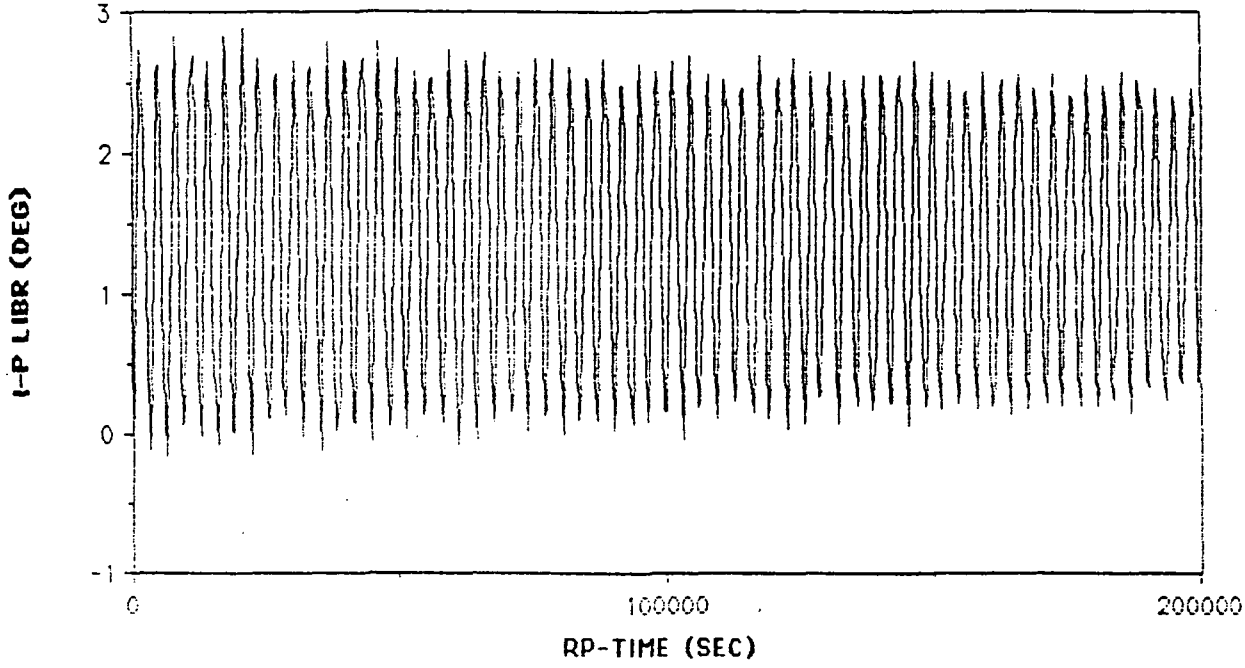

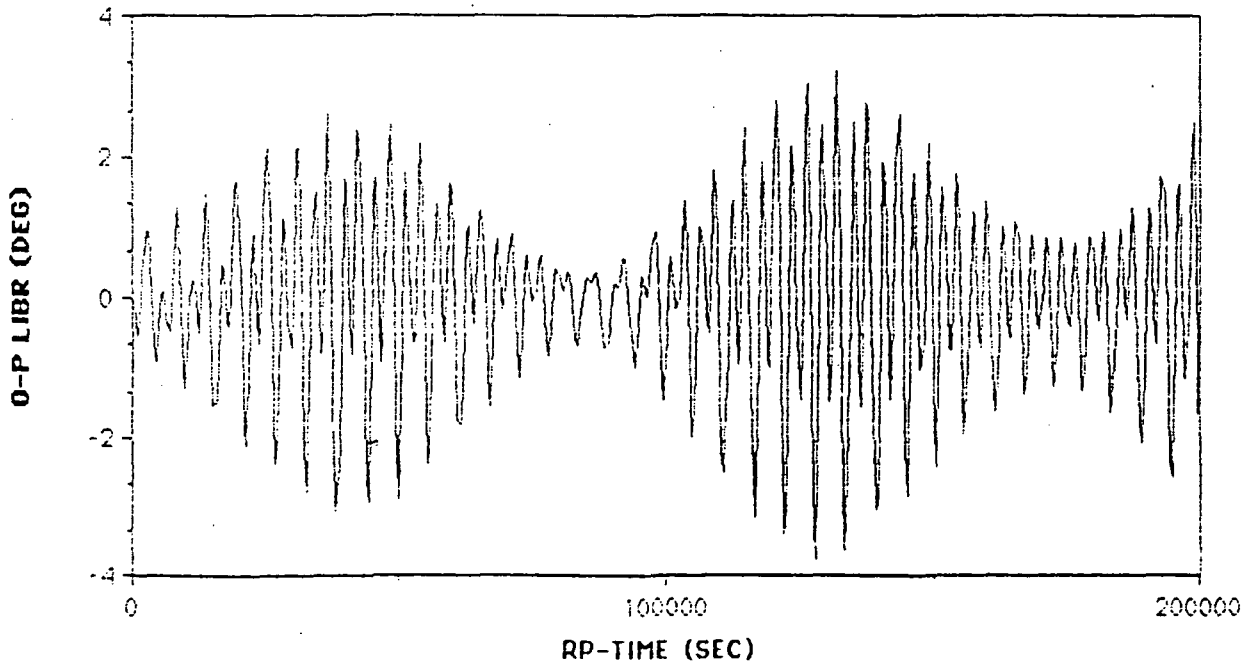

RUN 1

ORIGINAL PAGE IS
OF POOR QUALITY

1 week
Continuous power

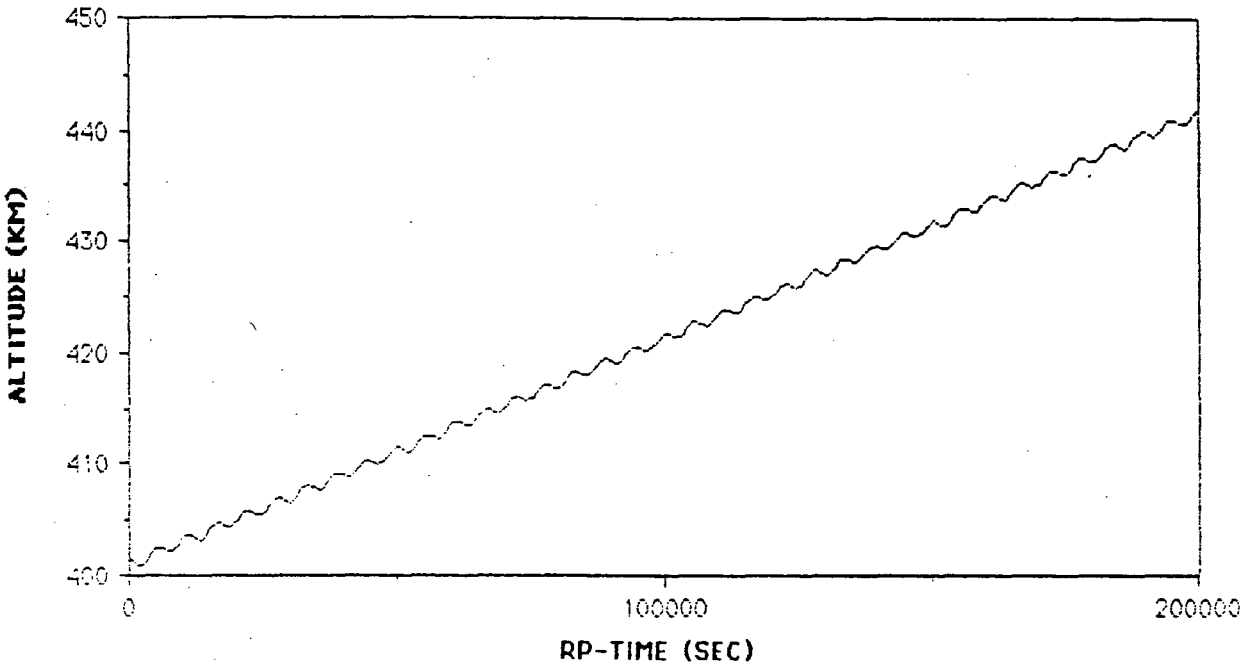

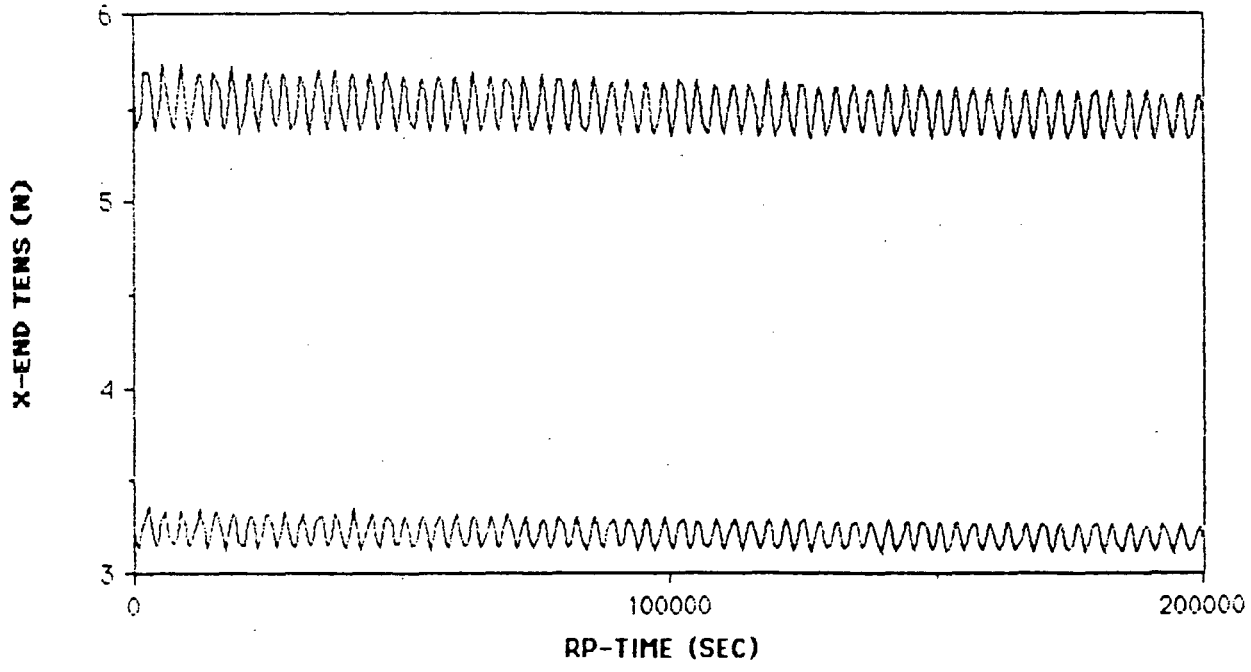

RUN 1

1 week
Continuous power

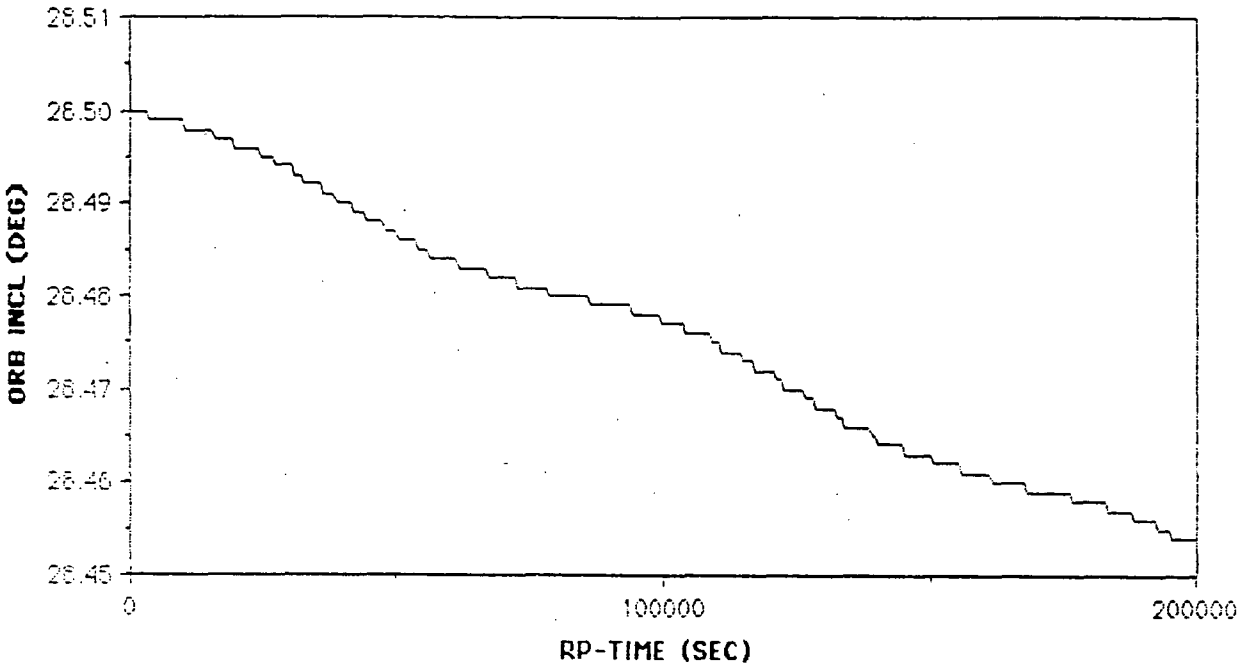

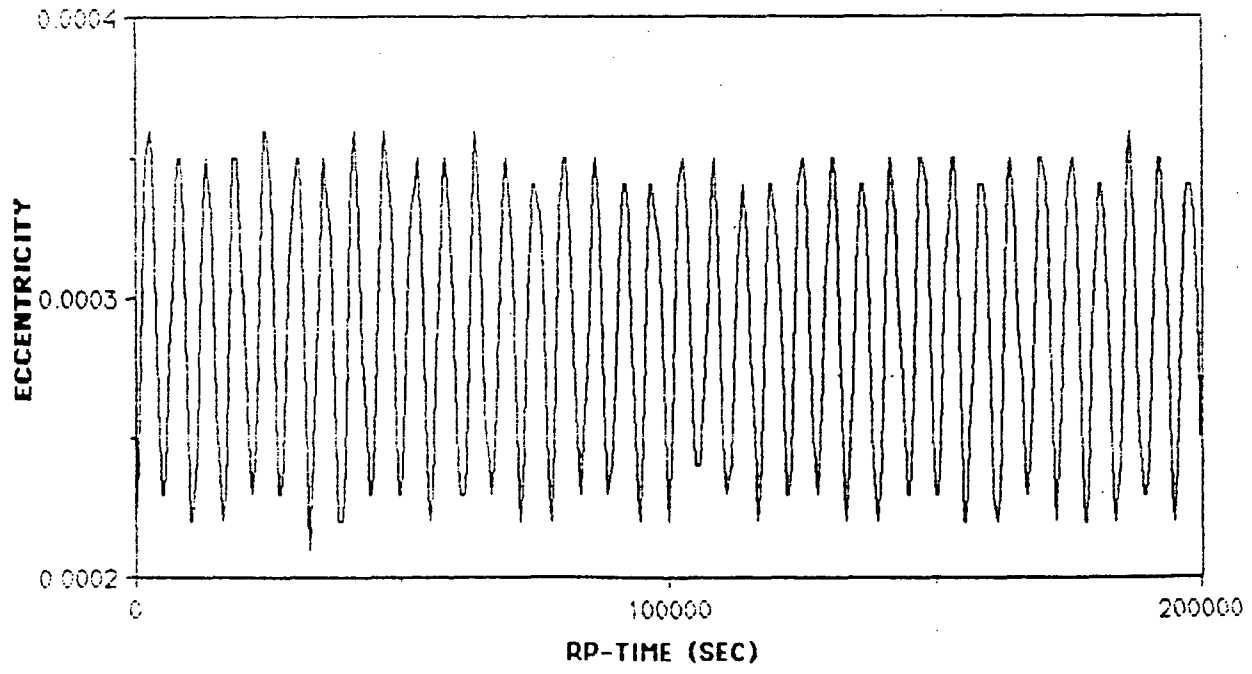

RUN 1

1 week
Continuous power

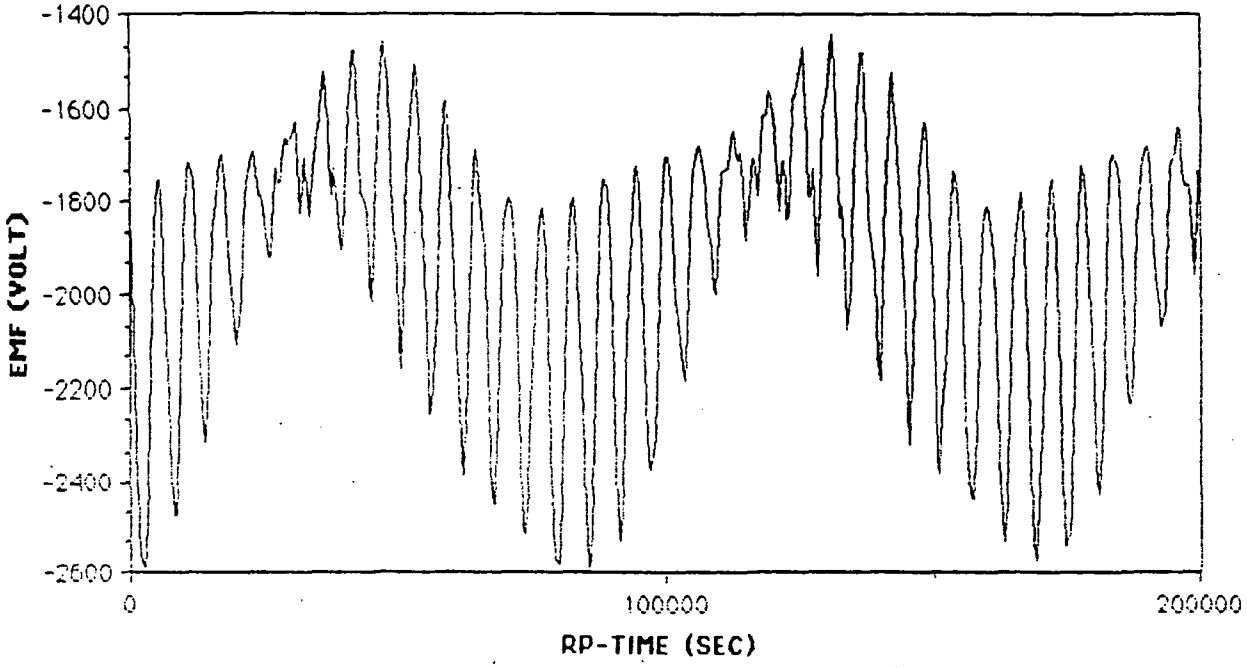

RUN 1

1 week
Continuous power

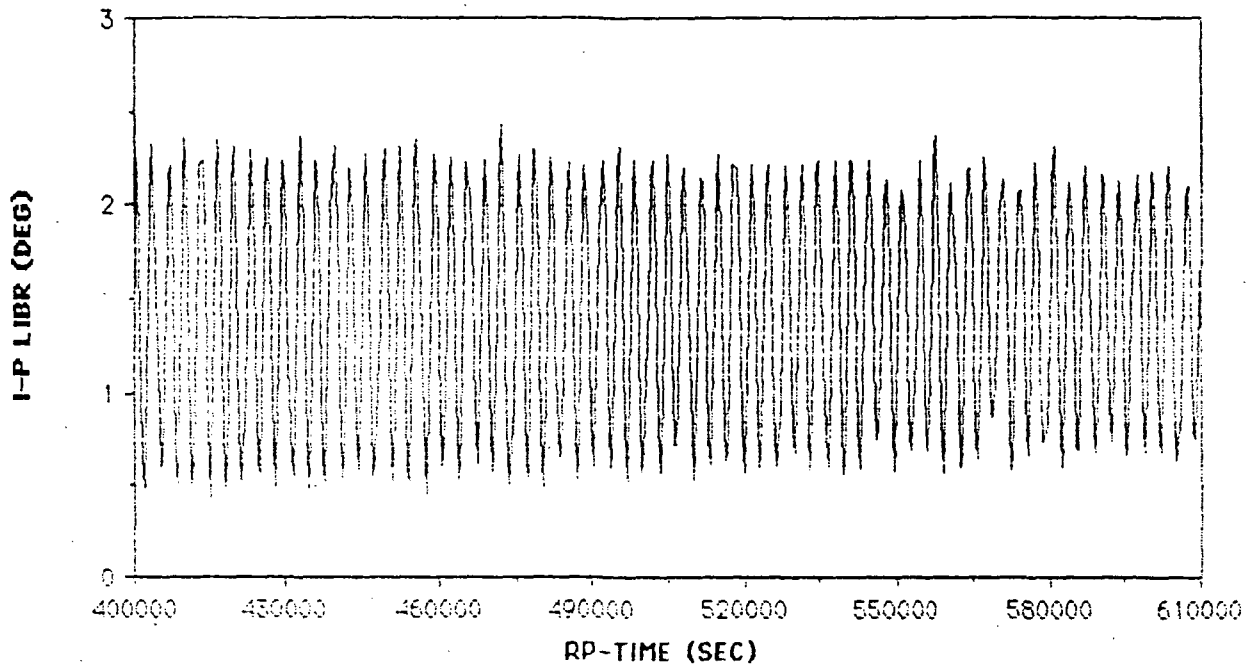

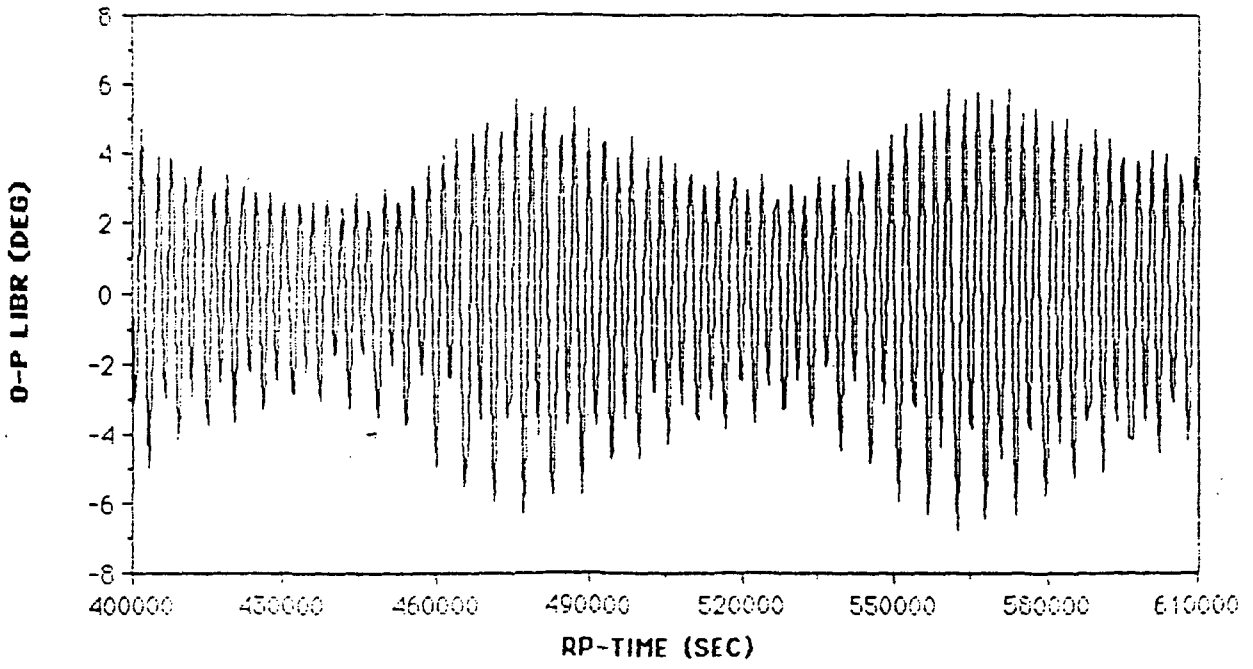

RUN 1

1 week
Continuous power

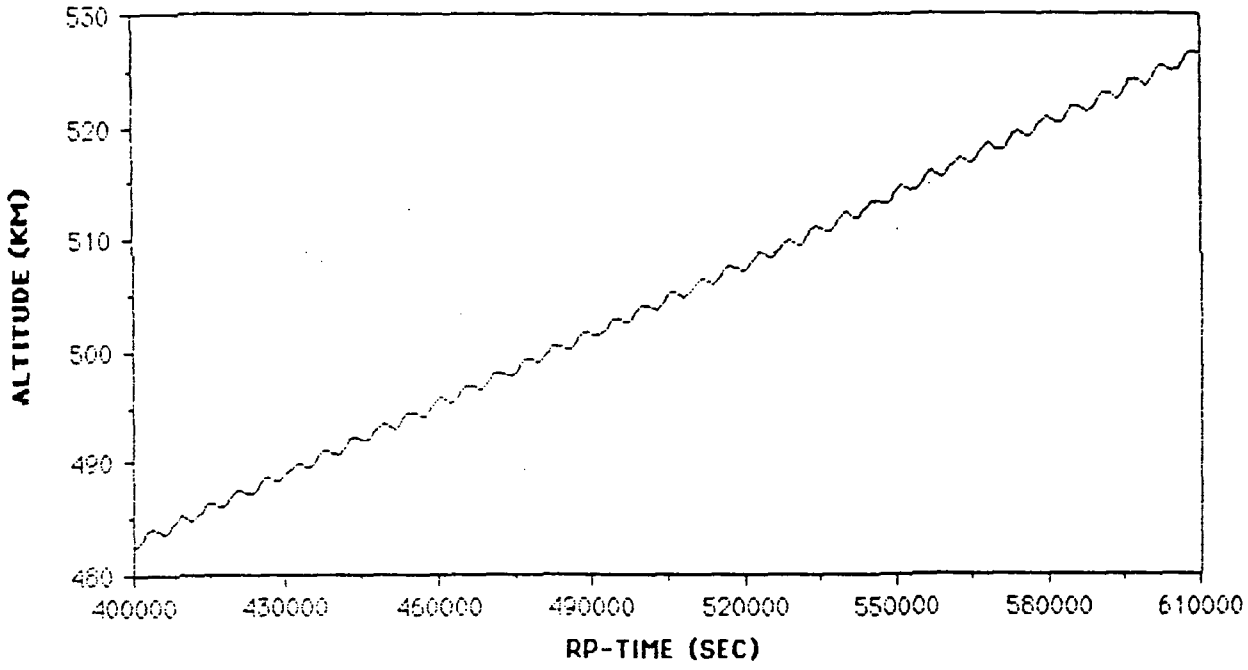

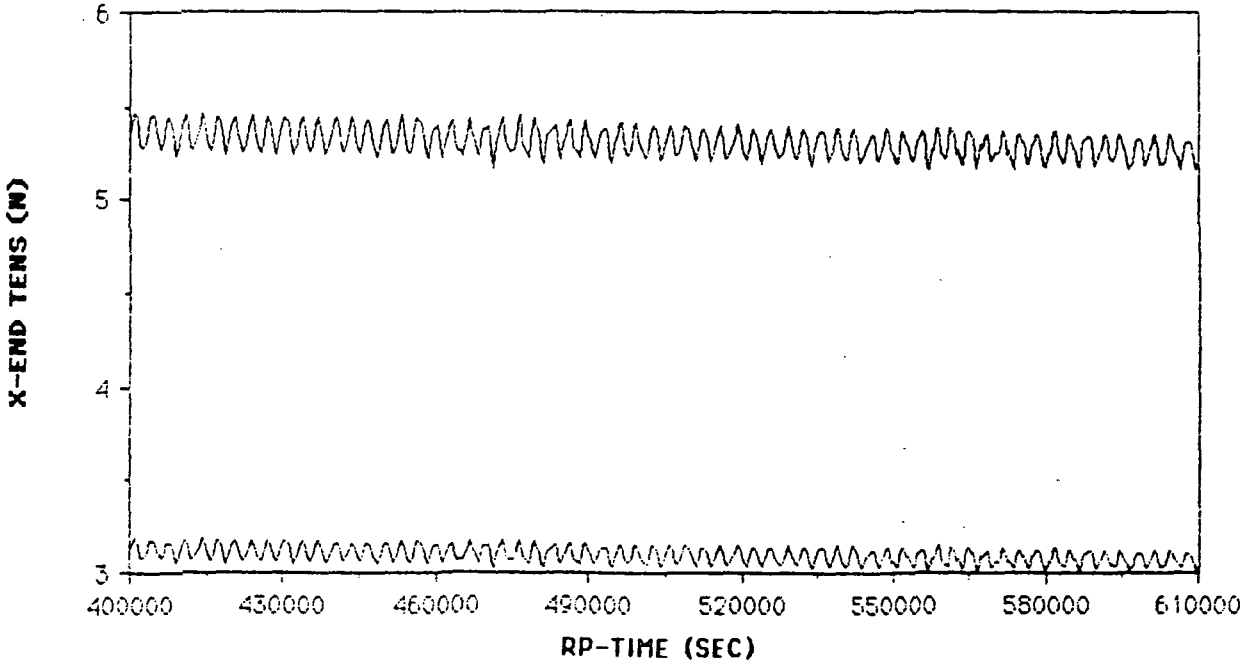

ORIGINAL PAGE IS
OF POOR QUALITY

RUN 1

1 week
Continuous power

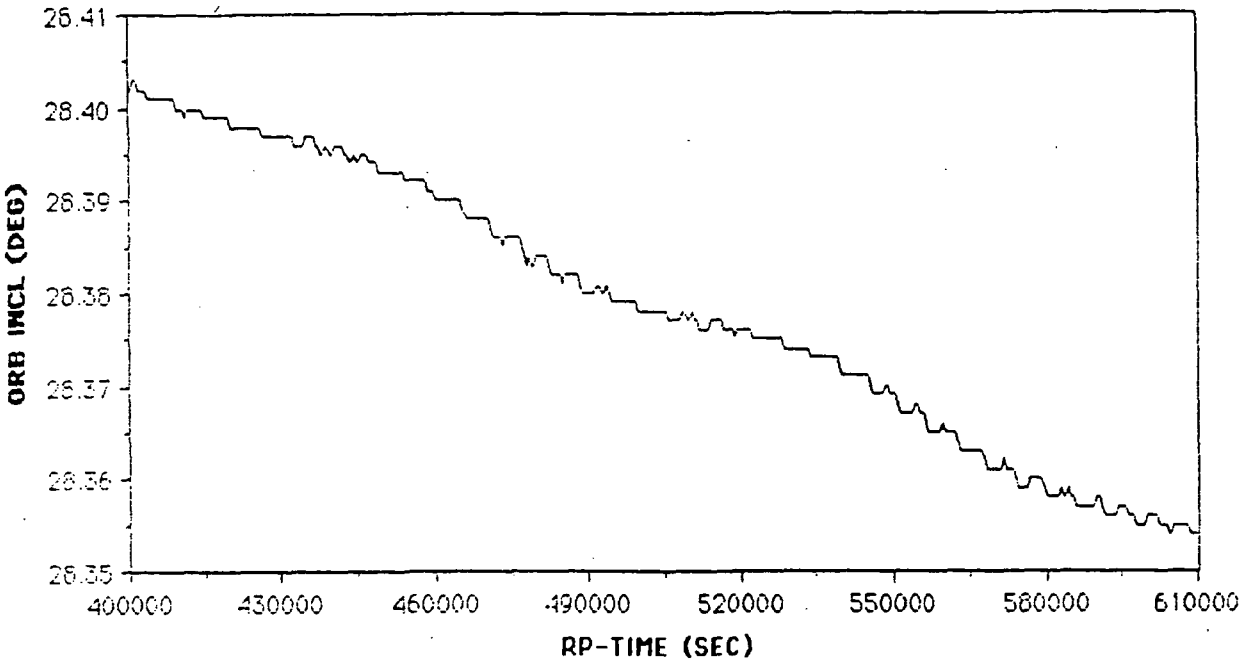

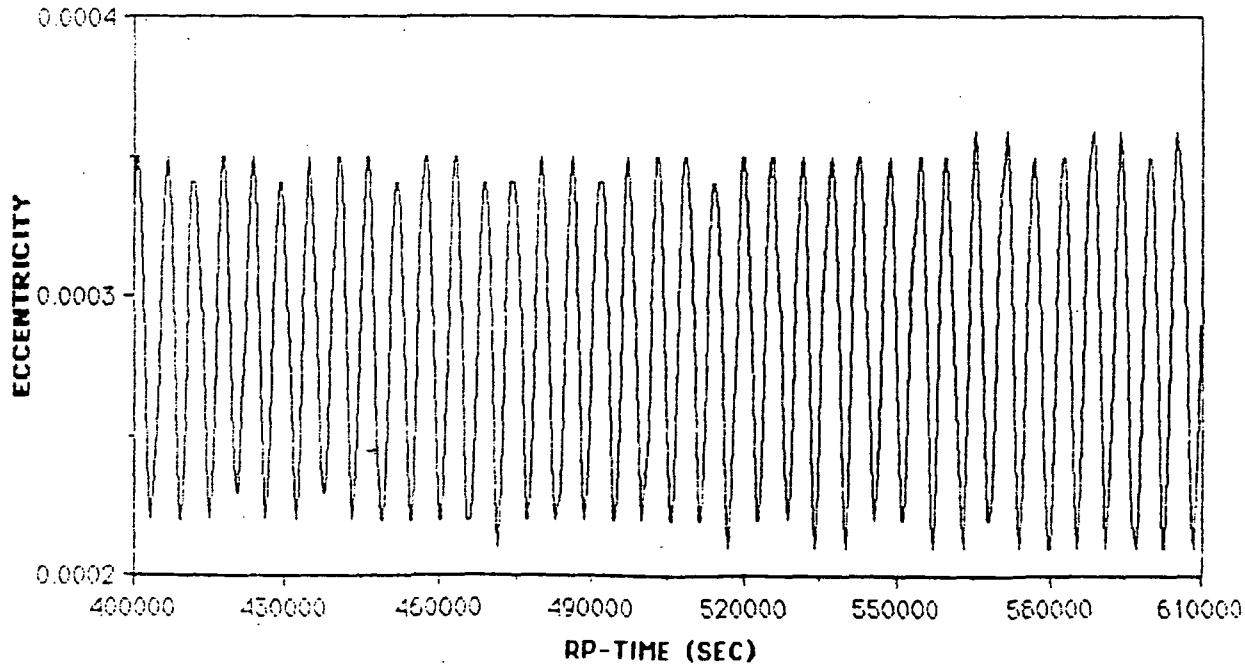

RUN 1

1 week
Continuous power

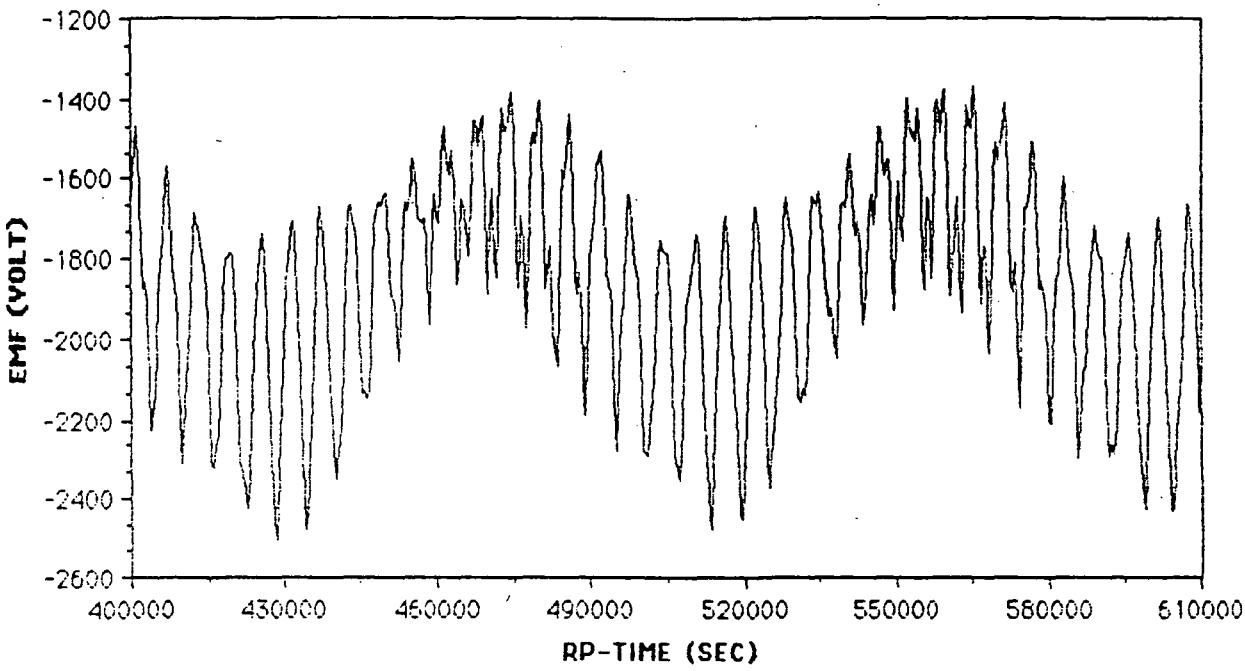

Run 2

1 week
Daytime only power

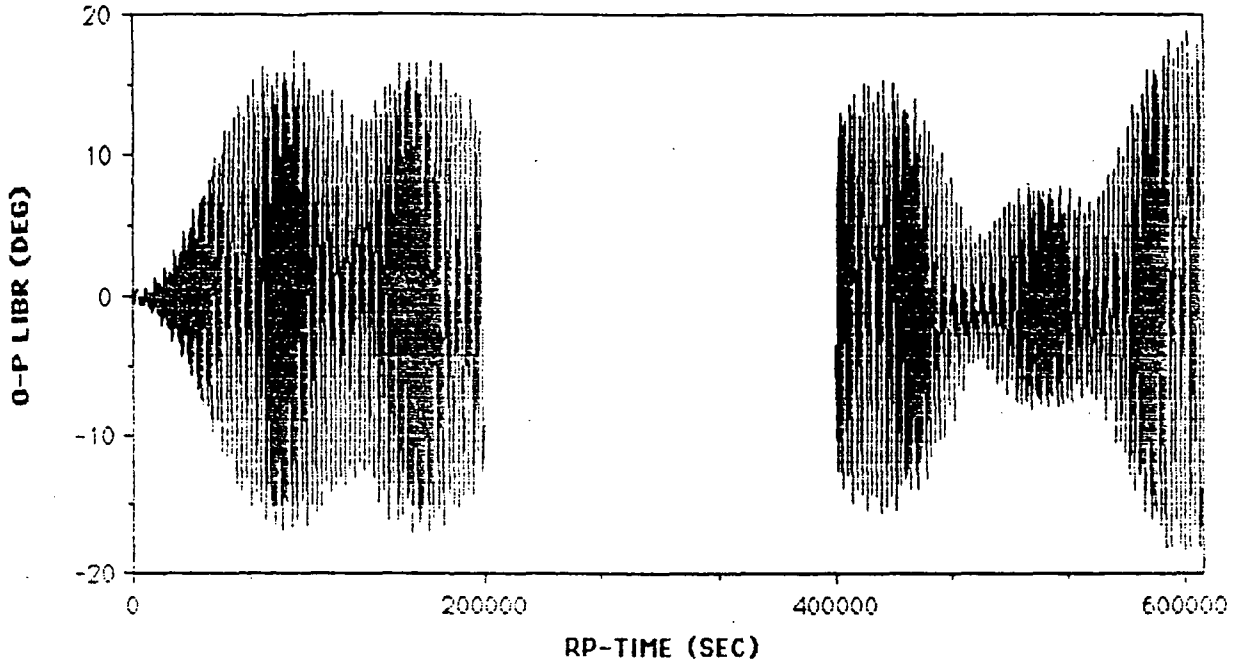

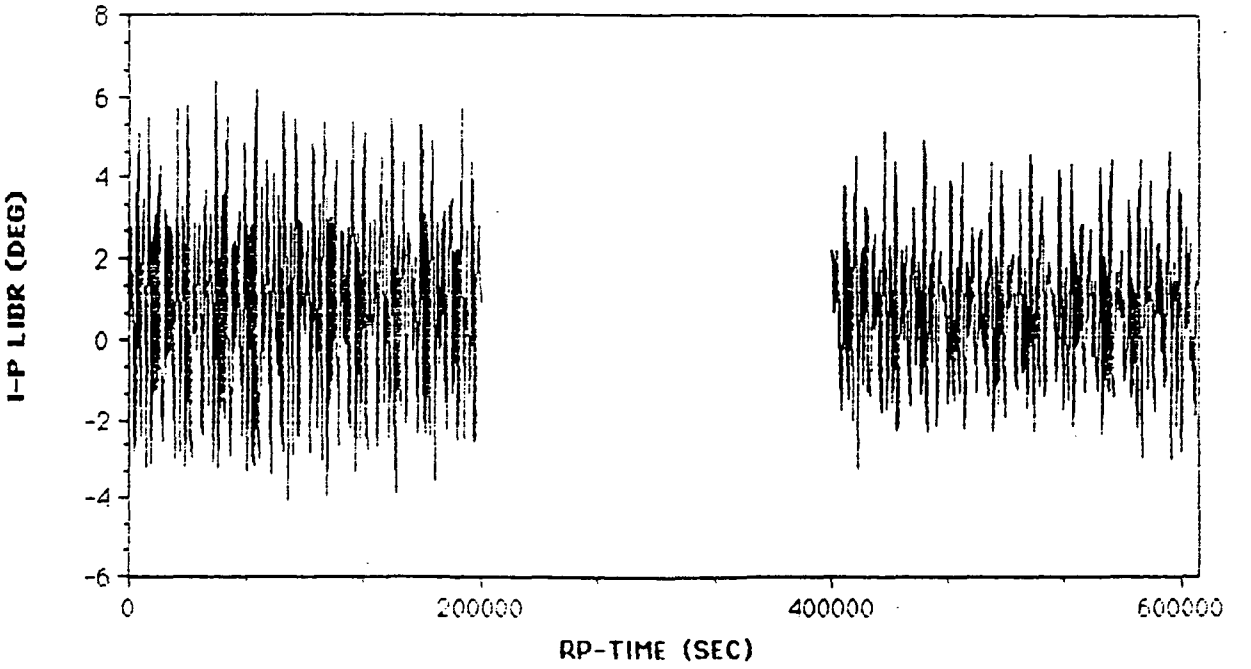

Run 2

1 week
Daytime only power

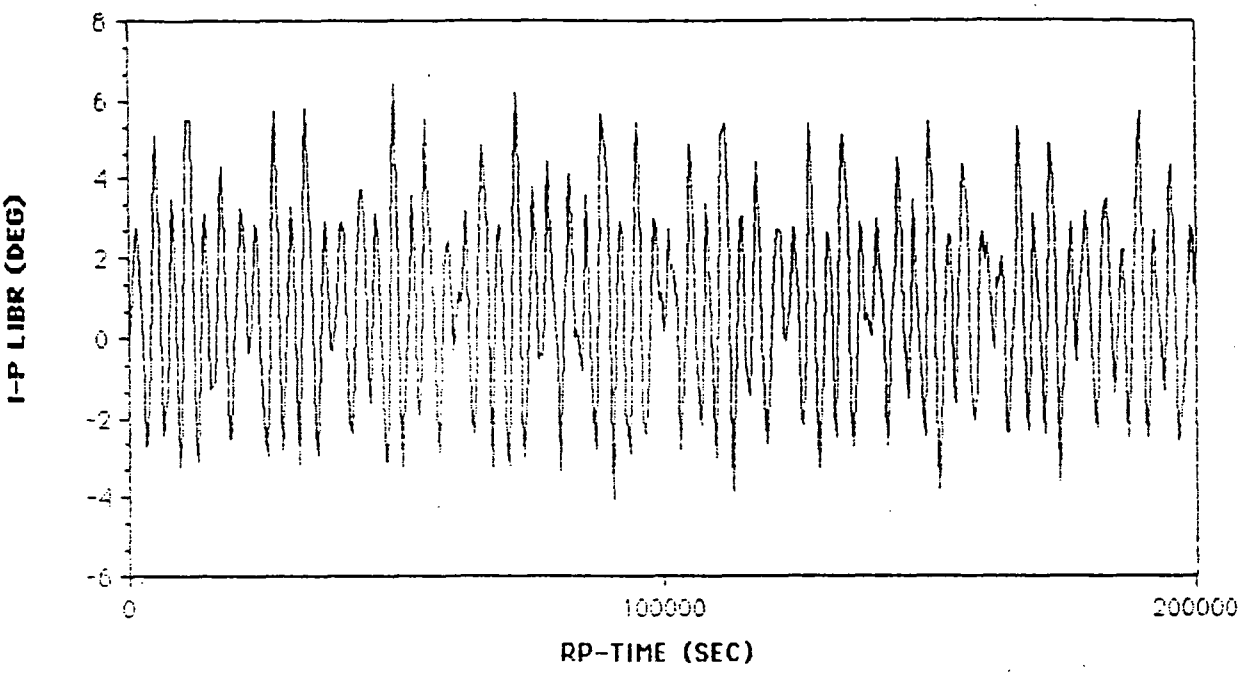

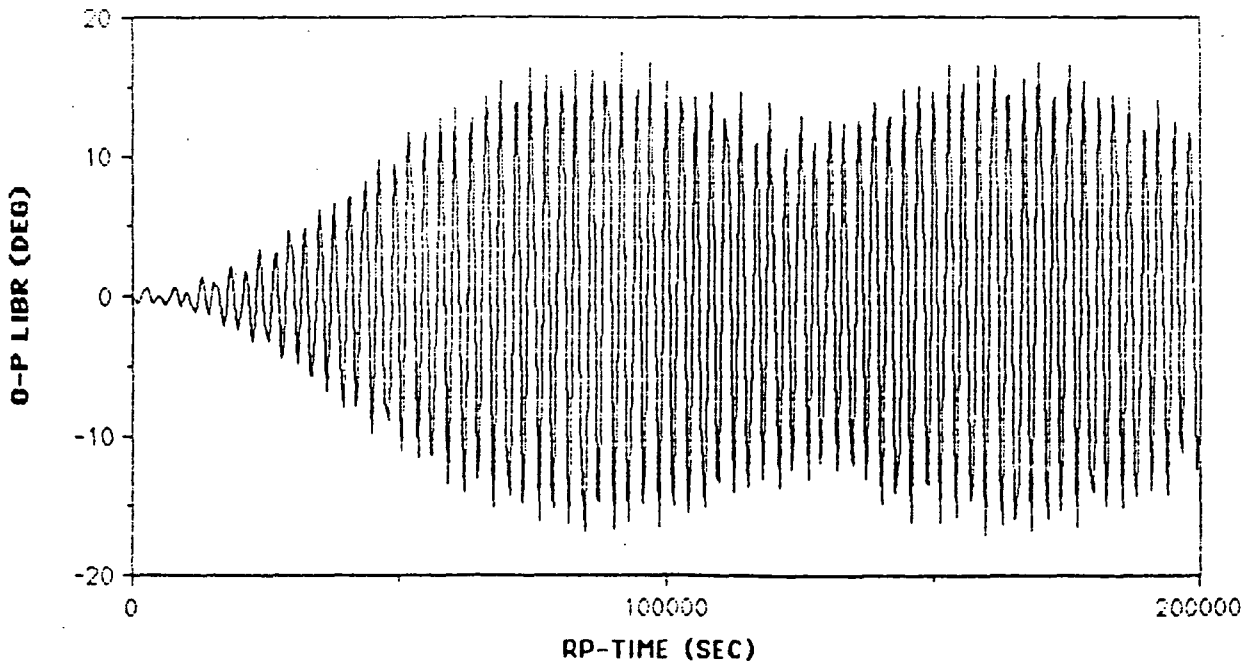

Run 2

1 week
Daytime only power

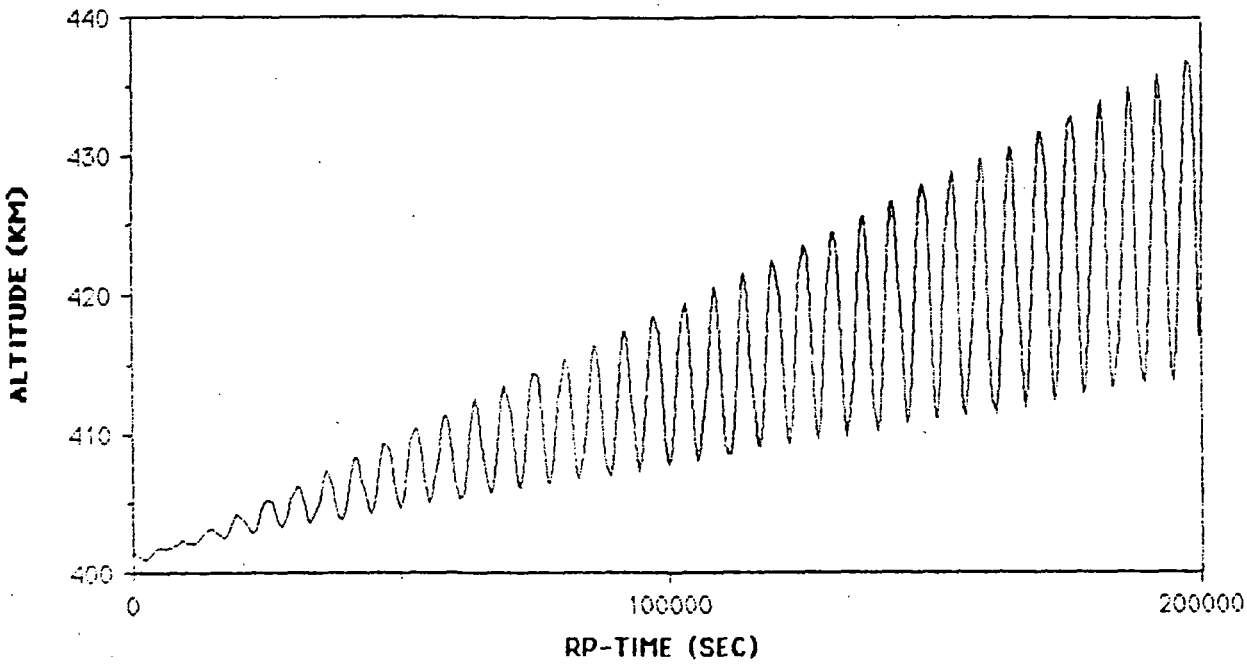

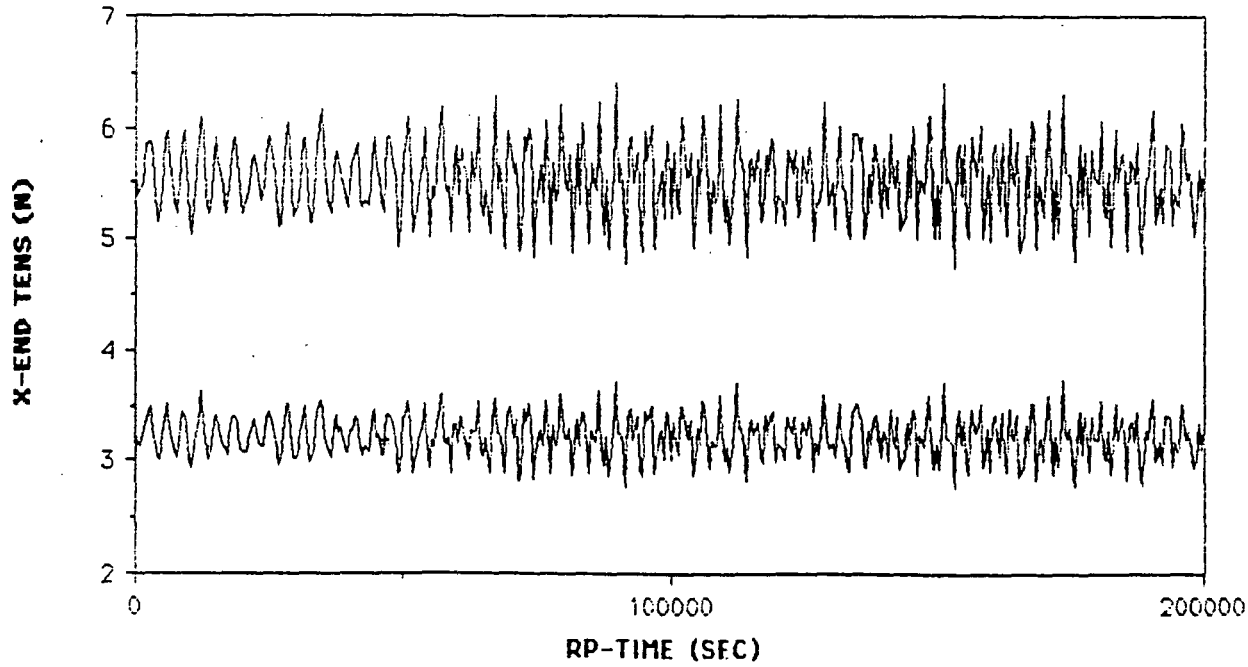

Run 2

1 week
Daytime only power

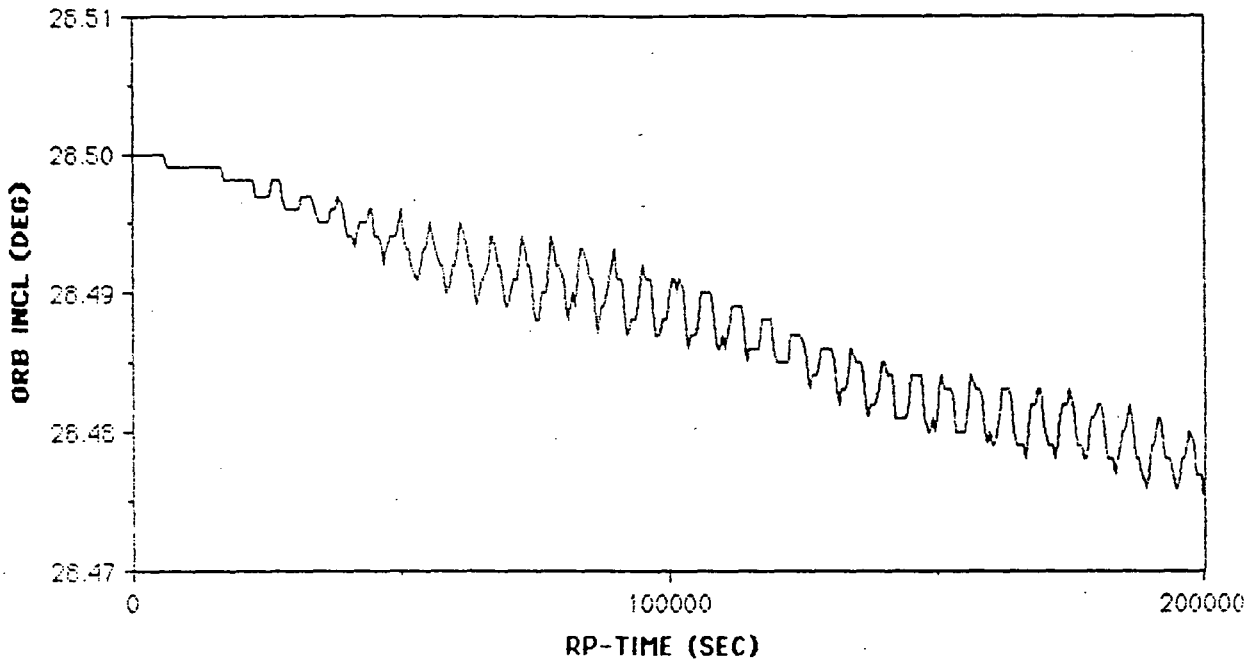

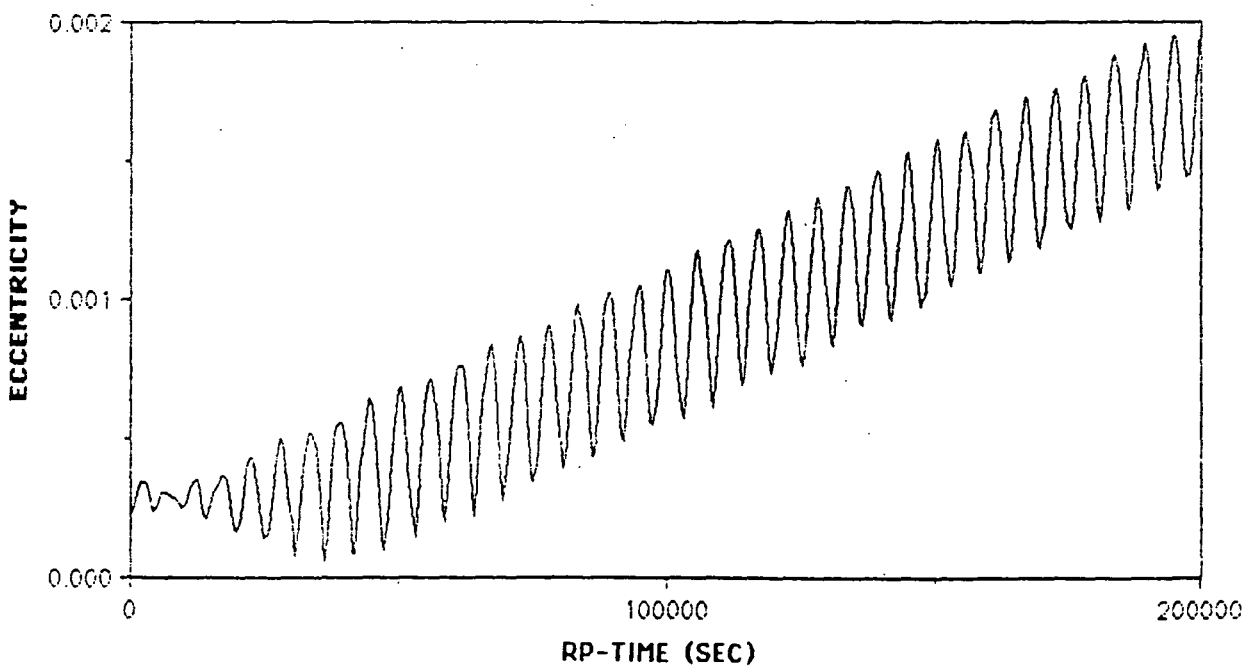

Run 2

1 week
Daytime only power

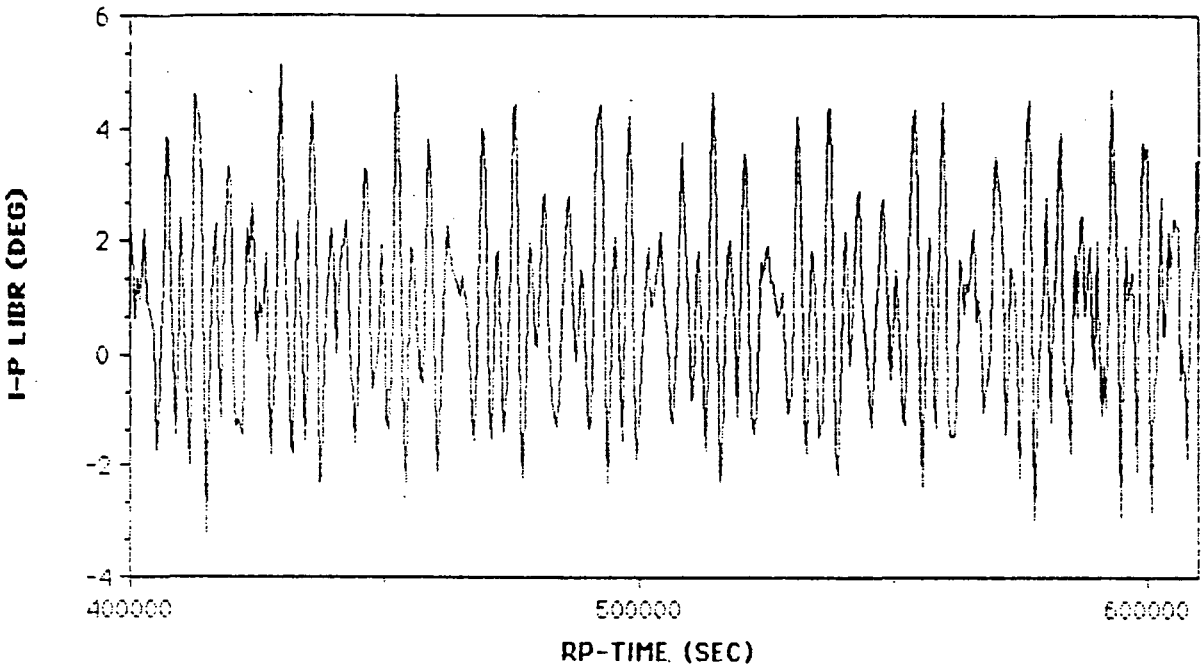

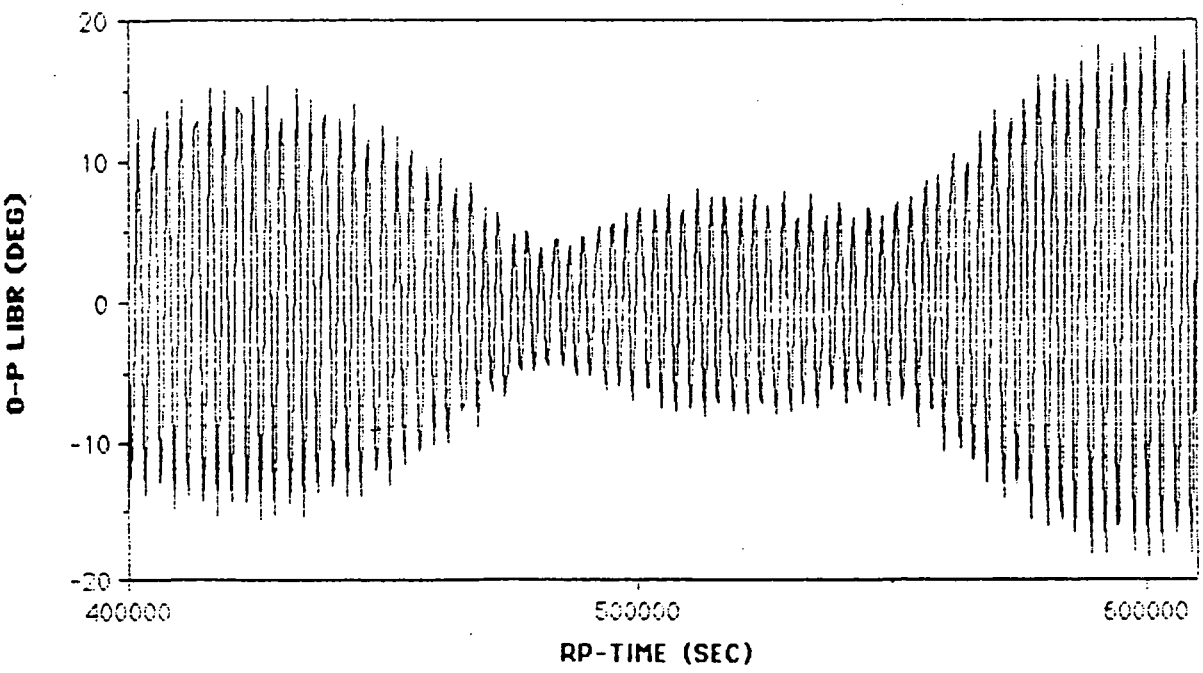

Run 2

1 week
Daytime only power

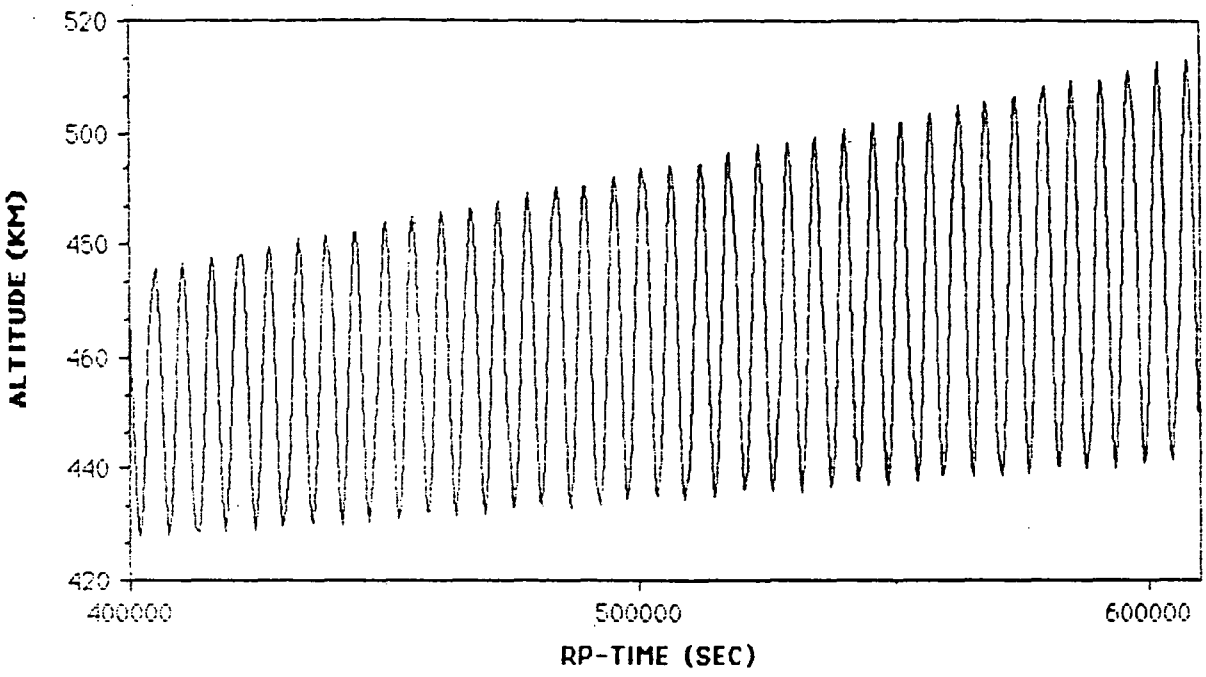

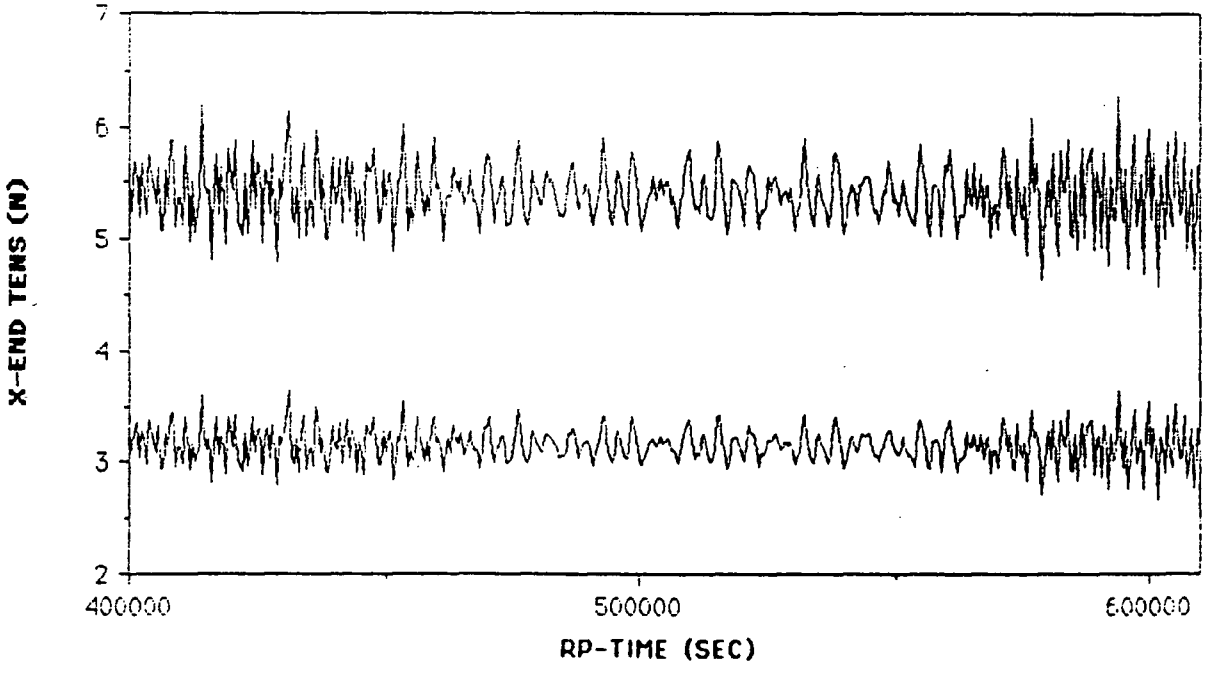

Run 2

1 week
Daytime only power

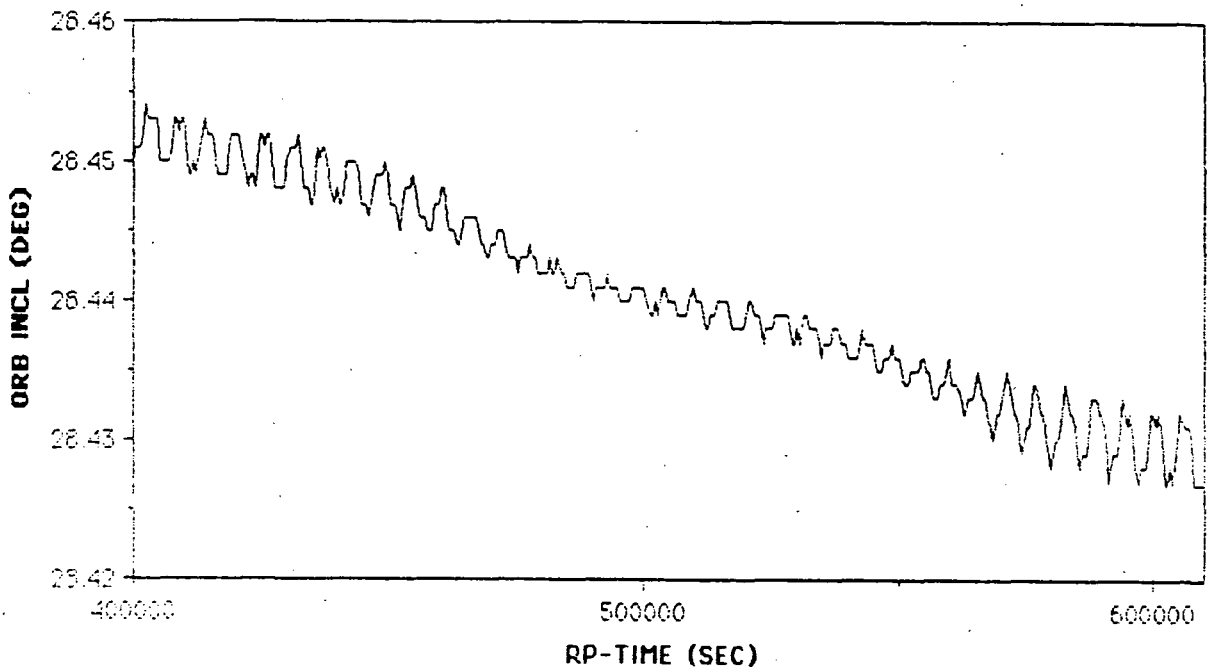

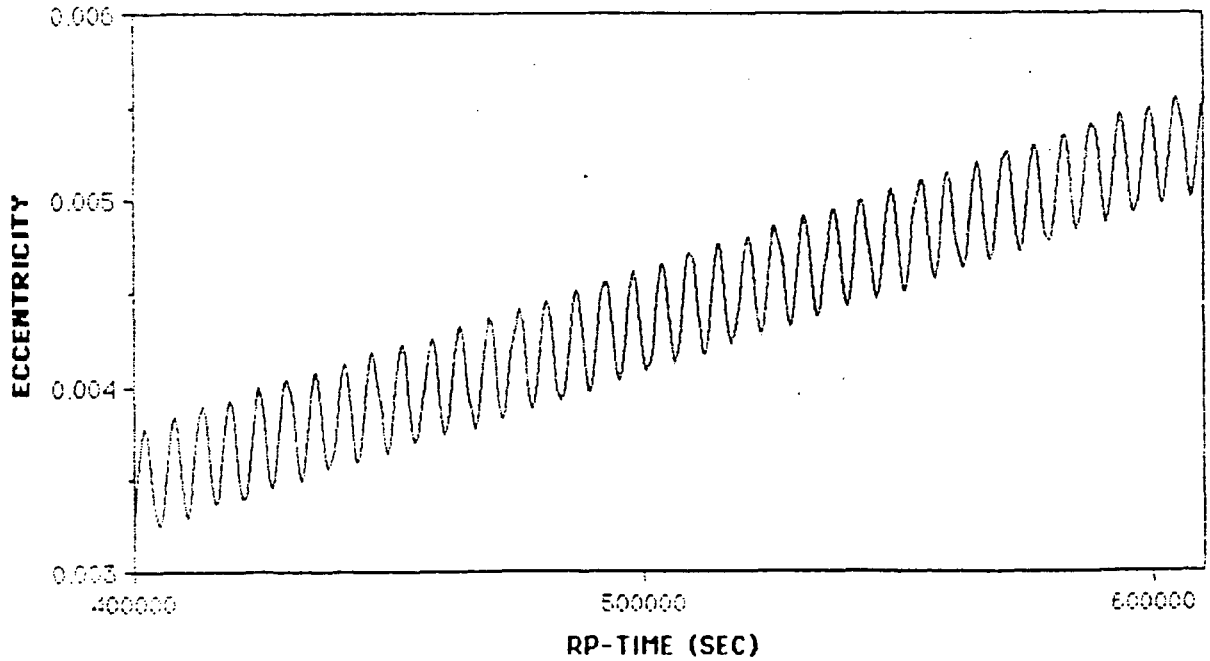

Run 3

2 days
High modulus tether
Daytime power only

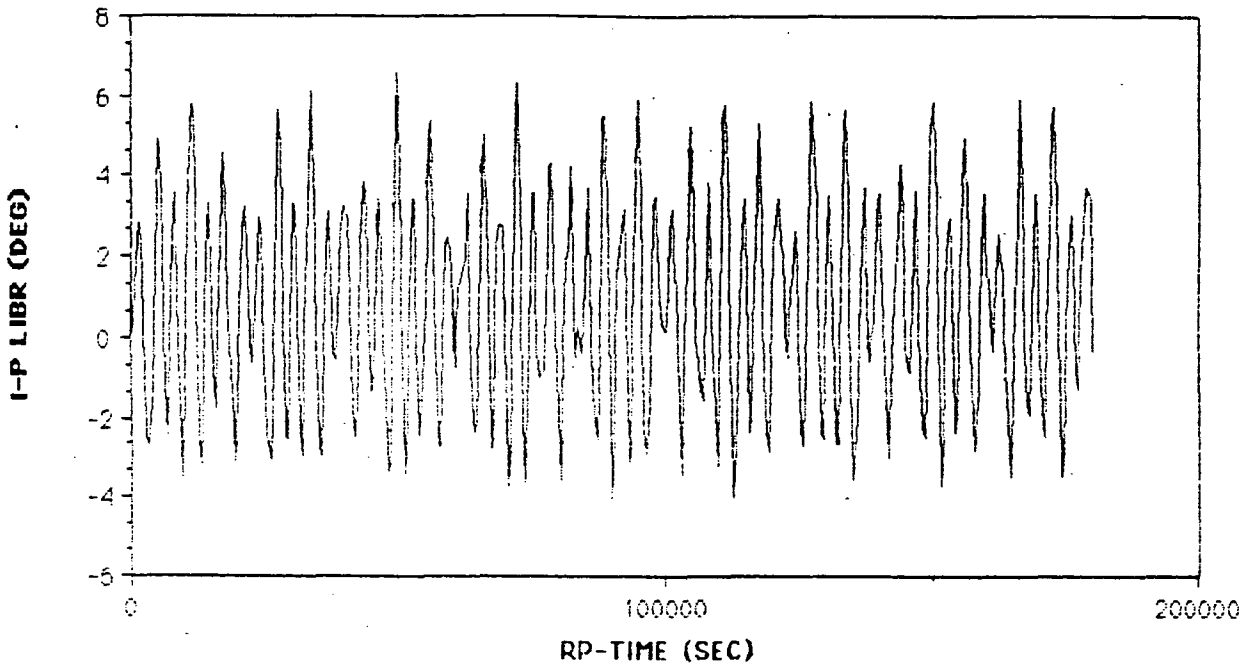

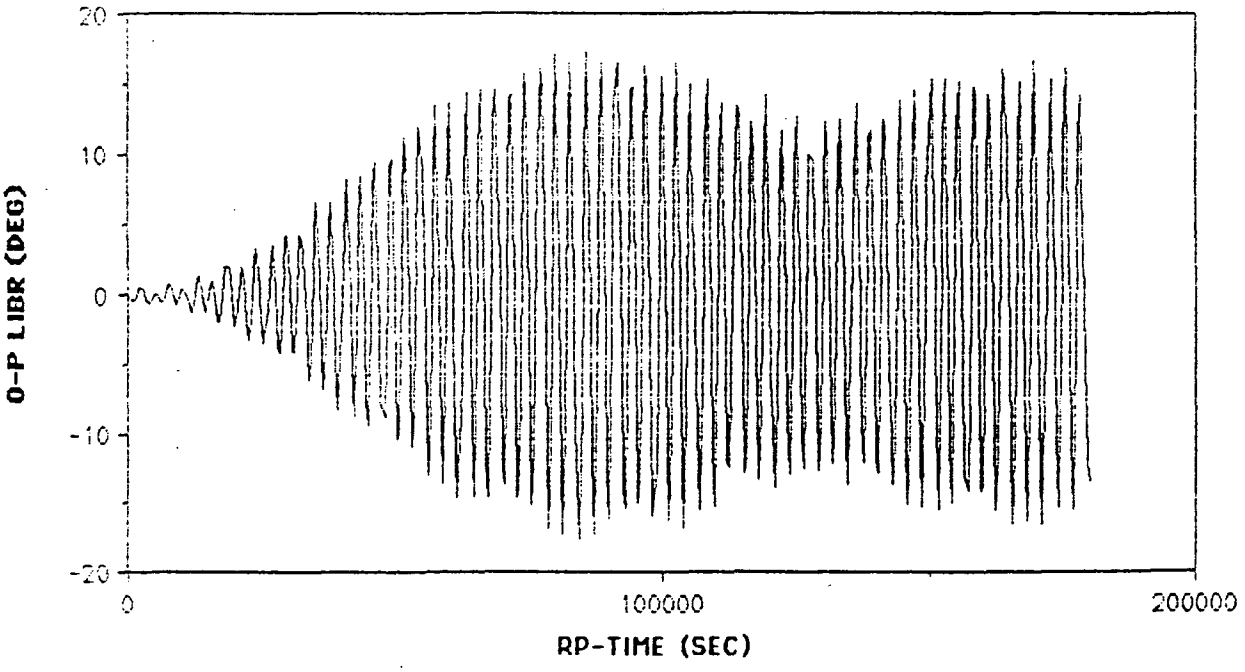

Run 3

2 days
High modulus tether
Daytime power only

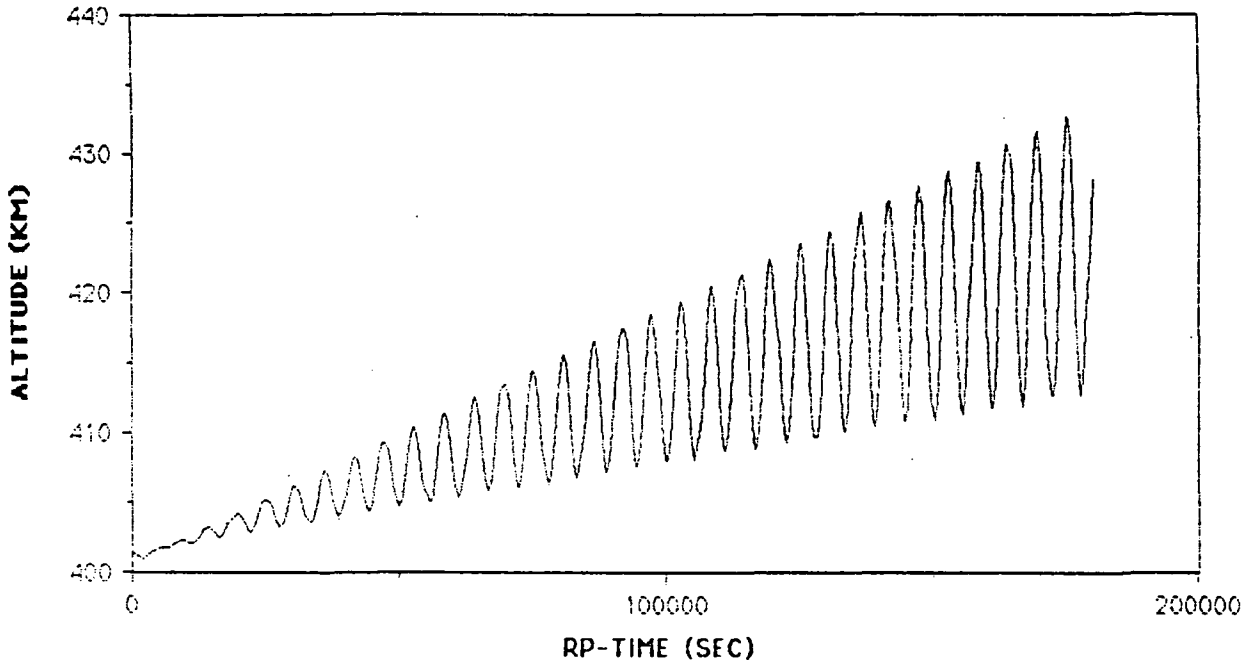

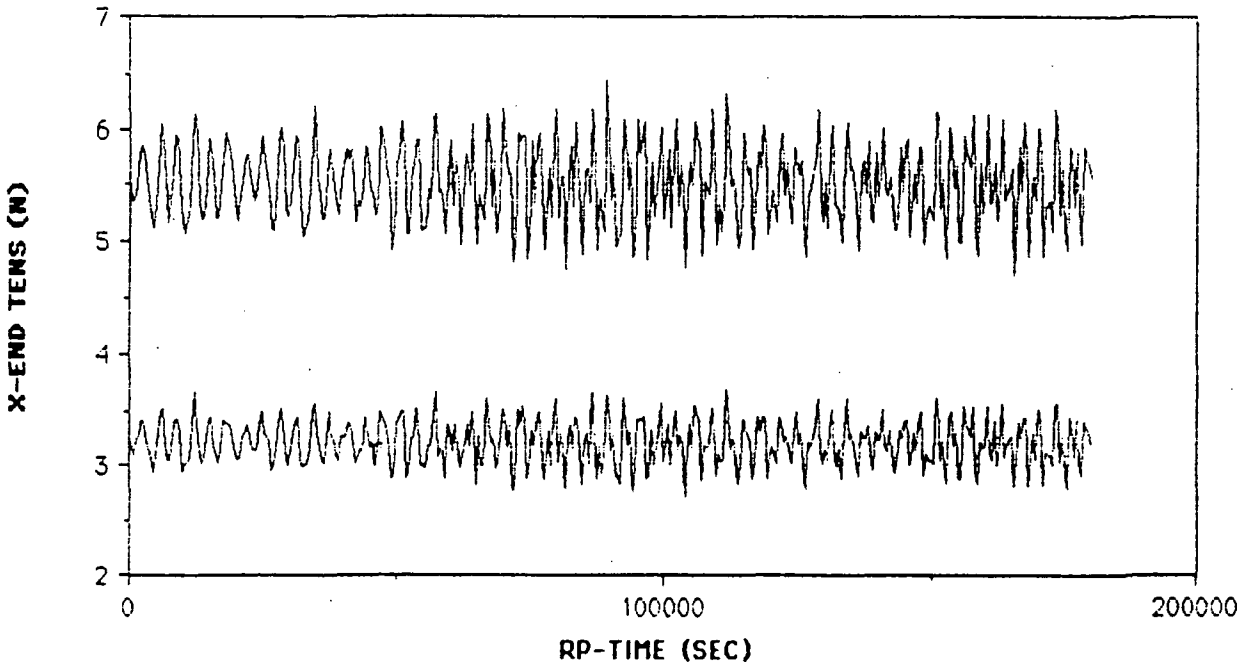

Run 3

2 days
High modulus tether
Daytime power only

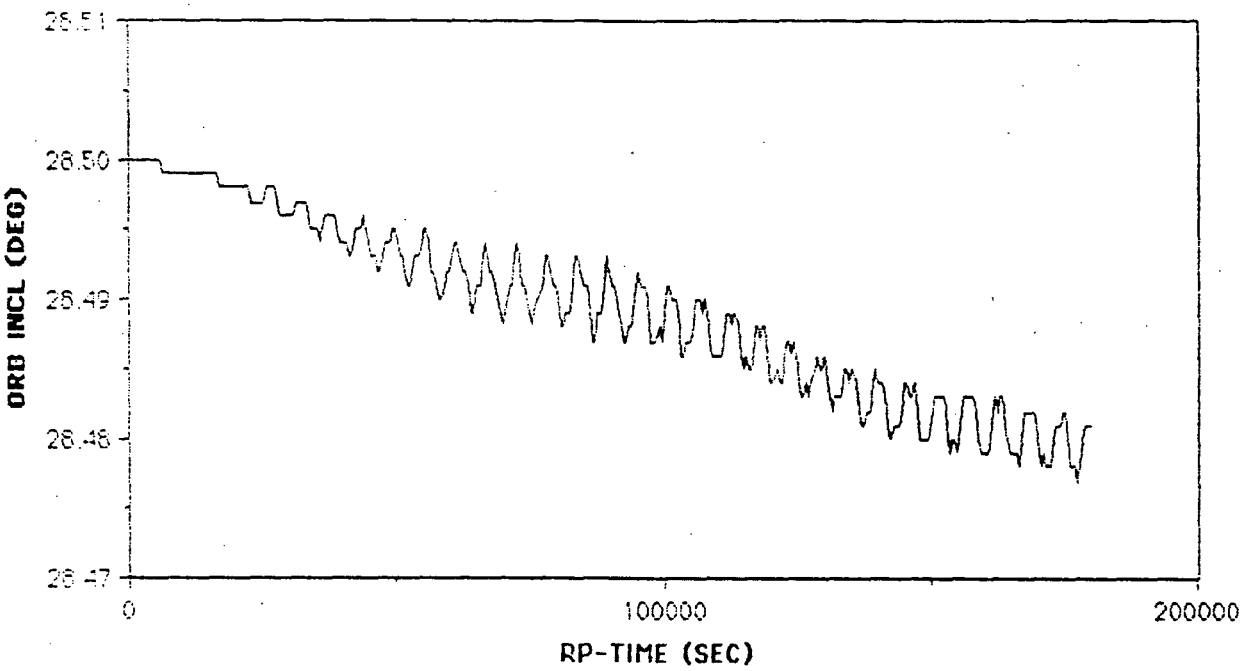

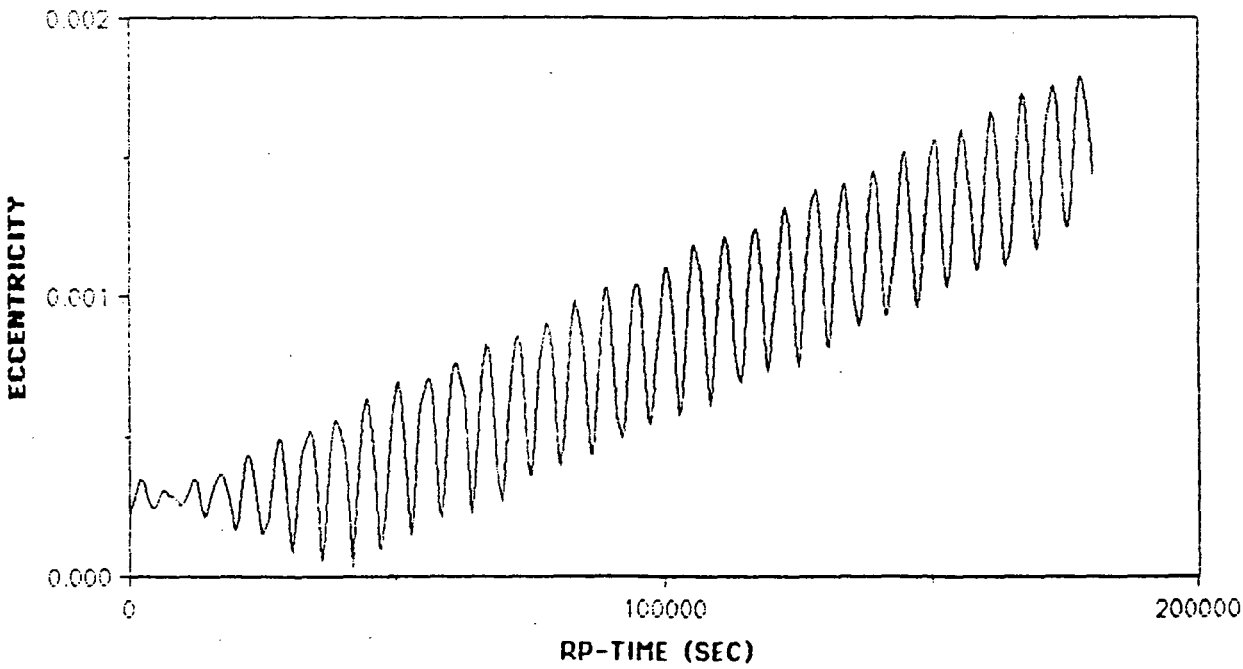

ORIGINAL PAGE IS
OF POOR QUALITY

Run 4

270,000 sec.
High modulus, light tether
Continuous power

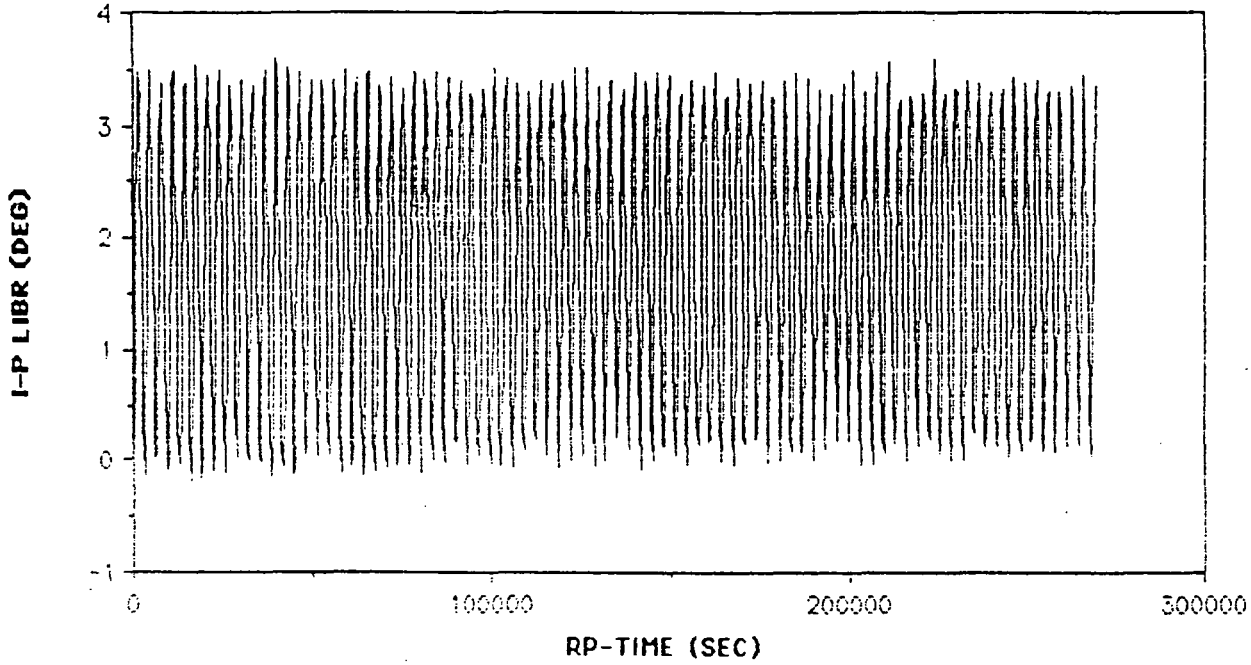

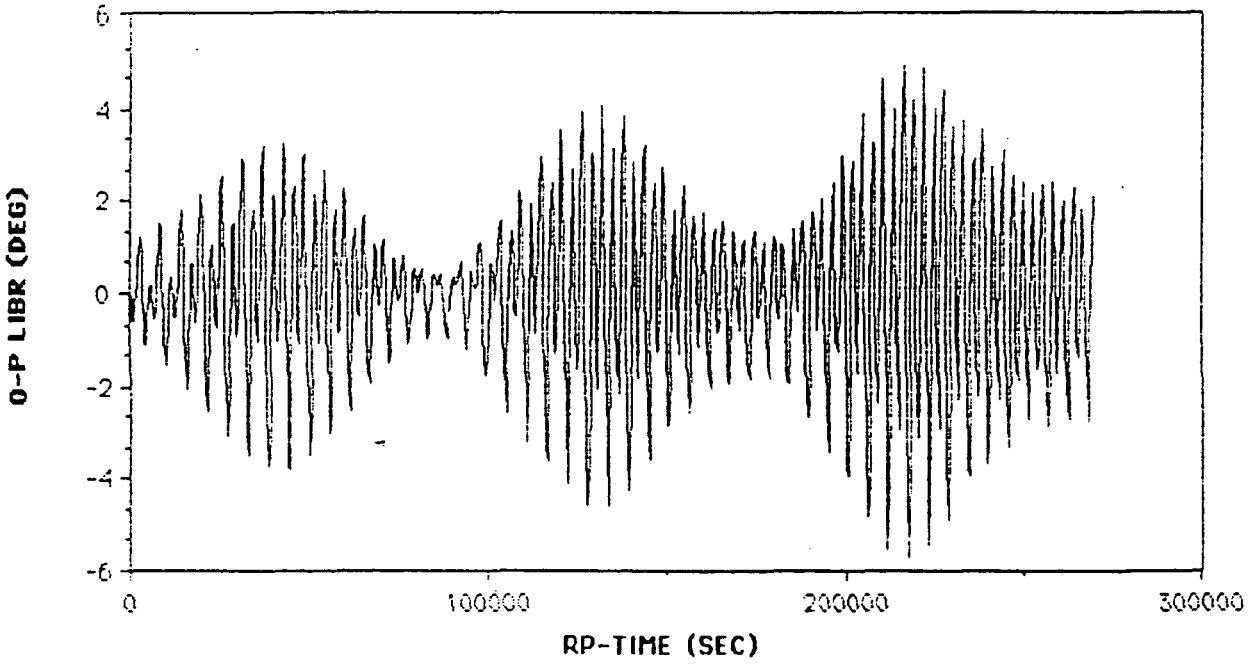

Run 4

270,000 sec.
High modulus, light tether
Continuous power

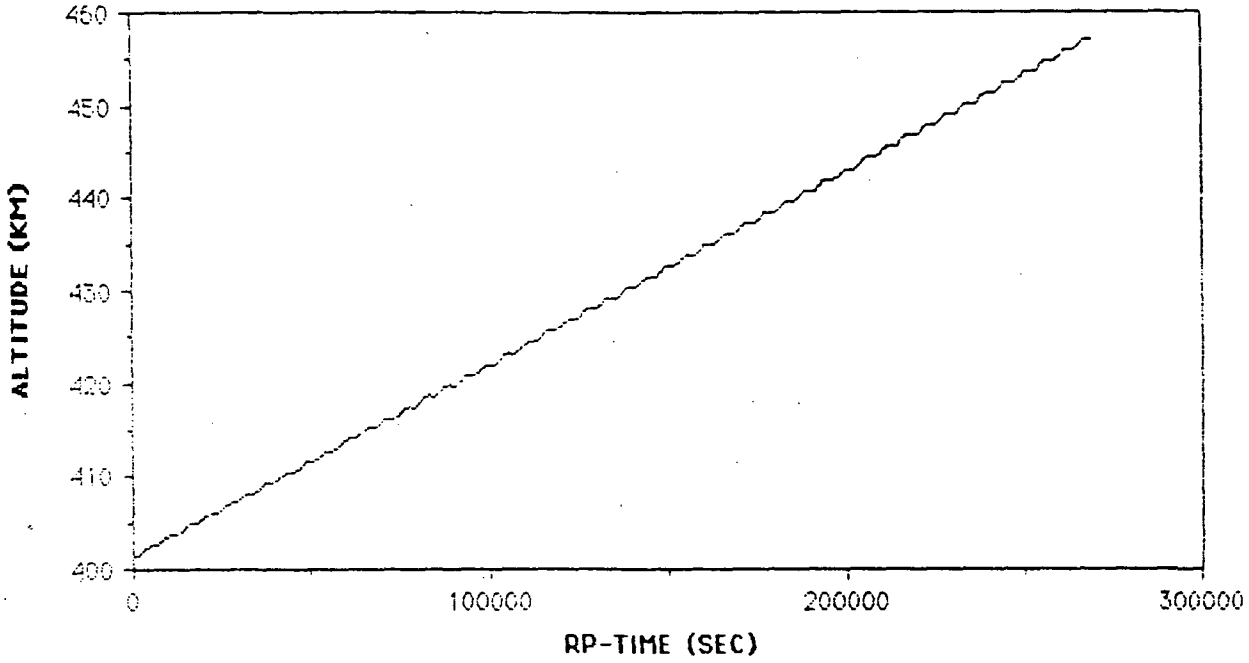

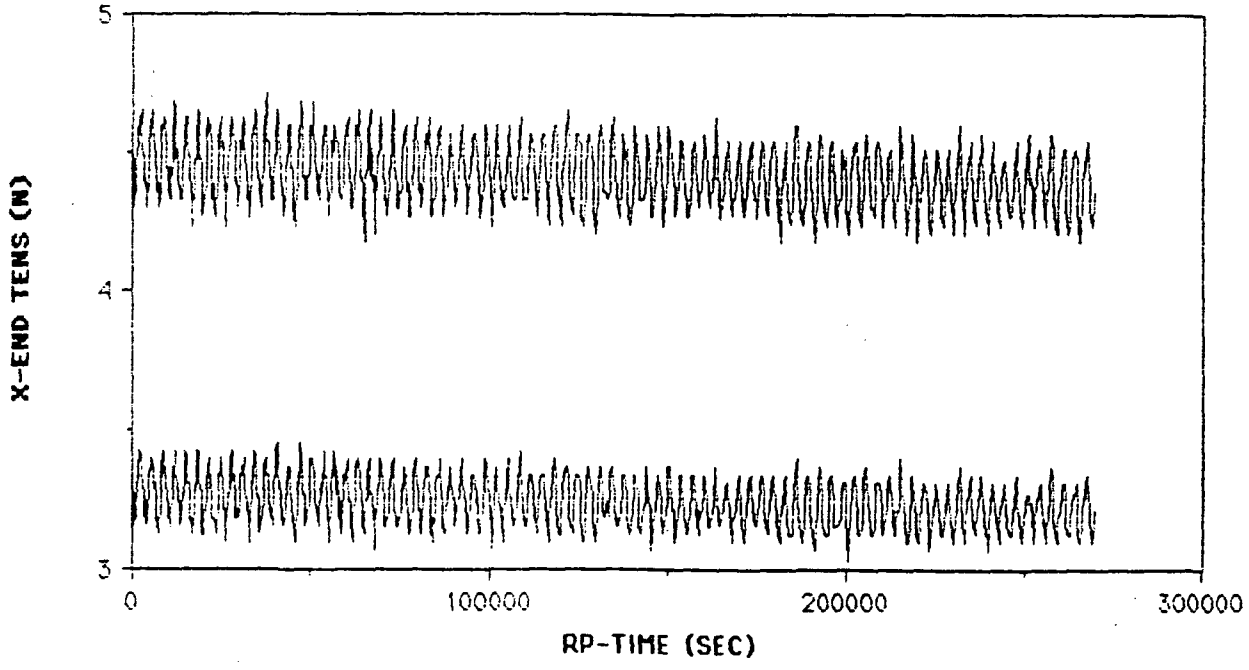

Run 5

200,000 sec.
High modulus, light tether
180 deg. longitude start
Daytime power only

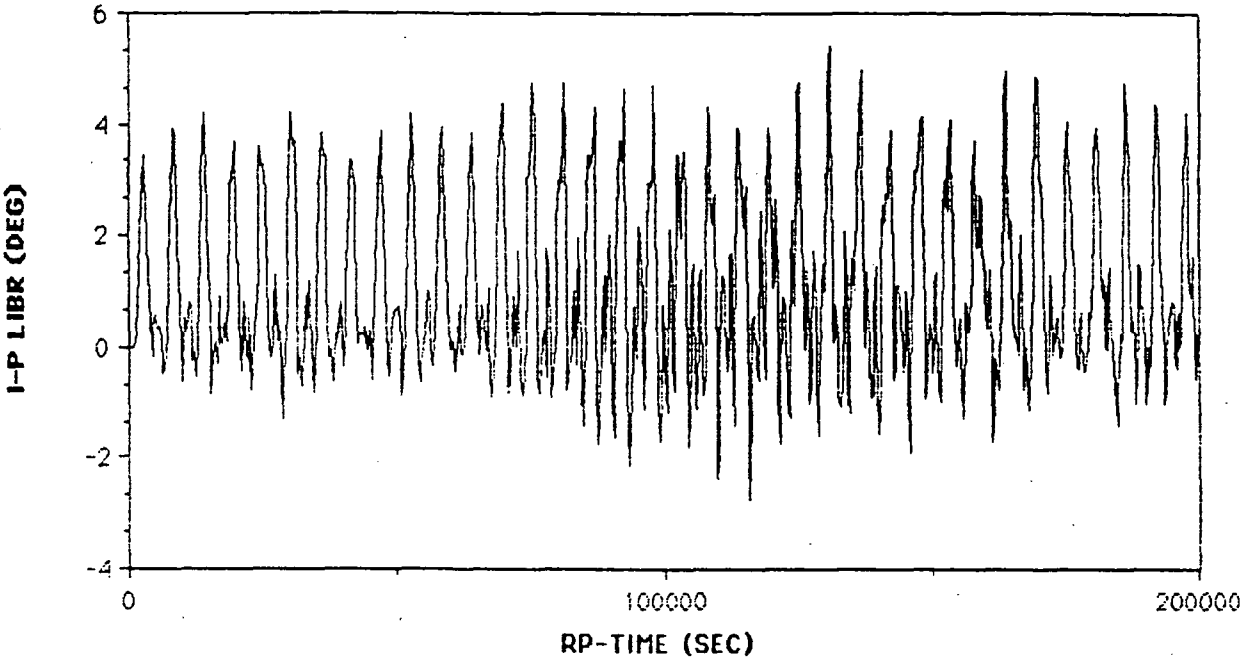

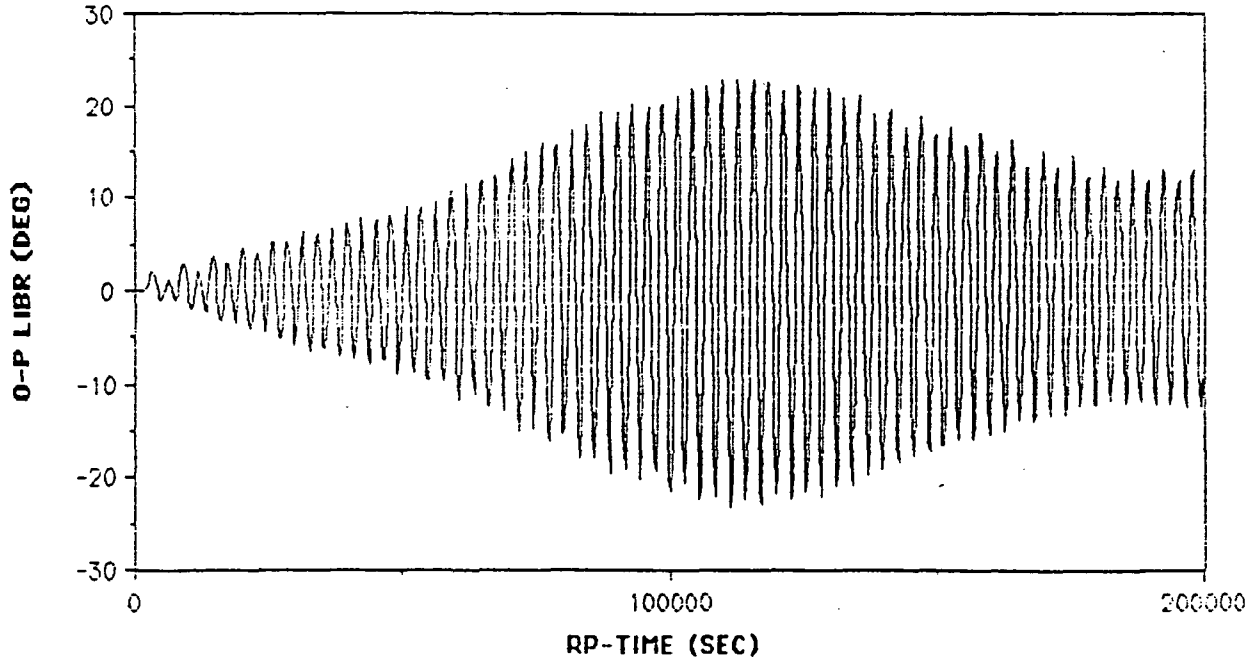

Run 5

200,000 sec.
High modulus, light tether
180 deg. longitude start
Daytime power only

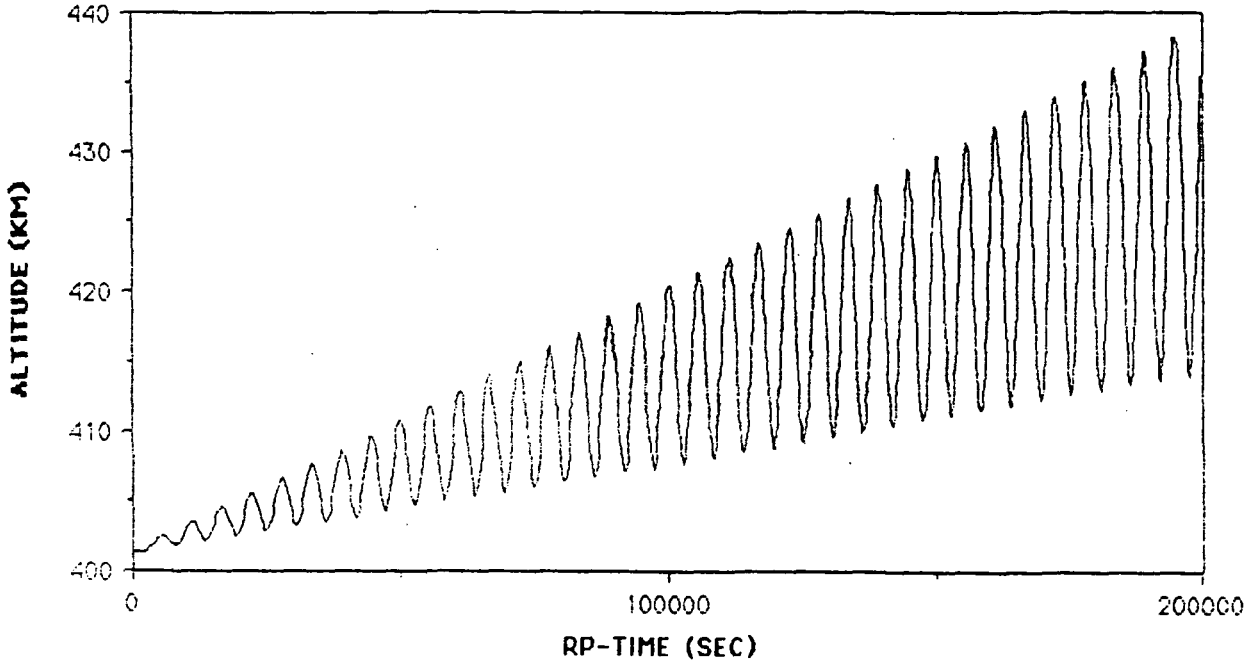

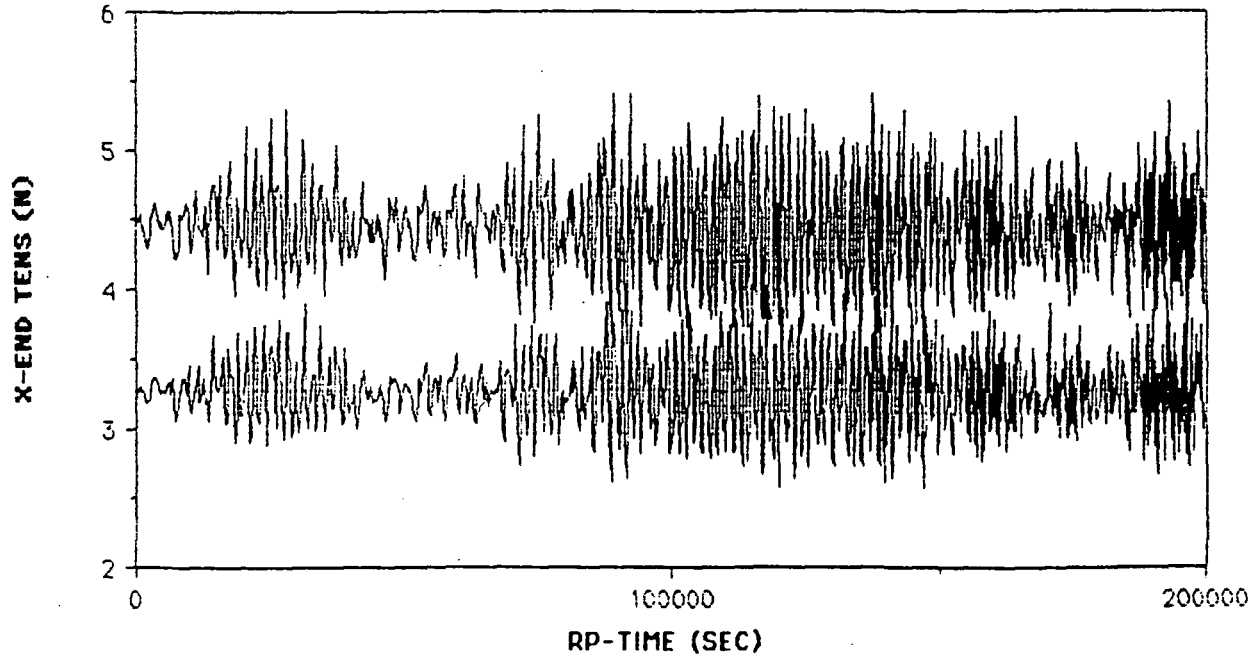

Run 6

100,000 sec.
High modulus, light tether, heavy endmass
180 deg. longitude start
Daytime power only

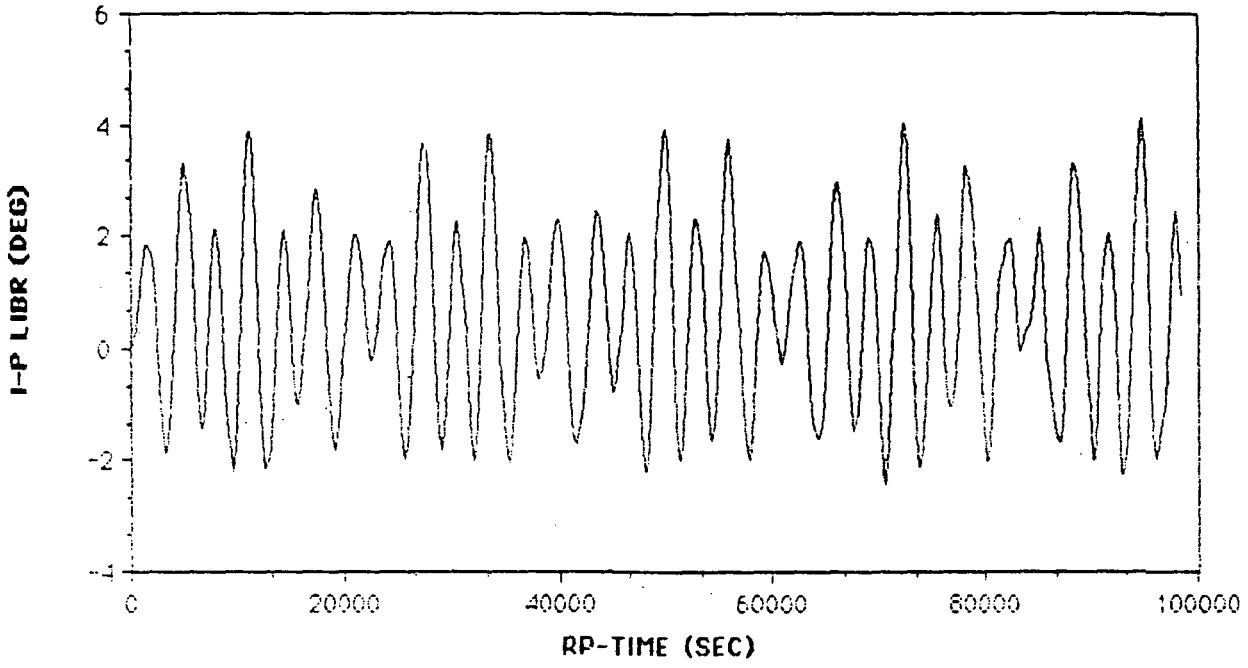

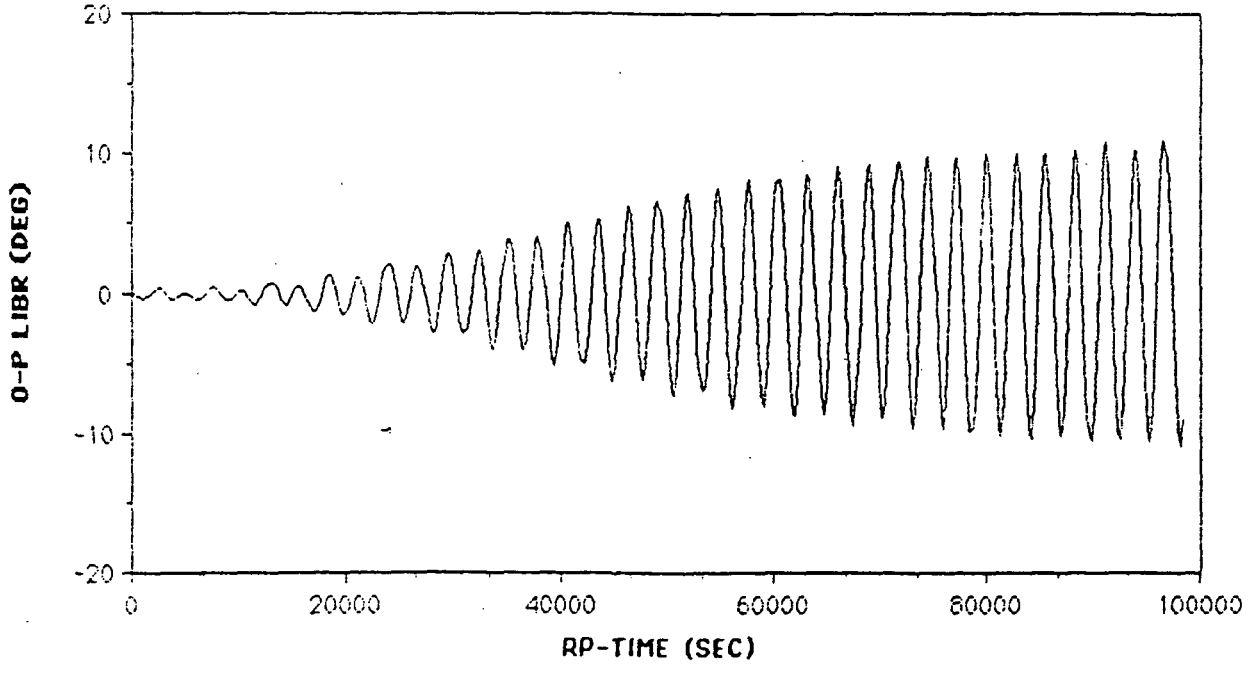

Run 6

100,000 sec.
High modulus, light tether, heavy endmass
180 deg. longitude start
Daytime power only

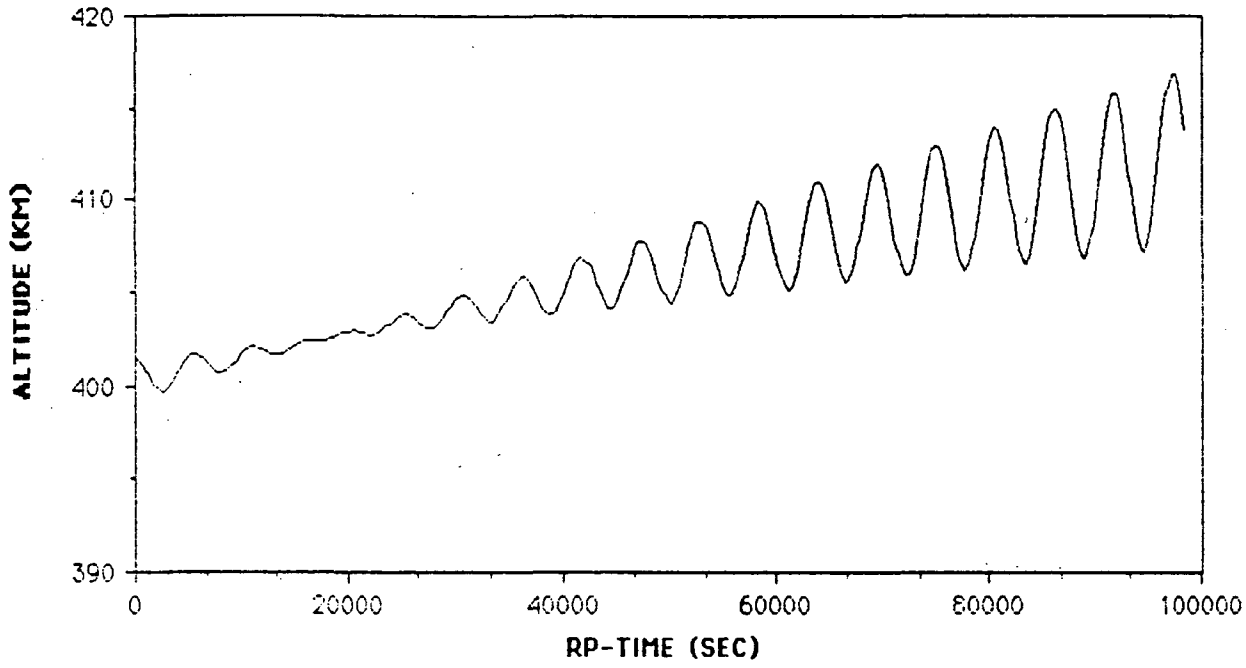

APPENDIX E

Interoffice Correspondence
TRW Space and Technology Group
Engineering and Test Division

TRW

Subject	Date	From
Comments on ESL Report to TRW on Electrodynamic Tether Stability	15 June 1988 88.L131.2-044	Dale Stuart D. Stuart for MAC
To	**cc**	**Location/Phone**
✓ D. Younkin	J. Bernier M.A. Chory	82/2045 536-2092

After reviewing the Energy Sciences Laboratories (ESL) report (Attachment 1) and the two accompanying video tapes, I made the following observations:

1. The first video tape shows extensive long-term simulation runs using a dumbbell tether model, however these runs were not requested in the SOW (Attachment 2), and there is no mention of these runs in the report (except the one-page guide to the monitor display). There is no explanation (during the narration of the runs) for the choice of initial conditions that deviate from the nominal vertical. The runs cover a simulated period of several weeks (?), and considerable discussion is provided about the results from these runs, which are of dubious value, considering the issues raised in item (2).

2. The second video shows the results from the GTOSS runs extending over a simulated time of about two days. The dynamic behavior shown during the run in which the tether is operating only in daylight exhibits the "jumprope" motion, and the tip motion develops in-phase (same frequency) in-plane and out-of-plane libration as the jumprope behavior develops and becomes the primary motion. These are significant effects not shown by the dumbbell model, and raise concern over the validity of the dumbbell simulation results.

3. In addition, there is no discussion about the significance of the jumprope motion, and no mention of the peculiar in-phase in-plane and out-of-plane libration. The simulation ends before it can be determined whether the motion diverges, since the tip motion is decreasing as the simulation ends. The discussion in the report (referring to longer runs) seems to indicate that this motion becomes bounded, and only "breathes" once the out-of-plane libration amplitude reaches 20 degrees, however, the jumprope motion looks anything but stable, and seems to be increasing in amplitude when the simulation ends. In general, much more discussion of the

GTOSS runs would have been expected, considering the large computational effort of running such a high-fidelity model, and the significance of the tether stability.

4. Only GTOSS runs 4 and 5 are shown in the video — runs 1 and 2 supposedly cover longer simulation time periods (1 week, as described in the report), and should have been shown if they answer some of the issues expressed in item (3) above.

A subsequent phone call to Joe Carroll at ESL provided some answers to the observations and concerns mentioned above.

Joe agrees that the dumbbell model has little validity in evaluating the long-term stability characteristics of the tether system. He said it was developed to get a feel for the contribution of the EM force to the out-of-plane librational behavior. ESL had not previously run simulations that included out-of-plane dynamics, and they wanted to become familiar with the behavior of a simple, un-driven tether (no EM force) before attempting to interpret the GTOSS simulation results.

Joe pointed out that the GTOSS simulation showed stable (bounded amplitude) out-of-plane librations for the daylight-operating case because the model included longitudinal damping in the tether, which absorbs enough energy to prevent divergence. (This stable behavior was not demonstrated in the dumbbell simulations.)

After submitting the report to TRW, ESL performed more GTOSS runs with a lower tether modulus (based on spiral twisted strands rather than solid aluminum), which lowered the tether longitudinal oscillation frequency and allowed them to use a larger time step and hence run the simulation for a longer time. Runs were performed for a simulated time of one month, and showed a maximum out-of-plane libration amplitude of about 18 degrees for the daylight-operation case. The minimum peak amplitude (due to the diurnal variation of the effective magnetic inclination) was roughly 70 percent of the maximum peak. Driving the tether at 4 kW would increase the maximum amplitude by only about 20 percent, according to Joe's rough calculations.

Some one-month GTOSS runs were also performed for the constant-operation case, and the out-of-plane librational motion remained bounded within about 4 degrees. If the power in the tether is reduced such that the total orbital energy imparted to the system matches the energy generated with the daylight-only operation, then the librational motion remains within 2–3 degrees. Joe said they intend to forward these additional results to TRW.

When asked about the in-phase behavior of the in-plane and out-of-plane libration appearing early in the daylight-operation GTOSS run, Joe replied that he had no idea why that should happen, and that he would take another look at it.

APPENDIX F

THE TRW TETHER STUDY TEAM

Project Manager	David L. Younkin
Deputy Project Manager	Dr. Neal D. Hulkower
20 kW PMG Tether Task	Robert Strommer John Biess Robert L. Anderson
Tether Characterization	Dr. Ronald C. Rossi ATD Materials Laboratory
Tether Tests and Simulation	Energy Sciences Laboratory J. A. Carroll John C. Oldson Matt Nilsen Hans Meissinger Dr. Dale Stuart